Imperial College London

Balancing Cryptoassets and Commodities: Novel Weighted-Risk-Contribution Indices for the Alternative Asset Space

Author Aikaterini Koutsouri
Supervisors Prof. W. J. Knottenbelt

Submitted April 2023

A thesis submitted in fulfilment of the requirements for the degree of Doctor of Philosophy

Centre for Cryptocurrency Research & Engineering,
Department of Computing,
Imperial College London

Centre for Cryptocurrency Research and Engineering,
Department of Computing,
South Kensington Campus,
Imperial College London,
South Kensington,
SW7 2AZ

Don’t be afraid to take risks and embrace failure. That’s where the best opportunities often lie.

Jim Simons

Declaration

I hereby declare that this thesis contains my own work and that all information derived from the research of others is properly acknowledged.

The formatting for this thesis is taken from the Thesis Template, authored by R. Robinson, available at https://github.com/mlnotebook.

Copyright

Acknowledgements

I would like to express my deepest gratitude to my supervisor, Professor William J. Knottenbelt, for his support and mentorship throughout my PhD journey. His exceptional expertise, patience, and encouragement have been pivotal in my personal and professional growth, and I am honored to have had the opportunity to work under his guidance.

I would also like to thank my fellow ACE358 colleagues, Alexei, Daniel, Dimitrios, Dominik, Dragos, Lewis, Paul, Rami, Sam, Sirvan, and Toshiko who have been a constant source of inspiration and fun. Our friendship and shared laughter have made the journey truly enjoyable and Monday fundays will always be a fond memory of mine.

I would also like to express my gratitude to CoinShares, for generously funding my PhD research. I am immensely grateful for the opportunity they have provided me, and I am proud to be associated with their esteemed organization.

I cannot thank my family enough for their unwavering love and support throughout my entire life. Their belief in my abilities and their constant encouragement have been the bedrock of my success. To my beloved parents, Katy and Dimitris, thank you for your countless sacrifices over the years and for your tireless efforts in shaping me into the person I am today. To my cherished siblings, Vicky, Ioannis and Natalia, thank you for always being there for me, both in the best and the most challenging of times.

Finally, I would like to express my deepest gratitude to my good friends, some in London and some back home, who have supported and motivated me throughout this journey. Your understanding, encouragement, and constant reassurances have been invaluable. Thank you for the much-needed distractions, the shared moments of joy and laughter, and for always being a safe harbor when times were difficult.

Abstract

This thesis aims to serve as a comprehensive guide for effective design, development and performance evaluation of novel Weighted-Risk-Contribution indices for the alternative asset space. We concentrate our focus on the quest for diversification and risk-reward balance by incorporating commodities into a crypto-asset allocation.

First, we introduce the CoinShares Gold and Cryptoassets Index, a novel index product that combines a basket of five cryptoassets with gold to enhance the risk profile while maintaining independence from traditional financial asset classes. By generalizing the theory of Equal Risk Contribution, we compare various asset allocation strategies and demonstrate the effectiveness of a crypto-gold weighting based on the Weighted Risk Contribution allocation scheme in terms of Sharpe Ratio.

To assess the resilience of the index, we further introduce a complete stress testing framework using ARMA–GARCH processes and copulas to simulate realistic market conditions and extreme events. The analysis reveals a superior risk-return profile for the CoinShares Gold and Cryptoassets Index compared to traditional market-cap-weighted cryptoasset indices. Furthermore, we employ Gaussian Hidden Markov Models and Markov-switching GARCH models to identify high-risk market conditions and demonstrate the stable risk-reward profile and superior performance of the index in terms of the Omega ratio, particularly for investors targeting wealth preservation and moderate annual returns.

Lastly, we seek to quantify the diversification benefits of incorporating commodities into cryptoasset portfolios by comparing the CoinShares Gold and Cryptoassets Index with a modified index that replaces gold with a basket of five commodities. Mean-variance spanning tests and simulation-based Dynamic Conditional Correlation GARCH models reveal statistically significant improvements in the efficient frontier for both indices. We conclude that the modified index is more suitable for investors seeking higher annual returns, while the original index is more appropriate for those with moderate annual return goals.

The aforementioned studies advance our understanding of portfolio diversification in the context of cryptoassets and emphasize the potential benefits of incorporating gold and other commodities into crypto-based index strategies, thereby providing valuable insights for investors and financial practitioners.

Contents

List of Figures

List of Tables

Chapter 1

Introduction

1.1 Publications & Thesis Outline

This thesis is built upon the following research publications:

1. Koutsouri, Aikaterini, Poli, Francesco, Alfieri, Elise, Petch, Michael, Distaso, Walter, and Knottenbelt, William J. (2019). "Balancing Cryptoassets and Gold: A Weighted-Risk-Contribution Index for the Alternative Asset Space." In Proc. 1st International Conference on Mathematical Research for the Blockchain Economy (MARBLE 2019), Santorini, Greece. [87].
2. Koutsouri, Aikaterini, Petch, Michael, and Knottenbelt, William J. (2020). "Stress Testing Diversified Portfolios: The Case of the CoinShares Gold and Cryptoassets Index." In Proc. 2nd International Conference on Mathematical Research for the Blockchain Economy (MARBLE 2020). [84].
3. Koutsouri, Aikaterini, Petch, Michael, an Knottenbelt, William J. (2021). "Performance of the CoinShares Gold and Cryptoassets Index Under Different Market Regimes." Cryptoeconomic Systems. [86].
4. Koutsouri, Aikaterini, Petch, Michael, and Knottenbelt, William J. (2021). "Diversification Benefits of Commodities for Cryptoasset Portfolios." In 2021 IEEE International Conference on Blockchain and Cryptocurrency (ICBC) [85].

Each publication cited herein acknowledges my position as the primary author and my role in guiding the research processes and presenting the findings within each work. I acknowledge the valuable contributions of my colleagues, particularly in assisting with the literature review and introductory sections. Their support played a significant role in the completion of this work.

The remainder of this thesis is organised as follows:

Chapter 2 introduces the basic concepts around the emerging digital assets class, including a description of blockchain technology and the historical evolution of the cryptoassets class. It presents characteristics of the cryptocurrencies that distinguishes them from traditional asset classes, as well as an introductory taxonomy for them. It also provides a thorough presentation of the technical prerequisites necessary to understand the work presented in subsequent chapters.

Chapter 3 presents the development of a novel index that provides investors with exposure to cryptoassets and physical gold, capitalizing on their unique characteristics: the high volatility of cryptoassets, the low volatility of gold, and their lack of correlation. This combination results in a reduction of price instability while increasing the average return per unit of volatility. The risk parity theory is extended to a Weighted Risk Contribution (WRC) approach, which proves to be a refined method for adjusting the index's exposure to the two asset classes, with moderate turnover and thus reduced operating costs. Additionally, the proposed framework considers various events exclusive to the cryptoasset domain, such as hard forks and airdrops, and devises appropriate policies to address them. This comprehensive approach ultimately culminates in the creation of an investable product with distinct features that render it a unique investment opportunity.

Chapter 4 discusses a comprehensive stress testing methodology and scenario-based risk management framework that is appropriate for assessing diversified portfolios. The approach combines univariate modelling of risk factors using ARMA and GJR-GARCH processes, Extreme Value Theory for extreme outcomes, and copulas for dependence structures and generates plausibility-constrained scenarios. The framework is then applied directly to the proposed index of chapter 3 and ultimately demonstrates the effectiveness of the Weighted Risk Contribution mechanism in mitigating risk, showcasing a superior risk-return profile compared to traditional market-cap-weighted cryptoasset indices. The methodology can be adapted for various risk factor shocks and potentially serve as a forward-looking portfolio optimization approach.

Chapter 5 proposes a method for market regime identification by utilizing Gaussian Hidden Markov Models (HMM) for intermediate trend-related states and Markov-switching GARCH models for volatility-related states. The two approaches in combination can be used to generate realistic simulated price paths that follow the market's cyclical patterns, switching between different regimes. It is shown that the simulation framework can be used for performance assessment purposes - utilising the Omega ratio metric - to ultimately evaluate a portfolio's suitability for investors with different risk tolerances and return targets. It is finally demonstrated that the described methodology can be incorporated in the index design process and the results further confirm the superiority of the WRC approach for the cryptoasset space.

Chapter 6 examines the diversification properties of commodities for cryptoasset investors and further proposes extending the original index in the commodities space. This is performed through the utilisation of mean-variance spanning tests which quantify the impact of adding constituents to a portfolio. The results reveal a significant shift in the efficient frontier for both global minimum variance and tangency portfolios upon the addition of physical gold and the inclusion of a broader commodity basket further confirms a statistically significant improvement, primarily through a shift in the tangency portfolio. Additionally, this chapter supplements the mean-variance spanning results with a Dynamic Conditional Correlation GARCH simulation specification, in order to compare the performance of the original and modified indices and their components in terms of risk metrics.

1.2 Research Motivation

Our work is motivated by the rapid emergence of cryptoassets as significant components of investment portfolios which calls for a deeper understanding of their characteristics and implications for financial risk management. With this in mind, the central theme of the thesis revolves around the challenges of integrating cryptoassets with traditional investment strategies and the developing robust methods to mitigate associated risks. We aim to provide concrete insights into the management and optimization of cryptoasset-inclusive portfolios, in a way that bridges the gap between traditional financial methods and the emerging field of cryptoassets. The research presented in this thesis is driven by four key points of motivation, summarised as follows:

1. **The Quest for Diversification:** The primary motivation of this thesis centers around the pursuit of diversification in investment portfolios through the inclusion of cryptoassets. With their distinct characteristics, particularly their low correlation with traditional asset classes, we hypothesize that cryptoassets offer unique opportunities to enhance portfolio diversification. Given the absence of risk-mitigating, cryptoasset-inclusive structured products at the time of writing this thesis, our initial aim is to introduce simple, yet effective, novel low-volatility indices that blend traditional investments with a selection of cryptoassets.
2. **Stress Testing in Post-Crisis Financial Systems:** The next component of the work presented delves into the realm of stress testing, a critical tool in financial risk management that gained prominence following the 2007 financial crisis. Our motivation stems from two key considerations: (i) risk management is a vital component in the development of any investment strategy and (ii) it represents an under-researched field in the context of cryptoasset portfolios as of the time this thesis was being developed.
3. **The Challenge of Market Regime Adaptation:** An additional motivation for this thesis arises from the challenge of identifying market regimes and assessing their impact on investment strategies. Driven by the lack of relevant research at the time of composing this thesis, we hypothesize the existence of several market regimes, each with distinct risk-performance characteristics. Our aims are twofold: (i) to uncover high-risk market states within the context of cryptoasset portfolios, and (ii) to evaluate the effectiveness of diversification strategies under various market conditions.
4. **Integration with Traditional Asset Classes:** A final point of motivation revolves around exploring the interplay between cryptoassets and traditional asset classes, especially commodities. Considering the scarcity of available relevant research, our goals are twofold: (i) to highlight the benefits and challenges of diversifying multi-asset portfolios with cryptoassets, and (ii) to determine the optimal balance between cryptoassets and conventional investments in order to meet a variety of investor objectives.

1.3 Contributions

The contributions of this thesis are summarised below:

Weighted Risk Contribution The first contribution of this thesis is the proposal of the Weighted Risk Contribution (WRC) allocation scheme, as a generalisation of the equal risk contribution portfolios. Ultimately we find that, in the context of crypto-based index solutions, the WRC allocation has historically proven to be more effective in terms of Sharpe Ratio than several alternative asset allocation strategies including Shannon's Demon, market capitalisation, equally weighted and equal risk contribution portfolios.

Digital Asset Indices The research and experimentation conducted within this thesis, eventually led to the release of the CoinShares Gold & Cryptoassets Index (CGCI), the first EU Benchmark Regulations (EU BMR) compliant index for the digital asset industry that combines cryptoassets and gold. In addition to this, two more index products have been released, the CoinShares Equally Weighted Crypto Index (CECI) and the CoinShares Gold and Bitcoin Index (CGBI). The former has been designed to provide a diversified exposure to the five most liquid cryptoassets, offering a way to replicate the original index's crypto-basket composition, while the later is a modification of the original index, replacing the crypto-basket component with Bitcoin. All indices rebalance once a month on the first business day of each month and are currently accessible on Bloomberg Terminals and Refinitiv (previously Reuters).

Cryptoasset Price Dynamics This thesis also utilises a set of tools to model the evolution of cryptoasset prices. This is done from a financial time series modeling perspective, employing various Autoregressive Moving Average (ARMA), Generalized Autoregressive Conditional Heteroskedasticity (GARCH), Hidden Markov Models (HMM), and regime-switching GARCH models to capture complex dynamics of pricing data. ARMA models are used to describe the autocorrelation structure in stationary time series, capturing mean reversion and short-term trends. GARCH models address the volatility clustering and conditional heteroskedasticity that is observed in returns time series, allowing for the estimation of time-varying volatility. HMMs enable the modeling of latent states underlying the observed data and provide insights into potential market regime changes and hidden processes affecting cryptoasset prices. Regime-switching GARCH models combine the GARCH framework with a Markov-switching mechanism, capturing shifts in the volatility of financial time series, thereby accounting for abrupt changes in market conditions. The aforementioned models help to advance the understanding of the crypto-market behavior and ultimately foster the growth and integration of cryptoassets into the broader financial ecosystem.

Multivariate Modeling & Relationship with Traditional Asset Classes An additional contribution of this thesis is the application of multivariate time series modeling techniques that allow us to unveil the relationship between cryptoassets and traditional asset classes. We demonstrate how copulas can be employed to capture the dependence structure between multiple financial time series while accounting for their individual marginal distributions. In the realm of financial time series, where assets often exhibit non-linear relationships and tail dependence, we show that copulas offer a flexible and powerful approach to model these complex structures. We show that they facilitate a more accurate representation of the joint behavior of financial assets and that they are suitable for applications such as portfolio optimization, risk management, and financial stress testing. Finally, we demonstrate the above advantages in practice by applying them to the price time series of cryptoassets and commodities, revealing valuable insights into the dependence structure between the two asset classes.

Performance Evaluation & Stress Testing Frameworks An additional contribution of this thesis is the combination of all the aforementioned modeling techniques to create comprehensive performance evaluation and stress testing frameworks for cryptoasset-containing portfolios. Univariate models are used to generate observations of the mean returns and volatilities for each asset in the portfolio while the regime-switching GARCH and HMM models can help account for changes in the market dynamics and volatility across different regimes, adding more realism to the simulation process. Also, Extreme Value Theory (EVT) is applied to estimate the tails of the residual distributions, enabling a more accurate representation of extreme events and copulas are then employed to account the potential impact of correlations shocks. Once the proposed models are fitted and the dependencies among the assets are captured, we suggest Monte Carlo simulations to be performed, in order to generate a large number of possible future scenarios for the assets' returns. The simulated paths are used to estimate the portfolio's performance under various market conditions and to calculate appropriate risk measures. Additionally, we demonstrate the importance of Mean-Variance spanning tests as a a statistical framework to evaluate the diversification benefits of adding new assets or asset classes to an existing investment portfolio. By assessing the impact of these additions on the efficient frontier, the tests help investors determine whether the new assets significantly improve the risk-return trade-off. The above concepts provide a comprehensive view of the asymptotic performance of the portfolio, enabling investors to make informed decisions regarding their investment strategies and risk management practices.

Chapter 2

Background

Blockchain technology emerged as a revolutionary innovation in the financial sector, offering a decentralized, distributed digital ledger for secure and transparent transaction recording. The technology gained popularity due to its ability to provide high levels of transparency and security, as well as its decentralized nature, which eliminates the need for intermediaries. Bitcoin, the first and most popular cryptocurrency, was created to serve as a decentralized digital currency without the need for central authorities or intermediaries. The cryptocurrency market has experienced numerous boom and bust cycles since Bitcoin's inception, driven by market speculation, media hype, and regulatory developments. Despite facing challenges, such as market volatility and high-profile exchange failures, the core blockchain technology remains resilient. With the 2008 financial crisis further prompting a shift towards alternative investments, cryptoassets are gaining popularity, as they offer opportunities for risk balance and portfolio diversification. Backed by blockchain technology, cryptoassets provide unique opportunities for investors, as they are independent from traditional financial systems and can act as a hedge against market uncertainties and currency devaluation. However, the volatile nature of digital assets and the rapidly evolving market landscape necessitate the implementation of robust risk and portfolio management techniques. By employing such strategies, investors can better navigate the complex and dynamic crypto-ecosystem, mitigating losses and capitalizing on promising opportunities.

This chapter introduces the unique characteristics of the cryptoasset class and highlights the importance of diversification and proper risk management in the portfolio contruction process.

2.1 Cryptocurrencies as Alternative Assets

2.1.1 A Brief History of Cryptocurrency and Blockchain Technology

Blockchain technology and Bitcoin are two concepts that are related and are now considered revolutionary technologies in the financial world. While the two terms are the most commonly cited when referring to the cryptoassets, it is important to distinguish between the two. The term "Blockchain" refers to a decentralized, distributed digital ledger that records transactions in a secure and transparent manner. Each node in the network has a copy of the entire blockchain and transactions are validated and added to the blockchain through a consensus mechanism. It is therefore a digital record-keeping system that is spread across a network of computers making it difficult to tamper with or corrupt. Each transaction is recorded in a block which is linked to the previous block forming a chain of blocks, hence the term "blockchain" [130, 146]. When a new transaction is initiated it is broadcast to all nodes in the network and the nodes validate the transaction using a consensus mechanism. After the transaction validation, the transaction is grouped with other transactions to form a new block and the block is added to the blockchain. To ensure the integrity and security of the blockchain, each block contains a cryptographic hash of the previous block. This makes it virtually impossible to alter any previous transaction on the blockchain without invalidating the entire chain. The technology has gained significant popularity due to its ability to provide a high degree of transparency and security [133].

Another very important reason for its popularity is its decentralized nature which eliminates the need for intermediaries [103]. This decentralized aspect has become popular among users due to its enhanced security, as it lacks a single point of failure, making it more resistant to hacking and data breaches. Unlike traditional financial systems where transactions are processed and verified by a central authority, the blockchain network is peer-to-peer meaning that transactions are validated by the participants on the network [31]. It fosters transparency and trust, as all transactions are recorded on a public ledger. It ensures data integrity and reduces reliance on intermediaries like banks, which can lower transaction costs and speed up processes. Furthermore, the immutability of blockchain records guarantees the integrity of transaction histories, essential for auditing and compliance.

Blockchain technology as we currently know it was created for the most popular cryptocurrency so far, named bitcoin. The emergence of digital currency dates back to 1983 when David Chaum, an American cryptographer, presented a preliminary version of anonymous cryptographic electronic money in a conference paper [33]. The primary objective of the concept was to create a decentralized currency that could be transferred without the need for central authorities such as banks. Chaum subsequently advanced this idea and created a proto-cryptocurrency named Digicash in 1995. To utilize this currency users had to install software that would withdraw funds from their bank accounts and transmit encrypted keys to the recipient before the funds could be transferred.

Nick Szabo's creation of Bit Gold in 1998 [132] is regarded by many as the direct predecessor of Bitcoin [107]. Bit Gold relied on participants dedicating their computer power to solve cryptographic puzzles with successful solvers receiving rewards [131]. Szabo's work combined with Chaum's earlier concept created something similar to Bitcoin but without a resolution to the issue of double-spending where digital data could be duplicated and reused without the involvement of a central authority.

A decade later in 2008 an individual or group using the pseudonym Satoshi Nakamoto published a white paper titled "Bitcoin - A Peer to Peer Electronic Cash System" [106] marking the birth of bitcoin and other cryptocurrencies. This groundbreaking event marked the beginning of a new era for decentralized digital currencies, which operate without central authorities or intermediaries to handle transactions. The Bitcoin project was registered on SourceForge.net [126], a platform dedicated to supporting open-source software development. It was evident at this point that Bitcoin was not intended to integrate seamlessly into existing governmental and financial systems; instead it aimed to establish an alternative system, free from hierarchical control and governed by a decentralized community [29]. Decentralized autonomy also played a crucial role in the Internet's early days where each network node functioned as an autonomous agent interacting with other agents through shared protocols [1].

From the inception of Bitcoin as a public network Satoshi demonstrated a keen awareness of the global financial system's shortcomings. The first data entry on Bitcoin's blockchain contained the message: "The Times 03/Jan/2009 Chancellor on brink of second bailout of banks," referring to an article discussing the potential need for the U.K. to support additional banks to remain solvent [66]. This aspect of the blockchain has since emerged as one of the most potent applications of the technology, embedding unalterable and transparent data that cannot be erased from digital history and is accessible to everyone [29]. The initial stages of Bitcoin were marked by exploration and progress with the community striving to fine-tune the technology and develop novel applications [110]. Despite initial doubts and opposition from traditional financial institutions and regulators, Bitcoin's popularity and adoption expanded swiftly. Presently, Bitcoin and other cryptocurrencies are extensively employed for transactions and investments while the underlying technology continues to advance and mature [133]. Currently, in the realm of terminology, "Bitcoin" is generally used to denote the Bitcoin network or the entire system. This term is applied when talking about the underlying technology, including the blockchain architecture, the Bitcoin protocol, or the comprehensive ecosystem that facilitates the functioning of this digital currency. On the other hand, "bitcoin" written with a lowercase "b" is specifically used in reference to the currency. This usage is common when talking about transactions, ownership, or the economics of the currency. This distinction helps in differentiating between the technological aspect (Bitcoin) and the financial or currency aspect (bitcoin).

Initially Bitcoin was the dominant use case but as the technology matured, developers started ex-

ploring other use cases. One example is the creation of Ethereum [30], a decentralized, open-source blockchain-based platform that was created to enable developers to build decentralized applications (dApps) with smart contract functionality. It was launched in 2015 by Vitalik Buterin and has since become one of the most popular blockchain platforms second only to Bitcoin. The Ethereum platform was developed using a new blockchain protocol that included a programming language called Solidity [142]. It enabled developers to write smart contracts which are self-executing agreements where the conditions of the deal between the buyer and seller are explicitly embedded in lines of code. Smart contracts are executed on the blockchain and cannot be altered once they have been deployed, ensuring that they are tamper-proof and transparent. One of the key advantages of Ethereum is its ability to support the creation of dApp, which are applications that run on a decentralized network of computers rather than on a central server. Ethereum dApps can be used for a wide range of purposes including financial services, gaming, social networks and more. Additionally, the platform has its own cryptocurrency called Ether (ETH) which is used to pay for transactions and to motivate developers to build on it.

One of the primary differences between Ethereum and Bitcoin is their consensus mechanisms. Bitcoin uses the Proof of Work (PoW) consensus mechanism which involves miners competing to solve complex mathematical problems to validate transactions and add new blocks to the blockchain. The first miner to solve the problem is rewarded with newly minted bitcoin. On the other hand, Ethereum has transitioned to the Proof of Stake (PoS) consensus mechanism. In PoS validators are chosen to validate transactions based on the amount of cryptocurrency they hold and are willing to lock up as collateral. Validators are rewarded with newly minted Ethereum for their service and their stake acts as a deterrent against malicious behavior as they would lose their collateral in the event of an attack. PoS is known for its energy efficiency and accessibility as it requires much less energy and specialized hardware compared to PoW [80].

Overall, the adoption of blockchain technology in the recent years has been slow but steady. Its complexity can be a significant barrier, especially for businesses lacking in-house blockchain expertise. Another very important aspect is the regulatory uncertainty and lack of clear legal frameworks in many regions, which create hesitancy among organizations to fully commit to its adoption. Additionally, concerns about scalability, energy consumption (particularly with proof-of-work models), and integration with existing systems pose challenges. Lastly, the relatively young stage of blockchain technology means there is a limited number of proven use cases, leading to cautious adoption as organizations and regulators seek to understand its implications and potential fully. Nevertheless, today it is being used in various industries [133] including finance, healthcare, real estate and supply chain management. The technology provides a secure and transparent way of recording transactions and storing data, which reduces the risk of fraud and corruption. Blockchain technology also enables the creation of decentralized applications that can operate without the need for intermediaries providing greater control and autonomy to users.

2.1.2 Evolution of the Cryptoasset Market

The cryptocurrency market has experienced several cycles of boom and bust since the introduction of bitcoin. The market cycles are characterized by periods of rapid price increases followed by significant price drops and are typically driven by a combination of market speculation, media hype and regulatory developments [3].

An early major cryptocurrency market cycle was initiated in 2011 with the escalation of bitcoin's price from less than $1 to $30 followed by a decline to approximately $2 [29]. During this phase, bitcoin remained the predominant cryptocurrency with the highest market capitalization and trading volume. Alternative cryptocurrencies (altcoins) were still in their nascent stage and had limited adoption. Mt. Gox was the principal bitcoin exchange responsible for a substantial percentage of global bitcoin trading [31]. However it experienced numerous security breaches and hacking incidents, culminating in its bankruptcy in 2014. This era was also marked by the operation of Silk Road, an online platform for illicit drug and goods trading that employed bitcoin as a mode of payment, until its closure by law enforcement in 2013 [98] thereby impacting bitcoin's credibility due to its potential to facilitate decentralized and anonymous transactions. Additionally, litecoin [89] one of the first altcoins that debuted in October 2011 gained traction as a faster and more scalable alternative to bitcoin and became the second-largest cryptocurrency in terms of market capitalization. At the same time various corporations such as WordPress, Reddit and Expedia began accepting bitcoin as a form of payment [110] boosting cryptocurrencies' awareness and adoption. However, both bitcoin and altcoins' prices demonstrated substantial volatility with sharp fluctuations over short intervals. For example in April 2013 bitcoin's price briefly escalated from $20 to over $260 before tumbling to approximately $60 [37]. Overall this period witnessed Bitcoin's dominance, the inception of altcoins and the increasing mainstream acceptance of cryptocurrencies despite notable security and volatility challenges that necessitated regulatory interventions.

Between 2013 and 2014 the market experienced significant evolution accompanied by the emergence of new altcoins the development of new use cases for cryptocurrencies as well as the increasing attention of regulatory bodies. The rise of altcoins during this period was fueled by several factors, including the growing dissatisfaction with Bitcoin's limitations particularly its transaction times and scalability [133]. Altcoins promised to offer better solutions to these problems attracting investors and traders who were looking for alternatives to Bitcoin and were designed initially to be more accessible to the average person with lower transaction fees and easier mining algorithms. The altcoin boom also coincided with a surge of interest in cryptocurrencies from mainstream investors [103], with many of them seeking to diversify their portfolios beyond bitcoin. Another significant development during this period was the emergence of initial coin offerings (ICOs) which allowed companies to raise funds by issuing their own digital tokens or coins [147]. The concept quickly gained popularity with numerous ICOs being launched in subsequent years. The altcoin development at the time was of course not without its challenge as many were created with little

or no oversight or regulation, leading to a proliferation of scams and fraudulent projects. Additionally, the rapid growth of altcoins led to increased volatility and instability in the cryptocurrency market [107] which was experiencing dramatic price swings over short periods of time.

The period between 2014 and 2016 saw the establishment of a larger number of altcoins, albeit in a more mature and stable market environment. This comes in contrast with the previously mentioned period, when the market was still in its infancy, with only a handful of established altcoins and a highly volatile environment. Tether (USDT), the first stablecoin, was also launched in October 2014 [97]. Being pegged to the U.S. dollar, it aimed to provide a stable alternative to volatile cryptocurrencies and facilitate digital transactions, while being tied to traditional fiat currencies. The altcoin boom of 2014-2016 was also marked by the emergence of new use cases for blockchain technology, particularly in the area of decentralized applications. Ethereum [101], launched in 2015, was the key driver of this trend and provided a platform for developers to build and launch decentralized applications on its blockchain. This period was also accompanied by increased regulatory oversight and scrutiny [112], as governments and regulators around the world began to take notice of the growing cryptocurrency market. This led to a more stable and legitimate market environment, as investors became more confident in the security and reliability of altcoins.

Another notable cycle occurred in 2017, when the cryptocurrency market experienced an unprecedented surge in prices. The beginning of this period saw the market cap of all cryptocurrencies at around $18 billion and by the end of the year, it had soared to over $600 billion [36]. This massive increase was driven by a surge in the popularity of ICOs as a fundraising method for new projects. ICOs raised billions of dollars in the same year and the market was flooded with projects, many of which promised to revolutionize various industries using blockchain technology. However, the lack of regulation and oversight also led to a number of scams and projects that failed to deliver on their promises. Meanwhile, bitcoin started the year with a market dominance of around 85%, but by the end of 2017, its dominance had dropped to around 38%. This was largely due to the rise of new cryptocurrencies and the ongoing scaling debate within the Bitcoin community, which eventually led to the creation of Bitcoin Cash (BCH) in August 2017 through a hard fork. Ethereum also gained significant traction in 2017, with its market cap increasing from around $700 million at the start of the year to over $70 billion by the end of it. Ethereum's native token, Ether (ETH), became the second-largest cryptocurrency by market cap and its growth was fueled by the platform's support for smart contracts and the use of its ERC20 token standard for the majority of ICOs. Throughout the same year, cryptocurrencies gained more mainstream attention, with major financial institutions expressing interest in the sector. Bitcoin futures were also launched by the Chicago Mercantile Exchange (CME) in December 2017 [58], further legitimizing the asset class. In December 2017, the cryptocurrency market reached its peak, with bitcoin's price soaring to nearly $20,000. However, this rapid growth was followed by a sharp correction in early 2018, as the market experienced a significant pullback.

The market continued to experience significant developments and shifts during 2018-2020. The year of 2018, often referred to as the "crypto winter", was marked by a decline in market enthusiasm, reduced ICO activity and an increased focus on regulatory compliance. Following the unprecedented bull run of 2017, Bitcoin's price fell from nearly $20,000 in December 2017 to around $3,000 by the end of 2018. As market volatility remained high, stablecoins emerged as an important component of the ecosystem. Tether (USDT) continued to dominate the stablecoin market, but other stablecoins also gained traction. After the prolonged "crypto winter" of 2018, the market began to show signs of recovery in 2019, with Bitcoin's price reaching over $13,000 in June before experiencing another correction. The market continued to recover throughout 2020, with Bitcoin's price climbing back above $10,000 and establishing a more stable support level. Decentralized Finance (DeFi) also began to emerge as a significant trend in late 2019, gaining momentum in 2020. DeFi platforms aimed to provide financial services, such as lending, borrowing and trading in a decentralized manner using blockchain technology. DeFi's growth continued in 2020, fueled by the rise of decentralized exchanges (DEXs) and innovative financial products like yield farming and liquidity mining. Meanwhile, despite the occasional market downturns, there was also a growing interest from institutional investors and an expansion of market infrastructure. Companies like Fidelity [52], Bakkt [6] and Grayscale [57] started offering cryptocurrency-related products and services, while traditional financial institutions such as JPMorgan and Goldman Sachs began exploring the market more seriously [124, 125]. These developments signaled a maturing market and increased acceptance of cryptocurrencies as an alternative asset class.

In 2021, the market experienced a strong bull run, with Bitcoin reaching an all-time high of around $64,000 in April before facing a correction in May. Ethereum and other altcoins also experienced significant price increases, with many reaching new all-time highs. Institutional adoption of cryptocurrencies also grew considerably, with major companies like Tesla making significant investments in Bitcoin [88] and institutional investors and hedge funds increasingly allocating portions of their portfolios to the digital asset class. Non-fungible tokens (NFTs) also became a mainstream phenomenon in 2021 [67], with digital artists, musicians and content creators using NFTs to monetize their work. The DeFi sector continued to grow and the total value locked (TVL) grew exponentially, reflecting its increasing popularity. At the same time, the market experienced additional regulatory developments and various jurisdictions, such as the European Union and the United States, tightened Anti-Money Laundering (AML) and Combating the Financing of Terrorism (CFT) requirements for cryptocurrency exchanges and other related businesses [141]. Additionally, in the United States, the Internal Revenue Service (IRS) intensified its focus on cryptocurrency tax compliance. Moreover, the U.S. Securities and Exchange Commission (SEC) continued to scrutinize cryptocurrency projects for compliance with securities laws [119]. The SEC also indicated its intention to regulate cryptocurrency exchanges and digital asset securities, with the aim of providing investor protection and ensuring market integrity. In December of the same year, the U.S. President's Working Group on Financial Markets released a report outlining recommendations for stablecoin regu-

lation, emphasizing the need for stablecoin issuers to be subject to federal banking oversight [137]. Additionally, many central banks explored the development and potential implementation of Central Bank Digital Currencies (CBDCs), digital versions of their national currencies [70].

In contrast, the year 2022 proved challenging for global markets, with the U.S. stock market, bond market and crypto markets experiencing significant declines. In response to inflation, central banks implemented higher interest rates, consequently diminishing investors' appetite for risk and prompting them to avoid speculative asset classes, including cryptoassets. Despite the initial flourishing of cryptoassets due to low interest rates and a robust economy, the market encountered a severe sell-off as central banks altered their course. Projects such as Terra [117] experienced a collapse and overleveraged centralized finance (CeFi) institutions, including Celsius Network and Voyager Digital, were compelled to file for bankruptcy protection [114]. By the end of the summer, the cryptocurrency market displayed signs of stabilization. Regrettably, this renewed confidence proved to be short-lived, as shocking disclosures about FTX's financial instability triggered a market downfall [120]. Despite the challenges, the fundamental blockchain technology remained intact, exemplified by Ethereum's triumphant transition to a proof-of-stake model [56]. Nevertheless, the failures and bankruptcies in 2022 have prompted calls for increased regulation and oversight in the crypto space to protect investors from fraud, theft and irresponsible lending practices.

Overall, throughout the years the cryptocurrency market has undergone numerous cycles of growth and decline since the inception of Bitcoin. Each phase has been marked by distinct developments and challenges, ranging from technological innovations, regulatory advancements and increasing mainstream adoption to security breaches, market volatility and high-profile failures. Overall, the events of 2022 have highlighted the need for enhanced regulatory oversight to ensure the long-term stability and sustainability of the cryptocurrency market, while continuing to foster innovation and adoption. Nevertheless, despite the recent market turbulence, the core blockchain technology remains resilient and continues to showcase its potential to revolutionize industries.

2.1.3 Cryptocurrencies as Alternative Assets and Taxonomy of Cryptoassets

The 2008 financial crisis prompted a reevaluation of investment strategies by financial advisors and wealth managers, who began considering alternative investment vehicles beyond traditional stocks and bonds. This shift was inspired by the remarkable performance of hedge funds during the crisis, with figures such as John Paulson and James Simons achieving exceptional returns [29, 148]. Overall, defining "alternative investment" is challenging, as definitions tend to change alongside the evolving investment trends. Alternative investments can be generically described as assets with unique economic and value-based characteristics that diverge from primary investments like stocks, bonds or cash. Their primary use-case for investors is to perform independently from traditional asset classes stocks and bonds, therefore providing risk balance during times of financial

turmoil. Considering the above, cryptoassets can be classified as alternative investments, likely to be increasingly incorporated into mainstream retail portfolios.

A unique feature that distinguishes cryptoassets from other asset classes is the underlying technology, as it was described in the previous sections. By investing in cryptoassets, investors can gain exposure to the growth potential of blockchain technology, which is often being hailed as a groundbreaking innovation with the potential to transform industries beyond finance [133]. Crypto-investors have the opportunity to yield significant returns as the technology matures and gains widespread adoption. Additionally, comprised of distributed and cryptographically secured digital ledgers, cryptoassets can be created, stored and transferred without the need for a central authority. This decentralization makes them fundamentally different from traditional assets, as they do not rely on central banks, governments, or other institutions for their value or operation. Additionally, cryptoassets evolve independently of traditional financial systems [144], which means their value is not tied to the performance of economies, interest rates, or inflation. This feature makes them a viable hedge against market uncertainties, currency devaluation and geopolitical risks. Independence from traditional financial systems not only provides investors with unique opportunities but also contributes to the overall diversification of their investment portfolios.

The landscape of digital assets is rapidly evolving, therefore it is beneficial to present a classification based on their underlying properties and intended use cases. By providing an organized framework, this can help participants in the digital asset ecosystem to better understand, evaluate and manage their exposure to this alternative asset class. Below is a categorization example:

Currency and Payment Tokens Currency and payment tokens are designed primarily to serve as a medium of exchange, unit of account, or store of value. These cryptoassets aim to facilitate the transfer of value between users, often with the goal of offering faster, cheaper and more secure transactions compared to traditional financial systems.

Currency and payment tokens can be categorized as follows:

1. Cryptocurrencies: These are digital or virtual currencies that employ cryptographic techniques to secure transactions and control the creation of new units. Bitcoin (BTC) is the most well-known example.
2. Stablecoins: These are a specific type of cryptocurrency designed to minimize price volatility by pegging their value to a reserve of assets, which could include fiat currencies, commodities, or other cryptocurrencies. Examples include Tether (USDT) and USD Coin (USDC).

Utility Tokens Utility tokens grant holders access to a particular service or functionality within a blockchain-based platform. These tokens are often used to incentivize participation in the network, facilitate transactions, or enable access to various features.

Utility tokens can be categorized as follows:

1. Network Tokens: These tokens are necessary for the proper functioning of a blockchain network and are often used to pay for transaction fees or access specific services. Examples include Ethereum's Ether (ETH), which is used to pay for gas fees on the Ethereum network and Binance Coin (BNB), used on the Binance Smart Chain.
2. Governance Tokens: These tokens allow holders to participate in the decision-making process of a decentralized organization, including voting on proposals, updates and changes to the platform. Examples include MakerDAO's Maker (MKR) and Compound's COMP tokens.

Asset-Backed Tokens Asset-backed tokens represent ownership or a claim on an underlying asset, which can range from physical commodities to financial instruments. These tokens are often designed to track the value of the underlying asset and can be traded on secondary markets. An example is PAX Gold (PAXG), a token backed by physical gold.

Non-Fungible Tokens (NFTs) NFTs are unique digital assets that represent ownership of a specific item or piece of content. Unlike other cryptoassets, NFTs are not interchangeable, as each token is distinct and indivisible. NFTs have gained popularity in various sectors, such as art, collectibles, gaming and virtual real estate.

For the remainder of this thesis we will make use of the term cryptoassets, a broad term that encompasses all assets using cryptographic technology, including cryptocurrencies, security tokens, utility tokens, and other types of tokenized assets. It is an umbrella term that refers to digital assets secured by cryptography.

2.2 Introduction to Basic Financial Concepts

2.2.1 Financial Index Products

A financial index is a mathematical construct that tracks the performance of a group of financial assets, such as stocks, bonds, commodities, or cryptocurrencies [72]. It represents a portfolio of these assets and serves as a benchmark to gauge the market's overall performance or a specific segment within it. Index products are financial instruments that track the performance of an underlying index, allowing investors to gain exposure to a diversified portfolio without directly purchasing each asset within the index.

There exist several types of index products and some examples include the following:

1. Index Funds: Index funds are passively managed investment funds designed to track the performance of a specific index. They aim to replicate the index's returns by holding the same assets in the same proportions as the index [72].
2. Exchange-Traded Funds (ETFs): ETFs are a type of investment fund and exchange-traded product, which means they are traded on stock exchanges. They typically track an index, offering investors a cost-effective way to gain exposure to a diversified portfolio [71].
3. Index Futures: Index futures are standardized contracts to buy or sell the value of an index at a specific future date. They allow investors to hedge against market risk or speculate on market movements. [73]
4. Index Options: Index options are financial derivatives that give the holder the right, but not the obligation, to buy or sell an index at a specified price on or before a specified date. They can be used for hedging, speculation, or income generation [74].
5. Index-linked Bonds: These are bonds whose interest payments and principal repayment are linked to the performance of a specific index. They can provide protection against inflation or offer exposure to specific market segments [75].

Over the years, index products have become essential in the traditional financial sector, providing investors an accessible, transparent and cost-effective method to invest in various assets [16]. With the growth of the cryptoasset market and increased interest from different types of investors, the demand for index products has risen significantly [69]. Cryptocurrencies' unique properties [92], such as decentralization, borderless transactions and programmable money, have led to the development of diverse index products catering to investors' needs. Given the distinct nature of the digital asset space and the opportunities arising from proper diversification and effective risk management, the upcoming chapters will present a methodological framework for creating, evaluating and monitoring cryptoasset indices. The approach will involve two asset classes, cryptoassets and commodities and will aim to optimize the resulting product's structure and enhance the understanding of its performance through various market cycles.

2.2.2 Diversification and Risk Management: A Synergistic Approach to Enhancing Portfolio Performance

Portfolio management is an essential component of the investment process that aims to assist investors achieve their financial objectives [19]. The primary functions of portfolio management include asset allocation, risk management and performance evaluation. Asset allocation refers to the process of determining the optimal mix of asset classes within a portfolio, based on the investor's unique characteristics, such as risk tolerance profile, investment horizon and financial goals. Portfolio management involves assessing and managing various types of risk, such as market, credit and liquidity risk and risk management refers to sets of tools that can assist investors in (i) minimising potential losses and (ii) maintaining portfolio stability. Performance evaluation involves monitoring the overall portfolio, comparing its performance against a set of established benchmarks and making necessary adjustments to remain aligned with investment objectives.

A key benefit of portfolio diversification is mitigating unsystematic risk, associated with individual assets or industries [127]. By allocating funds across various asset classes, industries and geographies, investors can protect themselves from company-specific or industry-specific events that adversely affect their portfolio. Additionally, it allows investors to participate in the growth potential of asset classes, which can contribute to a more stable and consistent growth trajectory over time. This approach helps investors capitalize on emerging trends and opportunities, which may lead to superior returns in the long run. In this context, cryptocurrencies can be considered a component of a well-diversified portfolio [28], albeit with certain caveats, as presented in the next sections. Finally, in terms of risk metrics, a well-diversified portfolio can deliver better risk-adjusted returns, as measured by the Sharpe ratio [122]. Therefore, for a given level of risk, a diversified portfolio is expected to provide higher returns than a concentrated one.

In regards to asset allocation methods, it is a fundamental investment principle aimed at minimizing risk and maximizing returns by allocating assets across a variety of investment types, industries and geographic regions. It is based on the premise that spreading investments across a wide range of asset classes, investors can mitigate unsystematic risk, reduce the impact of market fluctuations and enhance long-term growth potential. The concept can be traced back to the Modern Portfolio Theory (MPT), pioneered by Harry Markowitz in the 1950s [99]. MPT posits that investors can achieve an optimal risk-return trade-off by allocating their capital across a diverse set of assets with varying degrees of risk and return. Central to this theory is the idea that asset prices do not move in perfect correlation, which allows for the reduction of risk through diversification [47]. Moreover, MPT introduces the concept of efficient frontier, which represents the optimal set of portfolios with the highest expected return for a given level of risk.

More specifically, in Markowitz' theory of portfolio selection, the mean-variance optimization (MVO) approach provides investors with an effective mechanism of forming portfolios that trade off risk and expected returns. The optimization problem setting is constituted of $N \geq 2$ assets, denoted

as $S_1, S_2, \ldots, S_N$, with μ_i and s_i representing the expected return and standard deviation of S_i respectively and ρ_{ij} denoting the correlation coefficient of the returns of assets S_i and S_j for $i \neq j$. The $N \times N$ symmetric covariance matrix of returns is defined as $\Sigma = (\sigma_{ij})$ where $\sigma_{ij} = \rho_{ij}\sigma_i\sigma_j, i \neq j$ and $\sigma_{ij} = \sigma_i^2, i = j$. If x_i is the portion of the total fund invested in S_i, the expected return and variance of the constructed portfolio can be defined as $E[x] = \mu^T x$ and $Var[x] = x^T\Sigma x$, where $\mu = [\mu_1, \mu_2, \ldots, \mu_N]^T$ and $x = [x_1, x_2, \ldots, x_N]^T$. The set of satisfactory portfolios are represented as $X = \{x : Ax = b, Cx \geq d\}$, where A is an $m \times N$ matrix, b an m-dimensional vector, C a $p \times N$ matrix and d a p-dimensional vector. The main constraint of the asset weights is $\sum_{i=1}^{N} x_i = 1$ but further constraints such as maximum and minimum allocations or short-sale allowance can be assumed for X.

The set of efficient portfolios contains all feasible combinations of x_i values that maximize expected returns among all portfolios of given variance or equivalently, all combinations that minimize variance given a specific level of expected returns. This set constitutes the efficient frontier and is typically represented by a two-dimensional parabolic curve (referred to as the "Markowitz Bullet") along the upper edge of the scatter plot of all possible combinations in a risk-expected return space. The described MVO problem is typically formulated as a quadratic optimization problem:

$$\begin{aligned} \min_x \frac{1}{2} x^T \Sigma x \\ \mu^T x \geq R \\ Ax = b \\ Cx \geq d. \end{aligned} \tag{2.1}$$

The main limitation of the mean-variance portfolios is their sensitivity of the optimization problem solution to small changes of the input variables. Investors prefer heuristic, replicable methodologies that are not dependant on forward-looking approximations of individual asset returns. Some popular modifications include Minimum Variance and equally weighted approaches, as introduced by Benartzi and Thaler, 2001 [13]. Drawbacks of the former include large concentrations of low-risk components while the latter fail to take into account volatility behavior and asset cross-correlations.

When it comes to Quantitative Risk Management (QRM), it involves mathematical models and statistical techniques to measure, monitor and control various types of risk inherent in financial investments. In their work McNeil et al. [100] discuss the importance of investing in QRM and the various perspectives from which the concept can be approached. It emphasizes the significance of risk management in maintaining the smooth functioning of banking and insurance systems and the stability of the financial system as a whole and highlight how proper financial risk management can increase the value of a corporation and shareholder value. Broadly speaking, risk management

serves as a firm-wide language for discussing and pricing risk, addressing management and stakeholders' concerns about institutional solvency and profitability. QRM involves quantifying various risks, including credit, market, operational, insurance, liquidity, reputational, strategic or business risks. It further includes determining the acceptable probability of default (solvency standard) for the institution, often using external benchmarks for credit risk. The choice of horizon should align with capital planning or business cycles.

Overall, portfolio diversification and proper risk management work hand in hand, creating a powerful approach, able to improve portfolio performance. This synergistic method recognizes the importance of spreading investments across a wide range of asset classes as a means to counterbalance the inherent risks and uncertainties within financial markets. By ensuring that the portfolio is well-diversified, investors attempt to minimize the negative effects of individual asset underperformance or market volatility on their overall investment value. At the same time, incorporating risk management strategies involves a meticulous evaluation of potential hazards and weak spots within the portfolio, empowering investors to pinpoint, assess and address the risks associated with their investment decisions. By embracing this holistic approach, in the next chapters we present the delicate balance between risk and return, applied specifically for the emerging cryptoaasets class, ultimately maximizing its prospects for strong, long-term portfolio performance in an unpredictable and constantly evolving financial and technological environment.

The subsequent sections of this chapter provide an essential overview of quantitative methods related to the concepts of diversification, portfolio, and risk management, as outlined in the literature, serving as prerequisite knowledge for the later chapters of this thesis.

2.3 Quantitative Methods in Finance

2.3.1 Stochastic Processes in Finance

2.3.1.1 Univariate Risk Factor Modeling: ARMA-GARCH Models

Following the definitions of McNeil et al. [100], the value of a given portfolio at time t can be denoted as V_t and determined by information available at time t. The value V_t can be modelled as a function of time and an d-dimensional random vector $\boldsymbol{X}_t = (X_{t,1}, \ldots, X_{t,d})'$, observable at time t and therefore expressed in the form of $V_t = f(t, \boldsymbol{X}_t)$, which is typically referred to as mapping of risks. The change in the value of the portfolio will be $\Delta V_{t+1} = V_{t+1} - V_t$, the loss is defined as $L_{t+1} = -\Delta V_{t+1}$ and its distribution is referred to as loss distribution. In this study, we will ultimately be concerned with the distribution of ΔV_{t+1}, termed as the Profit and Loss (P&L) distribution.

In an attempt to obtain the P&L distribution, one can begin with expressing the evolution of each risk factor individually as an autoregressive moving average (ARMA) process, which accounts for autocorrelation and aims to model the conditional mean. A general ARMA model of order p_1, q_1 (where p_1 and q_1 denote the number of lags that explain linear dependence with past observations and past error terms), with non-zero mean μ and white noise term ϵ_t, can be written as:

$$X_t = \mu_t + \epsilon_t = \mu + \sum_{i=1}^{p_1} \phi_i (X_{t-i} - \mu) + \sum_{j=1}^{q_1} \theta_j \epsilon_{t-j} + \epsilon_t \tag{2.2}$$

Additionally, it is important to consider some financial time series stylised fact, which reject conditional homoskedasticity and suggest that volatility is stochastic and forecastable. Generalised autoregressive conditional heteroskedasticity (GARCH) processes can adequately account for volatility clustering. We can expect the GARCH-corrected time series to produce filtered conditional residuals that are nearly independent and identically distributed sequences, a key fact to enable us to examine extreme events at the tails of the distributions in the following sections.

By definition, any process X_t that involves a stochastic part Z_t (white noise process) and a time-dependent standard deviation σ_t, follows a GARCH(p_2, q_2) model if it satisfies the equations:

$$X_t = \sigma_t Z_t, \quad \sigma_t^2 = \omega + \sum_{i=1}^{p_2} \alpha_i X_{t-i}^2 + \sum_{j=1}^{q_2} \beta_j \sigma_{t-j}^2$$

The described GARCH model is a symmetric one, meaning that positive and negative returns have identical influence on volatility. Empirical evidence suggests that positive innovations to volatility correlate with negative market information (and vice versa), a phenomenon also referred to as leverage effect, and that positive returns should cause less uncertainty [100]. Glosten, Jagannathan, and Runkle [55] propose a way to account for this asymmetry (GJR–GARCH) through mod-

elling the positive and negative shocks on the conditional variance asymmetrically via the use of the indicator function I_t:

$$\sigma_t^2 = \left(\omega + \sum_{j=1}^{m} \zeta_j v_{jt}\right) + \sum_{i=1}^{p_2} \left(\alpha_i \epsilon_{t-i}^2 + \gamma_i I_{t-i} \epsilon_{t-i}^2\right) + \sum_{j=1}^{q_2} \beta_j \sigma_{t-j}^2,$$

In this case, ω is a volatility offset term, γ_j represents the leverage term and m denotes the number of external regressors v_j. The indicator function I_t takes on value of 1 in cases when $\epsilon_t \leq 0$ and 0 otherwise.

For a combination of the ARMA and GJR–GARCH approaches applied to a time series X_t, we let $\epsilon_t = X_t - \mu_t = \sigma_t Z_t$ denote the residuals with respect to the mean process (ARMA error). We assume that σ_t follows a GARCH(p_2, q_2) specification, where p_2 is the order of the squared innovation lag (ϵ_t^2) and q_2 is the order of the variance lag (σ_t^2) and finally obtain the asymmetric ARMA(p_1, q_1)–GARCH(p_2, q_2) equations:

$$\begin{aligned} X_t &= \mu + \sum_{i=1}^{p_1} \phi_i (X_{t-i} - \mu) + \sum_{j=1}^{q_1} \theta_j \epsilon_{t-j} + \epsilon_t \\ \epsilon_t &= \sigma_t Z_t \\ \sigma_t^2 &= \omega + \sum_{j=1}^{m} \zeta_j v_{jt} + \sum_{i=1}^{p_2} \left(\alpha_i \epsilon_{t-i}^2 + \gamma_i I_{t-i} \epsilon_{t-i}^2\right) + \sum_{j=1}^{q_2} \beta_j \sigma_{t-j}^2 \end{aligned} \tag{2.3}$$

The order of a suitable ARMA process for the conditional mean can be identified though the Akaike Information Criterion (AIC). We iterate over pairwise values of $p_1 \in [1, p_{\text{max}}]$ and $q_1 \in [0, q_{\text{max}}]$ and choose the combination that yields the AIC-minimal model. Heteroskedasticity and asymmetric tails can be accounted for through a GJR–GARCH) model, fitted using a Maximum Likelihood approach with an inferred Student-t distributed innovations (as it is commonly used in practice and considered adequate for most financial applications [100]).

The evaluation of the fitted model is inspected using residuals, since a low AIC cannot guarantee the validity of the model assumptions. Following [100], we differentiate between unstandardised and standardised residuals and denote the former with $\hat{\epsilon}_t$ and latter as $\hat{Z}_t$. Given the estimated ARMA parameters, unstandardised innovations are calculated recursively from the data X_t and the fitted values $\hat{\mu}_t$, $\hat{\epsilon}_t = X_t - \hat{\mu}_t$. Due to the finiteness of the data sample, initial values for $X_{-p_1+1}, \ldots, X_0$, $\epsilon_{-q_1+1}, \ldots, \epsilon_0$ can be inferred and disregarded in later analysis. Standardised residuals are given by $\hat{Z}_t = \hat{\epsilon}_t / \hat{\sigma}_t$, $\hat{\sigma}_t$ is calculated through the fitted GARCH part of Eq. 2.3 recursively and the starting value of $\hat{\epsilon}_t$ and $\hat{\sigma}_t$ may be similarly chosen at will.

The main assumption of GARCH models states that standardised residuals are independent and identically distributed (i.i.d.). This can be investigated visually through correlograms or through

strict white noise portmanteau tests. Alternatively, we can opt for (a) a Ljung-Box test on standardised residuals to check for evidence of serial autocorrelation, and (b) a Li-Mak test [91] on the standardised residuals to check for remaining ARCH effects.

2.3.1.2 Extension to Multivariate GARCH Models

In financial econometrics, it is important to consider the dependence structure in the second-order moments of asset returns. Multivariate GARCH models deal with the issue of correlation and their main application is studying the relationship between the volatilities of different markets. They are particularly useful for portfolio optimization, risk management, and understanding interdependencies between different assets. The main goal is to estimate the conditional covariance matrix of the multivariate time series, which provides information about the time-varying volatilities of individual assets and the time-varying correlations between them. Overall, they are more relevant than independent univariate models and improve the decision-making process in volatility prediction, portfolio selection and risk management.

Multivariate GARCH models can generally be expressed as:

$$\boldsymbol{r}_t = \boldsymbol{\mu}_t + \boldsymbol{\epsilon}_t, \quad \boldsymbol{\epsilon}_t = \boldsymbol{H}_t^{1/2} \boldsymbol{z}_t, \tag{2.4}$$

where $\boldsymbol{\epsilon}_t$ is the error term at time t, expressed through the mean-corrected time-series of $\boldsymbol{r}_t$, $E[\boldsymbol{\epsilon}_t] = 0$, $\boldsymbol{\mu}_t$ is the $n \times 1$ vector of the expected values of the asset returns $\boldsymbol{r}_t$, $\boldsymbol{H}_t$ is the $n \times n$ matrix of conditional variances of $\boldsymbol{\epsilon}_t$ at time t and $\boldsymbol{z}_t$ is the $n \times 1$ vector of the independent and identically distributed residuals. $\boldsymbol{H}_t^{1/2}$ can be obtained through the Cholesky factorisation of $\boldsymbol{H}_t$.

There exist different approaches of the multivariate GARCH setting that allow to specify the conditional covariance matrix $\boldsymbol{H}_t$. One method models the conditional variances and correlations rather than straightforwardly modelling the conditional covariance matrix. In this case, the conditional covariance matrix $\boldsymbol{H}_t$ is decomposed as follows:

$$\boldsymbol{H}_t = \boldsymbol{D}_t \boldsymbol{R}_t \boldsymbol{D}_t, \tag{2.5}$$

where $\boldsymbol{D}_t$ is the diagonal matrix of conditional volatilities $\boldsymbol{D}_t = \text{diag}(h_{1t}^{1/2}, \ldots, h_{nt}^{1/2})$, and $\boldsymbol{R}_t$ denotes the conditional correlation matrix of the mean-corrected time-series, ϵ_t.

Estimating the parameters typically involves maximum likelihood estimation, which can be computationally intensive due to the complex likelihood functions and the large number of parameters. Nevertheless, multivariate GARCH models are valuable tools for understanding the time-varying volatility and correlation structure of multiple time series and have numerous applications in finance and economics.

2.3.1.3 DCC-GARCH Models

This section is concerned with the issue of modeling the dependence structure of the time-varying volatilities and correlations of two asset classes through a Dynamic Conditional Correlation (DCC) GARCH model, as introduced by Engle and Sheppard in 2001 [50]. In this setting, both the correlation matrix $\boldsymbol{R}_t$ and the conditional variances $\boldsymbol{D}_t$ are time-varying and the DCC-GARCH is defined as:

$$\boldsymbol{r}_t = \boldsymbol{\mu}_t + \boldsymbol{\epsilon}_t, \quad \boldsymbol{\epsilon}_t = \boldsymbol{H}_t^{1/2}\boldsymbol{z}_t, \quad \boldsymbol{H}_t = \boldsymbol{D}_t\boldsymbol{R}_t\boldsymbol{D}_t, \tag{2.6}$$

The diagonal matrix $\boldsymbol{D}_t$ contains the time-varying volatilities, which can be expressed as univariate GARCH processes:

$$\begin{pmatrix} \sqrt{h_{1t}} & 0 & \dots & 0 \\ 0 & \sqrt{h_{2t}} & \dots & 0 \\ \vdots & \vdots & \ddots & \vdots \\ 0 & 0 & \dots & \sqrt{h_{nt}}, \end{pmatrix} \tag{2.7}$$

where

$$h_{it} = \alpha_{i0} + \sum_{q=1}^{Q_i} \alpha_q \epsilon_{t-q}^2 + \sum_{p=1}^{P_i} \beta_q h_{t-q}. \tag{2.8}$$

The given GARCH model is a symmetric one where positive and negative returns influence volatility in the same way. However, positive innovations to volatility practically appear to correlate with negative market information (and vice versa), while positive returns should cause less uncertainty. Glosten, Jagannathan, and Runkle [55] have proposed a way to account for this asymmetry (GJR–GARCH) through modelling the positive and negative shocks on the conditional variance asymmetrically via the use of an indicator function I_t.

There is no need for the univariate GARCH models to be of the same order and $\boldsymbol{\mu}_t$ in Eq. 2.6 can be expressed either as a constant vector or as a time-varying process. For the purposes of this study we choose a first order ARMA model for the conditional mean and a first order GJR–GARCH for each one of the univariate GARCH models:

$$\begin{aligned} r_t &= \mu + \phi_1(X_{t-1} - \mu) + \theta_1\epsilon_{t-1} + \epsilon_t \\ \epsilon_t &= \sigma_t Z_t \\ \sigma_t^2 &= \omega + \zeta_1 v_{1t} + \left(\alpha_1\epsilon_{t-1}^2 + \gamma_1 I_{t-1}\epsilon_{t-1}^2\right) + \beta_1\sigma_{t-1}^2, \end{aligned} \tag{2.9}$$

where ω is a volatility offset term and γ_1 represents the leverage term. The indicator function I_t takes on value of 1 for $\epsilon_t \leq 0$ and 0 otherwise.

2.3.1.4 Regime Switching GARCH Models

Regime switching models serve as a pivotal tool in capturing the cyclical nature of markets, offering insights into the transitions between different phases of market behavior. Regime-Switching GARCH models are specifically used for analyzing time series data with changing volatility dynamics. They combine the features of a GARCH model which accounts for time-varying volatility, with a regime-switching model which accounts for distinct states or regimes with different characteristics. The time series is assumed to switch between different volatility regimes, where each regime has its own GARCH process. The regime-switching component can capture abrupt changes or structural breaks in the volatility dynamics, which might be due to changes in the underlying process, such as economic or financial market conditions. They are used extensively in finance and economics for modeling and forecasting time series data with changing volatility patterns, such as stock returns, exchange rates, and interest rates.

We denote the daily value of a given financial instrument at time t by V_t and the daily logarithmic returns by r_t, which satisfy the moment conditions $E[r_t] = 0$ and $E[r_t r_{t-l}] = 0$ for $l \neq 0$ and $t > 0$. In an attempt to capture the time-varying volatility behavior, we express r_t in terms of a process that follows a regime-switching specification in its conditional variance h_t. The general mixture model, which allows for categorisation of the conditional variance dynamics in low, moderate and high-volatility periods, can be expressed as:

$$r_t \mid (s_t = k, \mathcal{I}_{t-1}) \sim \mathcal{D}(0, h_{k,t}, \boldsymbol{\xi}_k), \tag{2.10}$$

where the random variable r_t is modelled conditional on the regime s_t being in state k, the information set $\mathcal{I}_{t-1}$ represents any information about r_t that is observed up to time $t-1$ and $\mathcal{D}_k(0, h_{k,t}, \boldsymbol{\xi}_k)$ is a continuous distribution, corresponding to state s_t, with zero mean and time-dependent conditional variance $h_{k,t}$. Additionally, $\boldsymbol{\xi}_k$ denotes the shape parameters of the distribution of the independent and identically distributed standardised innovations $\eta_{k,t} \overset{\text{i.i.d.}}{\sim} \mathcal{D}_k(0, 1, \boldsymbol{\xi}_k)$ of the conditional variance process. Assuming that there are K different specifications of $h_{k,t}$, the latent variable s_t is defined on the discrete space $\{1, \ldots, K\}$. The definition of the regime-switching model defined by Eq. 2.10, requires specifying (i) the conditional variance dynamics, unique in each state $s_t = k$ and (ii) the state dynamics, driving the evolution of the variable s_t.

In regards to the conditional variances $h_{k,t}$ of r_t, we can adopt the approach of Haas et al. [59] and assume that they follow K separate GARCH type processes which evolve in parallel. Therefore, given time t, $h_{k,t}$ follows a GARCH specification, conditional on regime $k \in \{1, \ldots, K\}$ that prevails at time t:

$$h_{k,t} = h(r_{t-1}, h_{k,t-1}, \boldsymbol{\theta_k}), \tag{2.11}$$

where h is a function that denotes the GARCH expression of the conditional variance and ensures positivity and covariance stationarity and $\boldsymbol{\theta_k}$ are the model-specific parameters.

Assuming the ARCH model of Engle [48], we obtain:

$$h_{k,t} = a_{0,k} + a_{1,k} r_{t-1}^2, \tag{2.12}$$

where $k \in \{1, \ldots, K\}$, $\boldsymbol{\theta_k} = [a_{0,k}, a_{1,k}]$, $a_{0,k} > 0$ and $a_{1,k} \geq 0$. Additionally, we require $a_{1,k} < 0$ to ensure covariance stationarity in regime k. We further assume that the state process $s_t \in \{1, \ldots, K\}$ evolves according to a first-order ergodic homogeneous Markov chain, with $K \times K$ probability matrix $\boldsymbol{P}$, where:

$$\boldsymbol{P} = \begin{bmatrix} p_{1,1} & \cdots & p_{1,K} \\ \vdots & \ddots & \vdots \\ p_{K,1} & \cdots & p_{K,K}, \end{bmatrix}$$

where $p_{i,j}$ is the probability of transition from state $S_{t-1} = i$ to state $S_t = j$.

Similarly, if we assume that the conditional variance follows the GARCH model of Bollerslev [20], we have:

$$h_{k,t} = a_{0,k} + a_{1,k} r_{t-1}^2 + \beta_k h_{k,t-1}, \tag{2.13}$$

where $k \in \{1, \ldots, K\}$, $\boldsymbol{\theta_k} = [a_{0,k}, a_{1,k}, \beta_k]$, $a_{0,k} > 0$, $a_{1,k} > 0$ and $\beta_k \geq 0$. Covariance stationarity is ensured through $a_{1,k} + \beta_k < 1$.

For the model to be complete we also need to define the underlying distribution of the standardised residuals in each regime. We can assume a Student-t distribution, with the probability density function (PDF) given by:

$$f(t; \nu) = \frac{\Gamma(\frac{\nu+1}{2})}{\sqrt{\nu\pi}\,\Gamma(\frac{\nu}{2})} \left(1 + \frac{t^2}{\nu}\right)^{-\frac{\nu+1}{2}}$$

where $\Gamma(x)$ is the Gamma function.

Estimation of the specified model can be achieved through Maximum Likelihood approaches as described by Ardia et al. [4]. Given the Markov switching GARCH model parameters:

$$\boldsymbol{\Psi} = (\boldsymbol{\theta_1}, \boldsymbol{\xi_1}, \ldots, \boldsymbol{\theta_K}, \boldsymbol{\xi_K}, \boldsymbol{P}), , \tag{2.14}$$

where $\boldsymbol{\theta_i}$ are the GARCH parameters and $\boldsymbol{\xi_i}$ the parameters of the conditional distribution of the standardised innovations of state s_i and $\boldsymbol{P}$ the transition matrix, the likelihood function is given by:

$$\mathcal{L}(\boldsymbol{\Psi} \mid \mathcal{I}_T) = \prod_{t=1}^{T} f(r_t \mid \boldsymbol{\Psi}, \mathcal{I}_{t-1}), \tag{2.15}$$

where $f(r_t \mid \boldsymbol{\Psi}, \mathcal{I}_{t-1})$ denotes the density of r_t given its past observations $\mathcal{I}_{t-1}$. Maximisation of the logarithm of $\mathcal{L}(\boldsymbol{\Psi} \mid \mathcal{I}_T)$ gives the ML estimator $\hat{\boldsymbol{\Psi}}$.

2.3.1.5 Hidden Markov Models for Intermediate Trend Regimes

Building upon the discussion of Regime Switching GARCH models, we now turn our attention to Hidden Markov Models (HMM) as another powerful approach for deciphering market dynamics. This section introduces HMMs as a sophisticated yet practical tool for detecting and analyzing intermediate trend regimes in financial markets. HMMs offer a dynamic framework for modeling the probabilistic behavior of market states, allowing us to decipher patterns that are not immediately apparent. We let V_t denote the daily value of a financial instrument at day t and we express its weekly log-return with $R_t = \ln(V_{t,n}/V_{t,1})$, where $V_{t,1}$ is the value on the first day and $V_{t,n}$ is the value on the last day of the week. In an attempt to model its intermediate-trend, we assume that R_t can be described through a pair of stochastic processes $\{(S_t, R_t),\ t \in \mathbb{N}\}$ that follow a Hidden Markov Model (HMM) specification [54]. HMM specifications are a useful tool for modelling observation sequences, modelled as the output of a discrete stochastic process.

They are used for various tasks, including:

1. Determining the likelihood of a given observation sequence given the HMM parameters. This is typically done using the Forward Algorithm, which computes the probability of an observation sequence up to a particular time step.
2. Inferring the most likely sequence of hidden states given the observation sequence and the HMM parameters. This can be achieved using the Viterbi Algorithm, which finds the most probable path through the hidden states.
3. Simply estimating the HMM parameters (transition, emission, and initial state probabilities) given a set of observation sequences. The Baum-Welch Algorithm[9], an expectation-maximization (EM) algorithm, is commonly used for this purpose.

In this case, $\{S_t,\ t \in \mathbb{N}\}$ represents a Markov chain that is not directly observable and $\{R_t,\ t \in \mathbb{N}\}$ is a sequence of independent random variables conditional on S_t. At every time point t, the next state S_{t+1} is dependent only upon the current state S_t and the conditional distribution of R_t only depends on S_t.

The output variable R_t can be assumed to follow a Gaussian model $(\mu_k, \sigma_k,)$, conditional on state $S_t = k \in \{1, \ldots, K\}$ so that:

$$R_t \sim \begin{cases} \mathrm{N}(\mu_0, \sigma_0),\ S_t = 0 \\ \quad \vdots \\ \mathrm{N}(\mu_K, \sigma_K),\ S_t = K \end{cases} \tag{2.16}$$

The hidden state variable S_t is assumed to be defined on the discrete space $\{1, \ldots, K\}$. The $K \times K$ transition matrix is time-invariant and denoted with $\boldsymbol{P}$:

$$\boldsymbol{P} = \begin{bmatrix} p_{1,1} & \cdots & p_{1,K} \\ \vdots & \ddots & \vdots \\ p_{K,1} & \cdots & p_{K,K}, \end{bmatrix}$$

where $p_{i,j}$ is the probability of transition from state $S_{t-1} = i$ to state $S_t = j, 0 < p_{i,j} < 1 \, \forall i, j \in \{1, \ldots, K\}$ and $\sum_{j=1}^{K} p_{i,j} = 1 \, \forall i \in \{1, \ldots, K\}$.

The main assumptions of HMMs are the following:

1. probability of transitioning to the next hidden state depends only on the current hidden state and not on any previous states. Mathematically, this is represented as:

$$P(S_t|S_{t-1}, S_{t-2}, \ldots, S_1) = P(S_t|S_{t-1}).$$

2. The probability of emitting an observed symbol at a given time step depends only on the current hidden state and is independent of other hidden states and previous observations. Mathematically, this is represented as:

$$P(R_t|S_t, S_{t-1}, \ldots, S_1, R_{t-1}, \ldots, R_1) = P(R_t|S_t).$$

If applied to financial time series, autocorrelation effects in the returns time series will need to be eliminated through filtering with a first-order autoregressive process, AR(1).

The joint distribution of a sequence of a series of T observations $\{\boldsymbol{S}_{1:T}, \boldsymbol{R}_{1:T}\}$ is written as:

$$\begin{aligned} &\mathsf{P}(\boldsymbol{S}_{1:T}, \boldsymbol{R}_{1:T}) = \\ &\mathsf{P}(S_1)\mathsf{P}(R_1 \mid S_1) \prod_{t=2}^{M} \mathsf{P}(S_t \mid S_{t-1})\mathsf{P}(R_t \mid S_t) \end{aligned} \tag{2.17}$$

The definition of the probabilistic network described by Eq. 2.17 requires specifying the probability distribution over the initial state $P(S_1)$, the $K \times K$ transition matrix that describes the evolution of the state variable, $P(S_t \mid S_{t-1})$, and the output model $P(R_t \mid S_t)$.

The prior, transition and response parameters $\boldsymbol{\phi} = (\boldsymbol{\phi}_1, \boldsymbol{\phi}_2, \boldsymbol{\phi}_3)$ are estimated through the EM algorithm. Parameters can be estimated through an iterative process that seeks to maximize the expected joint log-likelihood of both the parameters, given the observed data and states:

$$\begin{aligned}\log(\mathsf{P}(\boldsymbol{S}_{1:T}, \boldsymbol{R}_{1:T}, \boldsymbol{\phi})) = \log(\mathsf{P}(S_1, \boldsymbol{\phi}_1)) \\ + \sum_{t=2}^{T} \log(\mathsf{P}(S_t \mid S_{t-1}, \boldsymbol{\phi}_2)) \\ + \sum_{t=1}^{T} \log(\mathsf{P}(R_t \mid S_t, \boldsymbol{\phi}_3))\end{aligned} \tag{2.18}$$

2.3.2 Diversification and Portfolio Management Strategies

2.3.2.1 Shannon's Demon

In 1960, Claude Shannon, a famous researcher in the field of Information Theory, presented a talk at MIT regarding stock markets and more precisely about an optimal growth-portfolio construction method. Based on the works of Kelly and Breiman, Shannon experiments with a way to generate extra growth using a diversification and rebalancing strategy (cf. [21, 128]) called Shannon's Demon [111]. In its experimental method, Shannon considers an asset that follows a random walk process without upward or downward trend. The portfolio is built using two uncorrelated assets, where half of available capital is allocated in some highly volatile asset and half of it in a risk free one. After each round, the investor has to decide whether to reallocate its wealth at risk or in cash respecting the original allocation.

The accumulated wealth after T rounds and L losses is $W_t = W_0[(1 + w_0 a)^{(T-L)}(1 - w_0 b)^L]$ where W_0 is the initial wealth, w_0 is the part of wealth reallocated in risk, a the percentage returns in an up-move proportional gain and b the percentage loss in an down-move proportional loss.

The objective is to maximize the expected growth rate, $E[g]$:

$$E[g] = p \log(1 + w_0 a) + q \log(1 + w_0 b)$$

where g is the average growth rate, $g = 1/T \log(w_t/w_0)$.

In the Shannon game set-up, the optimal fraction obtained from the optimization is:

$$w_0^* = \frac{pa - qb}{ab}$$

where p is the probability of profit and q is the probability of loss compared to the optimal full-bet fraction of capital in the buy-and-hold case.

Indeed, the rebalanced portfolio generates extra value compared to a buy-and-hold strategy under two specific conditions [43]: if $0 < \mu < \sigma^2/2$ (where the buy-and-hold might lose the initial value) or if $\sigma^2/2 < \mu < \sigma^2$, where μ and σ the mean and standard deviation of the normally distributed simple returns for the risky asset. Respectively, if the expected return is higher than σ^2, it is best to

fully invest in the risky asset. By maximizing the growth rate, the optimal fraction to invest at risk is equal to:

$$g^* = 1/2 \max[\log((1 + w_0 b)(1 - w_0 b))]$$

where the optimal weight is:

$$w_0^* = \mu/\sigma^2$$

Thus, the best choice of the risky asset among many risky assets is to one that provides the highest Sharpe ratio.

A case of two negatively correlated but volatile assets is also considered in [43]. In this scenario, it is shown that even with appealing diversification properties and positive expected returns, a buy-and-hold strategy to fails to grow the investors' wealth. Active management by rebalancing on the other hand can effectively add value in the long term.

Overall, the Shannon's Demon strategy is an alternative to the buy-and-hold strategy in order to generate growth even if the returns of both assets are negative. It provides a solution to Parrondo's Paradox [123] which states that a winning strategy can potentially emerge from the intelligent combination of two losing strategies. More generally, high volatility and low correlation provide extra-growth reducing portfolio risk due to the diversification and rebalancing effect [22]. However, the main limitation concerns the frequency of the rebalancing strategy, and a pertinent question is whether this frequency is enough to overcome the transactions costs (fees, commissions, taxes). That is, there is a trade-off between the advantages obtained by the Shannon's Demon strategy including lower risk and higher growth and the costs of rebalancing related to the transaction costs.

2.3.2.2 Equal Risk Contribution Portfolios

Optimal portfolio construction has been a topic of interest in academic literature for decades, with the mean-variance framework introduced by Markowitz [99] as the foundational method for efficient wealth allocation. Nevertheless, this framework encounters issues in practical application [96], as optimal portfolios often exhibit excessive concentration in a limited subset of assets, and are highly sensitive to input parameters. Alternative methods, such as portfolio resampling or robust asset allocation, have been proposed in literature [102, 140] to address these issues but also possess their own drawbacks [76, 118], including additional computational burden and inferior out-of-sample performance compared to traditional approaches.

In light of these challenges, investors often prefer heuristic solutions like the minimum variance and equally-weighted portfolios. The minimum variance portfolio is computationally simple and robust, as it does not rely on expected returns as a criterion; however, it suffers from portfolio concentration. The equally-weighted portfolio addresses this concentration issue by assigning equal weight to all assets considered. Nonetheless, the equally-weighted portfolio may result in

limited risk diversification if individual risks significantly differ.

Risk-based strategies have proved to be capable of reducing volatility in a way that does not impede market exposure, while outperforming standard strategies in unsteady markets. Equal Risk Contribution (ERC, also known as Risk Parity) is a well known risk-control strategy that achieves diversification both within and across asset classes. Its main goal is to bolster the portfolio's immunity to unforeseen drawdowns during stressful market periods. In contrast with the equally-weighted allocation scheme, a Risk Parity portfolio aims towards an equal distribution of the overall budget, expressed in terms of risk rather than capital. Moreover, ERC portfolios ensures a more balanced risk distribution compared to minimum-variance portfolios, which may lead to an over-concentration of risk in a limited number of positions [96]. Additionally, optimality arguments lend support to the ERC approach. Lindberg [93] shows that the solution to Markowitz's continuous-time portfolio problem, when considering positive drift rates in Brownian motions governing stock prices, is achieved by equalizing quantities related to risk contributions. Therefore, risk parity approaches offer a promising alternative to traditional portfolio construction methods, as they provide the diversification benefits of equally-weighted portfolios while accounting for individual and joint risk contributions of assets.

The Risk Parity optimisation problem setting is constituted of $N \geq 2$ assets $A_1, \ldots, A_N$, with μ_i, σ_i and σ_i^2 representing the expected return, standard deviation and variance of the returns of A_i respectively and ρ_{ij} denoting the correlation coefficient of the returns of A_i and A_j for $i \neq j$. The $N \times N$ symmetric covariance matrix of returns is defined as $\Sigma = (\sigma_{ij})$ where $\sigma_{ij} = \rho_{ij}\sigma_i\sigma_j, i \neq j$ and $\sigma_{ij} = \sigma_i^2, i = j$. If x_i is the amount to be invested in asset A_i, then the volatility (which is measured in terms of standard deviation) of the resulting portfolio $x = (x_1, \ldots, x_i)$ is computed as $\sqrt{x^T \Sigma x} = \sum_i x_i^2 \sigma_i^2 + \sum_i \sum_{j \neq i} x_i x_j \sigma_{ij}$.

In the ERC problem, we define the marginal risk contribution of asset A_i as:

$$\frac{\partial \sigma(x)}{\partial x_i} = \frac{x_i \sigma_i^2 + \sum_{j \neq i} x_j \sigma_{ij}}{\sigma(x)}$$

If $\sigma(x) = \sqrt{x^T \Sigma x}$ denotes the risk of the portfolio, the total risk contribution of asset A_i is given by $\sigma_i(x) = x_i \times \partial_{x_i} \sigma(x)$ and, through the Euler decomposition, the risk is expressed as:

$$\sigma(x) = \sum_{i=1}^{N} \sigma_i(x) = \sum_{i=1}^{N} x_i \times \frac{\partial \sigma(x)}{\partial x_i},$$

The desired risk-balanced portfolio is constituted in a way that all components contribute equally to the overall volatility; therefore $\sigma_i(x) = \sigma_j(x)$. The general Risk Parity portfolio construction

problem can be mathematically expressed as:

$$x_{ERC} = \left\{ x \in [0,1]^N : x_i \times \partial_{x_i}\sigma(x) = x_j \times \partial_{x_j}\sigma(x), \forall i,j, \sum_{i=1}^{N} x_i = 1 \right\}.$$

Through the problem expression, asset classes with reduced levels of volatility or correlation are favoured since their marginal risk contribution to the portfolio volatility will be lower. In [96], Maillard et al. show that if all correlations are the same then each constituent weight is defined as the ratio of the reciprocal of its volatility with the sum of the reciprocals of the volatilities of all constituents:

$$x_i = \frac{\sigma_i^{-1}}{\sum_{j=1}^{N} \sigma_j^{-1}}, i = 1, \ldots, N \tag{2.19}$$

Similarly, in the bivariate case, the vector of total risk contributions is given by:

$$\frac{1}{\sigma(x)} \begin{pmatrix} x_1^2\sigma_1^2 + x_1x_2\rho\sigma_1\sigma_2 \\ x_2^2\sigma_2^2 + x_1x_2\rho\sigma_1\sigma_2 \end{pmatrix}$$

Therefore, when $\rho = 0$, the constituent weights will be:

$$x_1 = \frac{\sigma_1^{-1}}{\sigma_1^{-1} + \sigma_2^{-1}}.$$

In [96], when the correlations are different, the authors propose solving the optimisation problem defined as

$$\min_x \sum_{i=1}^{N} \sum_{j=1}^{N} \left(x_i \left(\Sigma x\right)_i - x_j \left(\Sigma x\right)_j \right)^2 \tag{2.20}$$

with $x_i \in [0,1]$ and $\sum_{i=1}^{N} x_i = 1$. Here $(\Sigma x)_i$ denotes the i^{th} entry of the vector resulting from the product of Σ with x.

2.3.2.3 Mean-Variance Spanning Tests

The process of constituent selection in portfolio construction often raises the question of whether a set of additional assets can improve the risk-adjusted returns of a base asset set. Huberman and Kandel [68] address this issue and, given a set of K assets (benchmark assets) and a set of N additional assets (test assets), they test the hypothesis that the efficient frontier of K is the same as that of $K + N$. The concept of mean-variance spanning therefore states that a set of K assets spans a larger set of $N + K$ assets if the minimum-variance frontier of K assets is identical to the minimum-variance frontier $K + N$.

Relevant works in financial literature [42, 77, 90] analyse whether investors, given a set of K assets, can benefit through investing in an additional set of N assets. Following the definitions of Kan and

Zhou [77], we denote with $R_t = [R'_{1t}, R'_{2t}]$ the returns of the assets under consideration. Here R'_{1t} is a vector of length K, with the returns of the K benchmark assets at time t and R'_{2t} is a vector of length N, with the returns of the N test assets at time t. The expected returns and the covariance matrix of the $N + K$ assets are given by:

$$\mu = E[R_t] = \begin{bmatrix} \mu_1 \\ \mu_2 \end{bmatrix}, \; V = \text{Var}[R_t] = \begin{bmatrix} V_{11} & V_{12} \\ V_{21} & V_{22} \end{bmatrix}, \tag{2.21}$$

where $E[R_{1t}] = \mu_1$ and $E[R_{2t}] = \mu_2$, V_{11} is the covariance matrix of the K benchmark assets, V_{22} is the covariance matrix of the N test assets, V_{12}, V_{21} represent the covariances of the benchmark assets with the test assets. For the mean-variance spanning test setting, R_{2t} is projected on R_{1t}:

$$R_{2t} = \alpha + \beta R_{1t} + \epsilon_t, \tag{2.22}$$

where $E[\epsilon_t] = 0_N$ and $E[\epsilon_t R'_{1t}] = 0_{N\times K}$. In Eq. 2.22, α and β are given by $\alpha = \mu_2 - \beta\mu_1$ and $\beta = V_{21}V_{11}^{-1}$.

In matrix notation, assuming length T for the assets' time-series, we have:

$$R = XB + E, \tag{2.23}$$

where R is the $T \times N$ matrix of the test asset returns R_{2t}, X is the $T \times (K+1)$ matrix where each row is given by $[1, R'_{1t}]$, $t \in [1, T]$, $B = [\alpha, \beta]'$ and E is a $T \times N$ matrix where each row is given by ϵ'_t. The residuals ϵ_t are assumed to be independent and identically distributed as multivariate normal with zero mean and variance Σ.

Setting $\delta = 1_N - \beta 1_K$, the null hypothesis for spanning, provided by Huberman and Kandel [68], is given by:

$$H_0 : \alpha = 0_N, \delta = 0_N \tag{2.24}$$

The null hypothesis highlights the fact that mean-variance spanning tests are joint tests. Condition $\alpha = 0$ tests whether the test assets improve the tangency portfolio and $\delta = 0$ tests whether they improve the global minimum variance portfolio. The two conditions together imply that adding the N test assets to the base portfolio of K assets does not shift the efficient frontier significantly.

The null hypothesis in Eq. 2.24 can be rewritten as $H_0 : \Theta = 0_{2\times N}$, where $\Theta = [\alpha, \delta]'$. In this case, $\Theta = AB - C$, where

$$A = \begin{bmatrix} 1 & 0'_K \\ 0 & -1'_K \end{bmatrix}, \quad C = \begin{bmatrix} 0'_N \\ -1'_N \end{bmatrix}, \tag{2.25}$$

Mean-Variance spanning is presented in [77] as a likelihood ratio test (LR), based on the regression given by Eq. 2.22, and can accordingly be supplemented with the Wald (W) and the Lagrange multiplier (LM) tests. We define the estimation matrices

$$\hat{G} = TA\left(X'X\right)^{-1}A', \quad \hat{H} = \hat{\Theta}\hat{\Sigma}^{-1}\hat{\Theta}' \tag{2.26}$$

$\hat{\Sigma}$ in Eq. 2.26 is the unconstrained maximum likelihood estimator of the covariance matrix of error terms Σ. Denoting by $\hat{B}$ the estimator of B, we have:

$$\hat{B} = \left[\hat{\alpha}, \hat{\beta}\right]' = \left(X'X\right)^{-1}\left(X'R\right), \tag{2.27}$$

$$\hat{\Sigma} = \frac{1}{T}\left(R - X\hat{B}\right)'\left(R - X\hat{B}\right). \tag{2.28}$$

Further denoting by λ_1 and λ_2 the eigenvalues of $\hat{H}\hat{G}^{-1}$, with $\lambda_1 \geq \lambda_2 \geq 0$, we obtain the three test statistics:

$$\text{LR} = T\sum_{i=1}^{2}\ln\left(1+\lambda_i\right) \overset{\text{A}}{\sim} \chi^2_{2N}, \tag{2.29}$$

$$\text{W} = T\left(\lambda_1 + \lambda_2\right) \overset{\text{A}}{\sim} \chi^2_{2N}, \tag{2.30}$$

$$\text{LM} = T\sum_{i=1}^{2}\frac{\lambda_i}{1+\lambda_i} \overset{\text{A}}{\sim} \chi^2_{2N}. \tag{2.31}$$

All three tests have an asymptotic χ^2_{2N} distribution, although we must have W $\geq$ LR $\geq$ LM in finite samples [15, 27]. The three tests might produce conflicting results, with W favoring rejection and LM favoring acceptance. It is therefore important to perform all three tests when deciding upon the mean-variance spanning outcome.

The main determinant of the power of the spanning tests is the difference between the risk levels in the two minimum variance portfolios [77]. That is because, although spanning tests are joint tests, they weigh the estimates of the two constants according to their accuracy. In this case, the estimation of δ is statistically more accurate since it does not involve any estimations of expected returns. Additionally, a statistically significant shift in the minimum variance portfolio might not be as important to an investor as an improvement to the tangency portfolio. It is therefore suggested to examine the two parts of the hypothesis in Eq. 2.24 separately. This involves a step-down procedure which first examines whether $\alpha = 0_N$ through an F-test (F_1) and secondly the condition $\delta = 0_N$, also through an F-test (F_2). A rejection of the F_1 test will hint that the two tangency portfolios are different while the rejection of F_2 will indicate a significant difference in the minimum variance portfolios. The original hypothesis will be accepted only if both individual tests are accepted. F_1 has a central F-distribution with N and $T - K - N$ degrees of freedom, given

by:

$$\begin{aligned} F_1 &= \left(\frac{T-K-N}{N}\right)\left(\frac{|\bar{\Sigma}|}{|\hat{\Sigma}|}-1\right) \\ &= \left(\frac{T-K-N}{N}\right)\left(\frac{\hat{\alpha}-\hat{\alpha_1}}{1+\hat{\alpha_1}}\right), \end{aligned} \tag{2.32}$$

where $\hat{\Sigma}$ is an unconstrained estimate of the covariance matrix Σ and $\bar{\Sigma}$ is an estimate of Σ, conditional on $\alpha = 0_N$. Additionally, $\hat{\alpha} = \hat{\mu}'\hat{V}^{-1}\hat{\mu}$, $\hat{\mu} = \frac{1}{T}\sum_{t=1}^{T} R_t$, $\hat{V} = \frac{1}{T}\sum_{t=1}^{T}(R_t - \hat{\mu})(R_t - \hat{\mu})'$, $\hat{\alpha_1} = \hat{\mu_1}'\hat{V}_{11}^{-1}\hat{\mu_1}$. Here $\hat{\mu}$ and $\hat{V}$ represent the maximum likelihood estimates of the expected return and covariance matrix of the augmented portfolio, respectively.

Similarly, F_2 has a central F-distribution with N and $T-K-N+1$ degrees of freedom, it is independent of F_1 and is given by:

$$\begin{aligned} F_2 &= \left(\frac{T-K-N+1}{N}\right)\left(\frac{|\tilde{\Sigma}|}{|\bar{\Sigma}|}-1\right) \\ &= \left(\frac{T-K-N+1}{N}\right)\left[\left(\frac{\hat{c}+\hat{d}}{\hat{c}_1+\hat{d}_1}\right)\left(\frac{1+\hat{\alpha_1}}{1+\hat{\alpha}}\right)-1\right], \end{aligned} \tag{2.33}$$

where $\tilde{\Sigma}$ is an estimate of the residual covariance matrix Σ, conditional on $\alpha = 0_N$ and $\delta = 0_N$, $\hat{b_1} = \hat{\mu_1}'\hat{V}_{11}^{-1}1_K$, $\hat{c_1} = 1_K'\hat{V}_{11}^{-1}1_K$, $\hat{d_1} = \hat{\alpha}\hat{c} - \hat{b}^2$, $\hat{b} = \hat{\mu}'\hat{V}^{-1}1_{N+K}$, $\hat{c} = 1_{N+K}'\hat{V}^{-1}1_{N+K}$ and $\hat{d} = \hat{\alpha}\hat{c} - \hat{b}^2$. The mentioned constants will later also assist the geometrical interpretation of the performed spanning tests.

2.3.3 Fundamental Tools in Quantitative Risk Management

2.3.3.1 Multivariate Stress Testing for Efficient Risk Management

There are several definitions of stress tests in literature. Studer [129] describes stress tests as the concept of maximum loss over ellipsoidal scenario sets. The stress testing problem is also described by Breuer et al. [26] who propose a number of refinements to Studer's initial approach. According to [26], the quality of the stress test crucially depends on the definition of stress scenarios, which need to meet three requirements: plausibility, severity and suggestiveness of risk-reducing actions. Lopez [95] further refers to stress tests as risk management tools that aim to quantify the impact of unlikely, yet plausible, movements of financial variables on portfolio values.

Stress test design methods vary in practice and are typically divided into two main categories: univariate and multivariate. While univariate stress tests, also referred to as sensitivity analysis, are relatively easy to perform, they are considered insufficient, as they fail to incorporate the dependence structure of the identified risk factors. Multivariate approaches examine the effects of simultaneous changes in more than one variables and are usually scenario-based. Breuer et al.

[26] highlight the importance of an explicit choice of scenarios while Nyström et al. [109] identify the main elements of scenario-based risk management:

1. Recording the market value of the portfolio components
2. Generating scenarios based on a calibrated model of the portfolio behaviour
3. Estimation of the returns distribution
4. Application of risk measures in the obtained distribution

Regarding the model calibrations in step 2, Cherubini et al. [34] consider the bivariate equity portfolio case and suggest a univariate model for each of the two marginal distributions of the portfolio's risk factors , and one conditional copula approach for the underlying dependence structure.

Stylised facts on autocorrelations and volatility clustering, as proposed by Cont [38], suggest that (i) linear autocorrelations of returns are expected to be very small, (ii) autocorrelation function of absolute returns decays slowly as a function of the time lag and (iii) volatility events are stochastic and appear in clusters. Additionally, we expect (iv) asymmetric and heavy tails in the unconditional distribution of returns that exhibit power-law or Pareto-like behaviors. When examining conditional returns that have been corrected for heteroskedasticity, tails are less heavy.

2.3.3.2 Dependence Structure Modeling

In the preceding sections, we explored the application of GARCH models, focusing on how they help in understanding the volatility dynamics of financial markets through the analysis of GARCH residuals. These residuals, representing the deviations from the expected returns, provide key insights into market behavior under different volatility regimes. As we move towards a more holistic view of risk management, it is essential to extend our analysis beyond individual asset volatility to the interconnected nature of various assets within a portfolio.

Given a fitted semi-parametric distribution of the GARCH residuals, we have a foundation to simulate scenarios and examine the sensitivity of risk to different volatility specifications by adjusting the individually fitted constants. This approach, however, primarily considers assets in isolation. In a multivariate risk management context, where portfolio diversification and asset interdependence play critical roles, it is imperative to address the dependence structure among risk factors. This is particularly crucial in portfolios where decisions on composition are significantly influenced by cross-correlations among assets.

This leads us to the concept of copulas, a powerful statistical tool that allows us to model and analyze the dependence structure between different assets or risk factors. In subsequent chapters we will utilise the concept of copulas as a tool that allows us to decompose a joint probability distribution into its marginals. Copulas enable us to understand how assets move in relation to one another, especially during periods of market stress, thereby providing a more comprehensive risk assessment framework.

A d-dimensional copula is a distribution function with standard uniform marginal distributions, that represents a mapping of the unit hypercube into the unit interval in the form of $C : [0,1]^d \to [0,1]$. The practicality of copulas in multivariate distribution modelling is highlighted through Sklar's Theorem that states that, if F is a joint distribution function with margins $F_1, \ldots, F_d$, then there exists a copula $C : [0,1]^d \to [0,1]$ such that for all $x_1, \ldots, x_d$ in $\mathbb{R}$,

$$F(x_1, \ldots, x_d) = C(F_1(x_1), \ldots, F_d(x_d)).$$

Conversely, if C is a copula and $F_1, \ldots, F_d$ are univariate distribution functions, then the function F is a joint distribution function with margins $F_1, \ldots, F_d$. By further denoting with $F^{\leftarrow}(u) = \inf\{x : F(x) \geq u\}$ the generalised inverse distribution function of F, we obtain:

$$F(F_1^{\leftarrow}(u_1), \ldots, F_d^{\leftarrow}(u_d)) = C(u_1, \ldots, u_d)$$

Copulas lend themselves particularly useful for settings where the marginal distributions at hand have been defined in detail. Moreover, as confirmed by the latter expression of Sklar's Theorem, they express correlations on a quantile scale, since $C(u_1, \ldots, u_d)$ is the joint probability that each random value X_i lies below its u_i-quantile, allowing us to isolate the dependence of extreme outcomes, if necessary.

Given a copula C, its cumulative distribution function can be expressed as an integral over its density function, $c(u_1, \ldots, u_d)$:

$$C(u_1, \ldots, u_d) = \int_{-\infty}^{u_1} \cdots \int_{-\infty}^{u_d} c(u_1, \ldots, u_d)\, du_1, \ldots, du_d$$

Given this expression, copulas fall into two main categories: *implicit* and *explicit*, depending on whether the integral of the former equation possesses a simple closed-form (although those two categories are not mutually exclusive). Copulas of the former category do not necessarily have simple closed-form expressions and are implied by well-known multivariate distribution functions using Sklar's Theorem, while the latter possess closed forms.

For this study we consider two implicit copulas; the Gaussian and t-copula. Given a multivariate normal random vector $\boldsymbol{Y} \sim N_d(\boldsymbol{\mu}, \Sigma)$, its copula is a *Gaussian copula* and, under the copula property of invariance under monotone increasing transformations, it is the same as the copula of $\boldsymbol{X} \sim N_d(\mathbf{0}, P)$, where P is the correlation matrix of $\boldsymbol{Y}$. In two dimensions, the Gaussian copula is given by:

$$\begin{aligned} C_\rho^G(u_1, u_2) &= \Phi_P(\Phi^{-1}(u_1), \Phi^{-1}(u_2)) \\ &= \int_{-\infty}^{\Phi^{-1}(u_1)} \int_{-\infty}^{\Phi^{-1}(u_2)} \frac{1}{2\pi(1-\rho^2)^{1/2}} \exp\left(\frac{-(s_1^2 - 2\rho s_1 s_2 + s_2^2)}{2(1-\rho^2)}\right) ds_1 ds_2 \end{aligned}$$

where Φ and Φ_P denote the standard univariate normal distribution function and joint distribution function of $\boldsymbol{X}$ respectively, P is the correlation matrix and ρ is the correlation of X_1, X_2 (unique parameter of P in the bivariate case).

We can similarly define a 2-dimensional t-copula of $\boldsymbol{X} \sim t_d(\nu, \mathbf{0}, P)$ by introducing an additional parameter, namely the degrees of freedom:

$$C^t_{\rho,\nu}(u_1, u_2) = t_{P,\nu}(t^{-1}_\nu(u_1), t^{-1}_\nu(u_2))$$

where t_ν and $t_{P,\nu}$ are the standard univariate t distribution function and joint distribution function of $\boldsymbol{X}$ respectively with ν degrees of freedom, expectation 0 and variance $\frac{\nu}{\nu-2}$, and P is the correlation matrix of X_1, X_2. The degrees of freedom in the t-copula allows to adjust the co-movements of marginal extremes, and that makes t-copulas a popular choice for applications that aim to stress the tail dependencies of risk factors.

The estimation of the parameters $\boldsymbol{\theta}$ of a parametric copula C_θ is performed through maximum likelihood. If $\hat{F}_1, \ldots, \hat{F}_d$ denote estimates of the marginal distribution functions, we can construct a so-called *pseudo-sample* of observations from the copula that consists of the vectors $\hat{\boldsymbol{U}}_1, \ldots, \hat{\boldsymbol{U}}_d$, where

$$\hat{\boldsymbol{U}}_t = (\hat{U}_{t,1}, \ldots, \hat{U}_{t,d})' = (\hat{F}_1(X_{t,1}), \ldots, \hat{F}_d(X_{t,d}))'.$$

The marginal estimate $\hat{F}_i$ is obtained by the semi-parametric approach described in Section 2.3.3.3; the body of the distribution is approached empirically and the tails are given through a generalised Pareto distribution. The MLE is obtained through maximising:

$$\ln L(\boldsymbol{\theta}; \hat{\boldsymbol{U}}_1, \ldots, \hat{\boldsymbol{U}}_n) = \sum_{t=1}^{n} \ln c_{\boldsymbol{\theta}}(\hat{\boldsymbol{U}}_t)$$

with respect to $\boldsymbol{\theta}$, where $\hat{\boldsymbol{U}}_t$ denotes the pseudo-observation from the copula and $c_{\boldsymbol{\theta}}$ is the copula density. A goodness-of-fit test can be further used in order to evaluate whether the data is appropriately modelled. This is performed by comparing the empirical copula with a parametric estimate [53, 113]. We can then sample the vector $\boldsymbol{U}_t = (U_{t,1}, \ldots, U_{t,d})'$ and obtain the marginal distributions, through quantile transformation, that correspond to a defined dependence structure.

2.3.3.3 Tail Behavior Estimates

Stress scenarios aim to describe how the portfolio would perform under extreme market moves, a fact that yields the modelling process of the risk factors' tails crucial. Extreme Value Theory (EVT) approaches are specifically concerned with the asymptotic behavior of the left and right tails separately. The key assumption of EVT is that it considers i.i.d. sequences. The propagation of asymmetric, heavy-tailed characteristics in the GARCH standardised residuals [139] and their strict white noise behavior, allows for EVT application to the tails of their empirical distribution. Combined with

a non-parametric method for the centre, we can explicitly provide the filtered residual distribution for the fitted stochastic models described in Section 2.3.1.1 for further simulations.

There are two main approaches that isolate extreme values, block maxima and threshold exceedance models, with the latter being more useful in practice. This is due to the fact that the former study the time series of maxima of consecutive time-series blocks and therefore might disregard large (and often important) portions of the original dataset. In contrast, threshold exceedance methods study all events that exceed a specified high threshold.

Given a sequence of i.i.d. random values, the Generalised Pareto cumulative distribution function is given by:

$$G_{\xi,\beta}(x) = \begin{cases} 1 - (1 + \frac{\xi x}{\beta})^{-1/\xi}, & \xi \neq 0 \\ 1 - e^{-x/\beta}, & \xi = 0 \end{cases} \tag{2.34}$$

where ξ and $\beta > 0$ denote the shape and scale parameters, $x \geq 0$ when $\xi \geq 0$ and $0 \leq x \leq -\beta/\xi$ when $\xi < 0$. Given that $\xi < 1$, the GPD mean is $E(X) = \beta/(1-\xi)$. We further define the concepts of excess distribution over a threshold u along with the mean excess function, as they both play an important role in EVT. Given a random value X with a GPD cumulative distribution function $F = G_{\xi,\beta}$, the cumulative distribution function of the excess distribution over threshold u is given by:

$$F_u(x) = G_{\xi,\beta(u)}(x) = P(X - u \leq x \mid X > u) = \frac{G_{\xi,\beta(u)}(x+u) - G_{\xi,\beta(u)}(u)}{1 - G_{\xi,\beta(u)}(u)},$$

where $\beta(u) = \beta + \xi u$, $0 \leq x < \infty$ if $\xi \geq 0$ and $0 \leq x \leq -(\beta/\xi) - u$ if $\xi < 0$. The excess distribution remains a GPD with the same shape parameter ξ but with a scaling parameter that grows linearly with the threshold parameter u. The mean excess function of the GPD, describes the distribution of excess loss over the threshold u, given that u is exceeded, and is given by:

$$e(u) = E(X - u \mid X > u) = \frac{\beta(u)}{1-\xi} = \frac{\beta + \xi u}{1-\xi}, \tag{2.35}$$

In this case, $0 \leq u < \inf$ if $0 \leq u < 1$ and $0 \leq u \leq -(\beta/\xi)$ if $\xi < 0$. It can be observed that the mean excess function is linear in the threshold u, which is a characterising property of the GPD and will assist with the choice of u in later sections.

2.4 Research Landscape

As previously outlined, cryptoassets have gained recognition as viable investment options. Their unique characteristic of exhibiting minimal correlation with traditional asset classes, as noted in [10], means that even a modest allocation of cryptoassets in a portfolio can significantly enhance risk-adjusted returns, a point underscored by Burniske and Tatar [29]. Beyond enhancing returns, they also offer potential as a safe haven during financial crises. Despite these advantages, the cryptoasset market has, until recently, grappled with challenges stemming from unclear regulatory guidance. This uncertainty has spanned across various aspects, including the classification of assets, their tax implications, and responses to unique events within the cryptocurrency domain, such as forks.

However, the landscape has begun to shift over the past year, marked by the emergence of more mature and well-defined regulatory frameworks, as highlighted in [64, 121, 134]. This evolution in regulatory clarity has led to a growing institutional interest in cryptoasset-based financial instruments. Delving into these aspects, this thesis aims to navigate through the intricacies of the cryptoasset market, placing a strong emphasis on the development and application of robust financial tools and methodologies suitable for this dynamic and evolving landscape.

On the investment front, pure-crypto indices such as CRIX [138], CRYPTO20 [40], MVDA5 [105], and Bloomberg Galaxy Crypto Index [17] have been instrumental in offering broad market exposure. Yet, these indices are not without their challenges, primarily characterized by volatility levels that mirror those of individual cryptoassets. This reflects a critical limitation in their design – the lack of sophisticated risk control mechanisms beyond the basic strategy of diversification across their highly correlated constituents. Addressing these limitations forms a significant part of the research and analysis presented in this thesis.

Building on the understanding of the limitations and potential of diversified cryptoasset indices, as explored in the preceding section, the concept of stress testing emerges as a critical tool in risk management, especially in the volatile realm of cryptoassets. The origins of stress testing can be traced back to the early 1990s, predominantly utilized by banks for managing risks associated with their trading activities. The idea of using stress testing was only standardised in 1996 by the Basel Committee on Banking Supervision (BCBS) when an amendment was made to the first Basel Accord (Basel I) [7] that recognised stress testing as an effective way to measure risk. In the second Basel Accord (Basel II) [8], the BCBS asked banks to conduct internal stress testing. However, by the time the financial crisis began in 2007, Basel II was not yet fully implemented internationally, and most stress testing models were still in development.

The financial crisis is an example of a useful stress situation, when banks had to restrict their lending and the limitations of standard Value-at-Risk methodologies became apparent. At the time, most banks were not properly prepared to accommodate for this situation, which can be linked

to the lack of scenario-based risk management planning. Post financial crisis, stress testing has increased widely in implementation across jurisdictions and is used by banks, international organisations, national authorities and academics. Stress tests performed by banks are assessing whether there is enough capital on hand to withstand a potential financial disaster or economic crisis and the results are required to be made publicly available.

Stress testing is not only applied on evaluating risks from an organisational and industrial level; it can also be used to test investment portfolios in order to evaluate how they perform under unfavourable economic scenarios. Developing an adequate stress testing methodology, based on realistic market models and well-defined scenarios, is critical in understanding a portfolio's potential risks. Institutions and investors can then mitigate those risks by planning appropriate policies in advance.

In the cryptocurrency industry, while there have been numerous studies of price dynamics [35, 46, 82], there has been a lack of research in risk management for cryptocurrency-related investment products (e.g. cryptocurrency indices, funds, ETPs, etc.). There is, however, a growing awareness of the importance of this issue in the industry. Additionally, the US Federal Reserve is considering adding to their stress testing framework the scenario of a bitcoin market crash [18]. Nonetheless, there is still plenty of work to be done on the already-existing investment products in the cryptocurrency market by the product owners and potentially market supervisors. Hence, a further contribution of this thesis lies in introducing a scenario-based risk management framework tailored for cryptoasset products. We incorporate principles from the existing body of literature in traditional finance, with the goal of enriching the domain of cryptoasset risk management.

Moving beyond stress testing, an alternative approach to evaluating portfolio resilience is the analysis of market regime dynamics. This method focuses on understanding and predicting portfolio performance across diverse market conditions, offering a perspective on how investments respond to shifts in market conditions. Use cases of market regime studies span from Investment Banks who attempt to determine when market regime changes occur (e.g. Morgan Stanley Regime Switching Index, MSCEEMRI) to Central Banks aiming to estimate the occurrence probability of high-stress scenarios [44] in order to signal and mitigate financial risk. Methods including estimation of conditional volatilities are key for risk-monitoring processes and, while the original works of Engle [48] and Bollerslev [20] have been widely adopted and expanded by risk managers, studies highlight the presence of structural breaks in the dynamics of financial time-series.

The first application of regime switching approaches is found in the works of Hamilton [60] which examine how economic activity fluctuates between states of expansion and recession. Since then, Markov-switching approaches have extended to different specifications, with Hamilton and Susmel [61] presenting a conditional hetereoskedasticity (ARCH) setting with a Markov-switching specification in the state alteration. Other extensions are found in the works of Bauwens et al. [11] and Haas [59] which investigate stock market indices and categorise time periods according to volatility

changes. Other applications include attempts to forecast stock prices [62, 145], portfolio allocation methodologies [39, 108] and univariate Value-at-Risk (VaR) estimations [116].

In the cryptoasset space, previous studies have investigated single-regime generalised conditional heteroskedasticity (GARCH) model estimations [35, 45]. The highly volatile nature of cryptoassets has made the original works of Engle [48] and Bollerslev [20] around Generalised Autoregressive Conditional Heteroskedasticity (GARCH) models, a popular choice when evaluating price fluctuations. GARCH-type models are commonly used in financial time series modeling, in cases where time-varying volatility and volatility clustering are observed, and earlier studies have examined their application in the cryptocurrency space as well. Chu et al. [35] examine various specifications of univariate GARCH-type models for twelve, major at the time, cryptoassets and assess them according to their ability to estimate Value-at-Risk. Multivariate settings are also typically considered, with Katsiampa [78] employing an Asymmetric Diagonal BEKK (named after Baba, Engle, Kraft and Kroner [49]) multivariate GARCH setting to examine the individual conditional variances as well as the volatility co-movements of five major cryptocurrencies. Overall, results reject normality and homoskedasticity and time-varying conditional correlations are persistent and positive. Kim et al. [81] also utilise multivariate approaches and examine the relationship between Bitcoin, Gold and the S&P 500 index using a variety of Dynamic Conditional Correlation models (DCC) GARCH specifications. Results demonstrate a positive time-varying relationship between the examined markets.

Nevertheless, the weaknesses of single-regime models have been highlighted in existing literature, with Molnár and Thies [135] detecting structural changes in Bitcoin pricing data. Ardia et al. [5] address the switch in the Bitcoin returns process through a Markov-switching GARCH model (MS-GARCH) whose parameters adapt to variations in the unconditional variance. They show that the 2-state MSGARCH approach in volatility modeling improves one–day ahead VaR predictions. Koki et al. [83] study cryptoasset prices via a Non-Homogeneous Pólya Gamma Hidden Markov (NHPG) model. Their findings identify two states – high and low volatility, with frequent transitions between the two – and the proposed model is characterised by good in-sample performance but poor posterior out-of-sample predictions.

Despite existing research on crypto-market dynamics and the diversification potential of cryptoassets, there remains a gap in understanding how different allocation strategies perform under varying market conditions and align with individual investor goals. Bridging this gap, another goal of this thesis is to apply regime-switching models to identify high-risk market states in diversified crypto portfolios and evaluate the suitability of various strategies for investors with distinct annual return objectives.

The inclusion of cryptoassets in investment portfolios has also been a point of interest in recent studies. One of the main steps of portfolio optimisation is selecting a target function that needs to be optimised. Investors that are interested in mitigating risk, may choose to form a portfolio that is

constructed through minimisation of the standard deviation. Another popular choice is constructing a portfolio that gives the highest expected return per unit of risk. The Sharpe ratio is a metric that is used on this occasion, and is defined as the return divided by the standard deviation of the investment. Maximising the Sharpe ratio produces a "risk-efficient" allocation that is commonly referred to as the tangency portfolio. While the Sharpe ratio is the most commonly used risk–return assessment metric by investors, its main disadvantage is that it accounts only for the first two moments of the returns distribution (average asset return and standard deviation). The Omega ratio [79], defined as the probability-weighted ratio of gains over losses given a specific level of threshold return, is an alternative metric that is used in portfolio theory to address the shortcomings of the Sharpe ratio. Asset allocation methods can also follow simplistic approaches, such as equally-weighted portfolios. Recent studies have examined the applications of the aforementioned principles of modern portfolio theory in investment strategies that include cryptoassets.

In [94], Liu considers ten major cryptoassets and examines the out-of-sample performance of commonly-used asset allocation strategies. Results demonstrate that diversifying across the crypto-market improves risk-adjusted performance, with the equal-weighting scheme achieving the best results in terms of Sharpe ratio. Brauneis and Mestel [23] also assess the risk-adjusted performance of cryptoasset portfolios, based on the traditional Markowitz mean-variance framework. The authors employ different mean-variance strategies to form diversified portfolios of 500 cryptoassets and compare their performance to individual cryptoasset investments. They also consider two benchmarks for performance comparison, an equally-weighted portfolio and the CRIX [138] market capitalisation index. In terms of the Sharpe ratio, they conclude that naïvely diversified portfolios outperform single cryptoasset investments and mean-variance optimised portfolios.

Castro et al. [32] suggest a framework that maximises the Omega ratio. They consider four diversified investment portfolios and conclude that, while crypto-exposure improves returns, it also increases risk. Bedi and Nashier [12] construct diversified portfolios, denominated in USD and converted to GBP, EUR, JPY and CNY and conclude that CNY, JPY and USD portfolios record significantly higher gains if they include Bitcoin. Wu and Pandley [143] also examine the impact of including Bitcoin in a portfolio of stocks, bonds, currencies, real estate and commodities. Results confirm that investors can benefit from holding a small amount of Bitcoin in their portfolios. For a comprehensive overview of cryptocurrency trading-related research, readers can consult the works of Fang et al. [51]

Henriques and Sadorsky [63] refer to gold as a safe haven asset with important diversification capabilities and recognise that its elimination from investment portfolios can potentially negatively impact their risk-return profile. Motivated by the occasional referral to Bitcoin as digital gold, they examine whether Bitcoin can replace physical gold in traditional investment portfolios and how such scenario would impact the risk-adjusted returns. Their approach uses multivariate GARCH models to minimise variance, given a target return and is applied to a US benchmark portfolio

that includes gold and a portfolio that substitutes gold for bitcoin. They conclude that the bitcoin-containing portfolio ranks higher in terms of risk-adjusted returns. Nevertheless, their model assumes daily rebalancings with no restrictions on short sales and is limited in historical data up to 2018, therefore disregarding a large portion of recent market dynamics.

The diversification properties of cryptoassets are also examined by Antipova [2]. Empirical results show that global portfolios display better performance when they utilise the crypto-market as a diversification mechanism. Additionally, it is shown that better results are achieved when portfolios are exposed to multiple cryptoassets rather than solely Bitcoin. Optimization approaches on crypto-containing portfolios have also been studied, with Brauneis et al. [24] examining a traditional mean-variance framework. Castro et al. [32] suggest maximising the Omega ratio when optimising cryptoasset-based portfolios and consider four investment portfolios, two of which contain stock market indices in addition to cryptoassets. They conclude that, while crypto-exposure improves returns, it also increases risk. A detailed, comprehensive overview and analysis of further research work around cryptocurrency trading is presented by Fang et al. [51].

Notwithstanding past studies on crypto-market dynamics and the diversification properties of cryptoassets, their combination with traditional asset classes remains a relatively unexplored topic of discussion. This thesis will be specifically concerned with examining the diversification benefits of commodities for the cryptoasset space, ultimately aiming to gain insight into how their inclusion in cryptoasset portfolios affects the mean-variance frontier.

Chapter 3

Mitigating Risk in Cryptoasset Investments

Bitcoin is foremost amongst the emerging asset class known as cryptoassets. Two noteworthy characteristics of the returns of non-stablecoin cryptoassets are their high volatility, which brings with it a high level of risk, and their high intraclass correlation, which limits the benefits that can be had by diversifying across multiple cryptoassets. Yet cryptoassets exhibit no correlation with gold, a highly-liquid yet scarce asset which has proved to function as a safe haven during crises affecting traditional financial systems. As exemplified by Shannon's Demon, a lack of correlation between assets opens the door to principled risk control through so-called volatility harvesting involving periodic rebalancing. In this chapter we ultimately propose an index which combines a basket of five cryptoassets with an investment in gold in a way that aims to improve the risk profile of the resulting portfolio while preserving its independence from mainstream financial asset classes such as stocks, bonds and fiat currencies. We generalise the theory of Equal Risk Contribution to allow for weighting according to a desired level of contribution to volatility. We find a crypto–gold weighting based on Weighted Risk Contribution to be historically more effective in terms of Sharpe Ratio than several alternative asset allocation strategies including Shannon's Demon. Within the crypto-basket, whose constituents are selected and rebalanced monthly, we find an Equal Weighting scheme to be more effective in terms of the same metric than a market capitalisation weighting.

This chapter was published at the 1st International Conference on Mathematical Research for Blockchain Economy in 2019 [87].

3.1 Background and Methodology

3.1.1 Motivation

Regardless of the creation of new financial products, many investors still see the crypto market as being unacceptably risky due to its high volatility – something not unusual for an emerging asset class. Although volatility poses challenges in terms of increased uncertainty, there are also benefits to be had from its proper management through diversification and regular rebalancing [22]. This is was exemplified in section 2.3.2.1 by the so-called Shannon's Demon approach in which two, ideally uncorrelated, assets – at least one of which is highly volatile – are periodically rebalanced to maintain an ideal target allocation. The resulting expected growth rate is greater than the arithmetic mean of the individual expected growth rates, while the variance of the returns is less than the mean of the individual variances [111, pp. 201–209].

In theory, this strategy would be well-suited for the volatile cryptoasset class and an uncorrelated wealth-preserving asset class. Although there are plenty of candidates to consider, not all are properly suited. For example, traditional wealth-preserving assets such as property or museum-quality fine art are illiquid [115]. An asset such as gold is much more appropriate because of its low volatility, high liquidity and ability to act as a hedge [10, 25, 45]. Gold is also more suitable in this context than other precious metals such as platinum or silver, since the latter, unlike gold, have not historically served as a hedge or safe haven during times of financial turmoil [65].

As reviewed in previous sections, existing pure-crypto indices do not incorporate mechanisms for effective risk control. By contrast, the purpose of the study presented in this chapter, put forth jointly by researchers at Imperial College London and CoinShares, is to propose a low-volatility index that combines an uncorrelated asset (gold) with a basket of cryptoassets, using weighted-risk contribution as a rebalancing mechanism. By decreasing volatility levels, it yields superior risk-adjusted returns when compared to a number of alternative strategies, including holding cryptoassets or gold alone. Further, the proposed index presents a moderate turnover, which translates into moderate operating costs.

3.1.2 From Equal to Weighted Risk Contribution Allocations

One potential concern about the Equal Risk Contribution scheme is that, because it belongs to the family of inverse volatility weighting, it can generate allocations that are too concentrated towards assets with low volatility or low correlation, causing the undesired effect of low diversification inside a portfolio when no constraints are introduced.

This has indeed what happened to many Risk Parity funds. When low rates were set by Central Banks in the most advanced economies, sovereign bonds returns reached an unprecedented low level of volatility and an unconstrained minimisation resulted in an extremely high weight for this

asset class. When Central Banks moved on to raise rates, Risk Parity portfolios found themselves too exposed to that risk and suffered important losses. In this case, when it comes to the weighting of cryptoassets alone, the risk of a similar scenario is somehow less of a concern, because of the similar level of volatility between cryptoassets and because of their high level of correlation.

We can address this issue by allowing the proportion of risk contribution by each asset class to be configurable. As examined in the previous section, following [96], the vector of risk contributions in the two-asset case given weighting $x = (x_1, x_2)$ and correlation ρ is:

$$\frac{1}{\sigma(x)} \begin{pmatrix} x_1^2\sigma_1^2 + x_1x_2\rho\sigma_1\sigma_2 \\ x_2^2\sigma_2^2 + x_1x_2\rho\sigma_1\sigma_2 \end{pmatrix}$$

Considering the case of uncorrelated assets ($\rho = 0$), and supposing that we desire the risk contribution of asset 1 to be α times the risk contribution of asset 2, we need to solve for x_1 in:

$$x_1^2\sigma_1^2 + x_1x_2\rho\sigma_1\sigma_2 = \alpha\left(x_2^2\sigma_2^2 + x_1x_2\rho\sigma_1\sigma_2\right) \overset{\rho=0}{\Rightarrow} \tag{3.1}$$

$$x_1^2\sigma_1^2 = \alpha\left(x_2^2\sigma_2^2\right) \tag{3.2}$$

Given $x_i \in [0, 1]$ and $\sum_{i=1}^{2} x_i = 1$ this yields:

$$x_1 = \frac{\sqrt{\alpha}\,\sigma_1^{-1}}{\sqrt{\alpha}\,\sigma_1^{-1} + \sigma_2^{-1}} \tag{3.3}$$

In the next sections we present how the weighted risk contribution scheme can be utilised in the creation of an index product, where x_1 will represent the proportion of the investment allocated towards a basket of cryptoassets whose components are equally weighted, while x_2 is the proportion invested in gold. The risk contribution ratio is set as $\alpha = 4$, indicating that 80% of the total risk emanates from the crypto-basket.

3.2 Applications

3.2.1 CGCI: Balancing Physical and Digital Gold

CoinShares Gold and Cryptoassets Index The research presented in this chapter led to the launch of the CoinShares Gold and Cryptoassets Index (CGCI), the first EU Benchmark Regulations (EU BMR) compliant index for the digital asset industry that combines digital assets and gold. The CGCI is available on Bloomberg and Refinitiv (formerly Reuters) under the ticker symbol COINCGCI and .COINCGCI, respectively[1].

3.2.1.1 Design Goals

In this section we present how the concepts of the previous chapters can be used to design an index product for the digital asset space. The general aim is to propose a solution for investors that wish to gain diversified exposure to the cryptoasset space, in a way that yields a superior risk-return profile when compared to holding such assets in isolation, while being orthogonal to traditional financial markets. The objective the study is the design and implementation of an index that should meet the following goals:

1. Provide exposure to the alternative asset space in a way that is orthogonal to traditional financial markets;
2. Be comprised of a small number of liquid, investable constituent assets;
3. Exhibit a relatively stable composition in terms of constituents with asset weights that do not vary dramatically between rebalancing periods, leading to low or moderate turnover;
4. Utilise some means of principled risk control leading to lower volatility;
5. Be specified in a clear and unambiguous manner to facilitate validation and reproducibility;
6. Hold constituent assets on a long-only basis;
7. Not make use of leverage.

In terms of Goal 4, historical volatility of cryptoassets has remained at much higher levels compared to other asset classes while correlation among single non-stablecoin cryptoassets is persistent, displaying some signs of time variability. Therefore, constructing an index constituted only of cryptoassets offers very little prospect of diversification irrespective of the methodology used and hence, less prospect of bringing down its volatility. Gold returns, on the other hand, have been much less volatile than those of cryptoassets and have displayed a very low time varying correlation with cryptoassets (see Fig. 3.1). Gold was therefore the ideal candidate to include alongside cryptoassets with the purpose of considerably reducing volatility.

[1] A full index methodology document has been made available online by the index owner, CoinShares (Holdings) Limited (www.coinshares.com), and the Benchmark Administrator and Calculation Agent, Compass Financial Technologies (www.compassft.com).

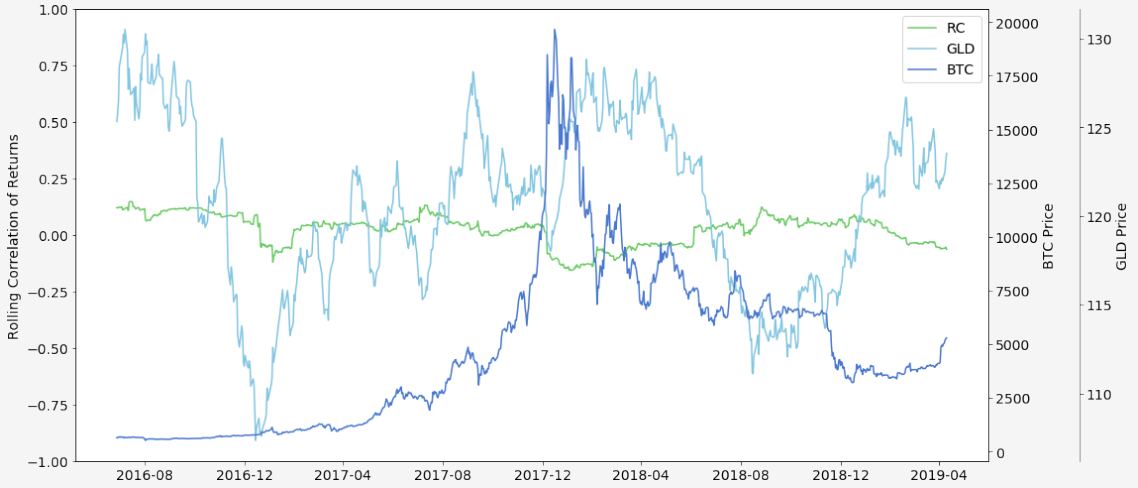

Figure 3.1: 180-Day Rolling correlation (RC) between daily returns of Bitcoin (BTC) and Gold (GLD)

3.2.1.2 Constituent Eligibility and Selection

The index is composed of a fixed number of constituents including five cryptoassets and SPDR Gold Shares (GLD), the largest gold ETF. The cryptoasset constituents of the index are the top five eligible cryptoassets based on the 6-month rolling mean of free-float market capitalisation. By restricting the index to the top five cryptoassets we are less likely to encounter liquidity issues. Selection of constituents occurs on a monthly basis.

We determine whether a cryptoasset is eligible to be selected, based on the following requirements:

1. Trades in USD;
2. Is not linked to the value of a fiat currency;
3. Has at least a 6-month history of trading on a reputable exchange;
4. Has been on its native blockchain for at least 6 months;
5. Is not an ERC20 token;
6. Is not a privacy-focused coin (e.g. Monero, ZCash);
7. Has not suffered a major chain reorganisation in the last 6 months, and is not subject to a forthcoming contentious hard fork before the next selection is due to take place.

3.2.1.3 Constituent Weighting

For the weighting of the constituents, we choose a bi-level approach that involves studying the historical volatilities of the crypto-basket and gold separately in order to inform the crypto–gold asset allocation decision. That is because if GLD is added to a basket of five cryptoassets for a global allocation scheme, the correlation structure between all six assets cannot be ignored and the constituents' weighting procedure cannot be performed through Eq. (2.19) directly. Also, in

order to be able to produce a robust estimation of covariance matrices, the behaviour of the two asset classes would have to be studied only in time spans where exchanges for both are open. The bi-level approach on the other hand allows for exploitation of all available market data.

Regarding the formation of the crypto-basket, due to the persistent levels of correlation between non-stablecoin cryptoassets, any Risk Parity approach is expected to lean towards an Equally Weighted allocation whose risk level is not significantly improved. Therefore, due to its much more convenient reproducibility compared to Eq. (2.20) and the fragility of Eq. (2.20) when the covariance matrix is barely positive semi-definite, an Equally Weighted scheme is employed within the crypto-basket.

Taking into consideration the former, and the lack of a significant correlation between gold and cryptoassets, the index is calculated following a two-stage allocation scheme that involves:

1. Computation of the historical volatility of (a) the equally weighted crypto-basket, and (b) gold;
2. Asset allocation among the crypto-basket and gold expressed as the bivariate weighted risk contribution problem presented in Section 3.1.2.

3.2.1.4 Rebalancing Schedule

In order to capture the diversification benefits of the time-varying correlations between gold and crypto highlighted in Figure 3.1, a monthly rebalancing frequency is chosen. This is coupled with the monthly reselection of the top five eligible cryptoassets in terms of rolling free-float market capitalisation. This approach allows the index to represent the rapidly evolving market conditions. Additionally, the rebalancing frequency is low enough to ensure that there is no dramatic impact on the turnover of the cryptoasset portfolio and hence transaction costs can be maintained at an acceptable level.

3.2.1.5 Index Calculation

The Index base level is set on 1 000 on January 1st, 2016:

$$\text{Index}_0 = 1\,000 \tag{3.4}$$

The Index level on day t from January 2nd, 2016 onwards is calculated as:

$$\text{Index}_t = \frac{\sum_{i \in N_t} P_{i,t} \times x_{i,t}}{D_t} \tag{3.5}$$

where

- N_t is the set of the 6 selected assets (5 cryptocurrencies and gold) on day t
- $P_{i,t}$ is the closing price for asset i on day t expressed in USD

- $x_{i,t}$ is the weight of asset i on day t as computed through the WRC allocation scheme at the beginning of the month
- D_t is the Index Divisor on day t

The Index Divisor is used so that assets weight rebalancing and substitution do not alter the Index level. It is calculated using the following formula:

$$D_t = \frac{\sum_{i \in N_t} P_{i,t-1} \times x_{i,t}}{\sum_{i \in N_{t-1}} P_{i,t-1} \times x_{i,t-1}} \times D_{t-1} \tag{3.6}$$

The Divisor on January 2nd, 2016 is calculated as:

$$D_1 = \frac{\sum_{i \in N_1} P_{i,0} \times x_{i,1}}{1\,000} \tag{3.7}$$

where

- N_1 is the set of the selected assets on January 2nd, 2016
- $P_{i,0}$ is the closing price for asset i on January 1st, 2016 expressed in USD
- $x_{i,1}$ is the weight of asset i on January 2nd, 2016

Equations (3.5 – 3.7) are equivalent to computing recursively the value of the Index using the weighted average of its constituent's returns:

$$\text{Index}_t = \sum_{i \in N_t} \frac{P_{i,t}}{P_{i,t-1}} x_{i,t} \times \sum_{i \in N_{t-1}} \frac{P_{i,t-1}}{P_{i,t-2}} x_{i,t-1} \times \cdots \times \sum_{i \in N_1} \frac{P_{i,1}}{P_{i,0}} x_{i,1} \times 1\,000 \tag{3.8}$$

This implies:

$$\text{Index}_t = \sum_{i \in N_t} (1 + R_{i,t})\, x_{i,t} \times \text{Index}_{t-1}, \quad t = 1, 2, \ldots \tag{3.9}$$

where

- $R_{i,t}$ is the return of asset i from time $t-1$ to time t
- Index_0 is the base level of the Index set at 1 000 on January 1st, 2016

Figure 3.2 shows how the index value would have evolved over the period January 2016 to April 2019. A detailed breakdown and comparison of index performance is presented in Section 3.2.2.

3.2.1.6 Hard Fork and Airdrop Policy

Hard Fork Policy A 'Hard Fork' occurs when a change is made to the transaction validation rules of a cryptoasset's underlying blockchain protocol in a way that is not compatible with its earlier version. Nodes that wish to continue to participate are expected to upgrade to the new version of the protocol's software. Usually such a fork is planned and accepted by the overwhelming

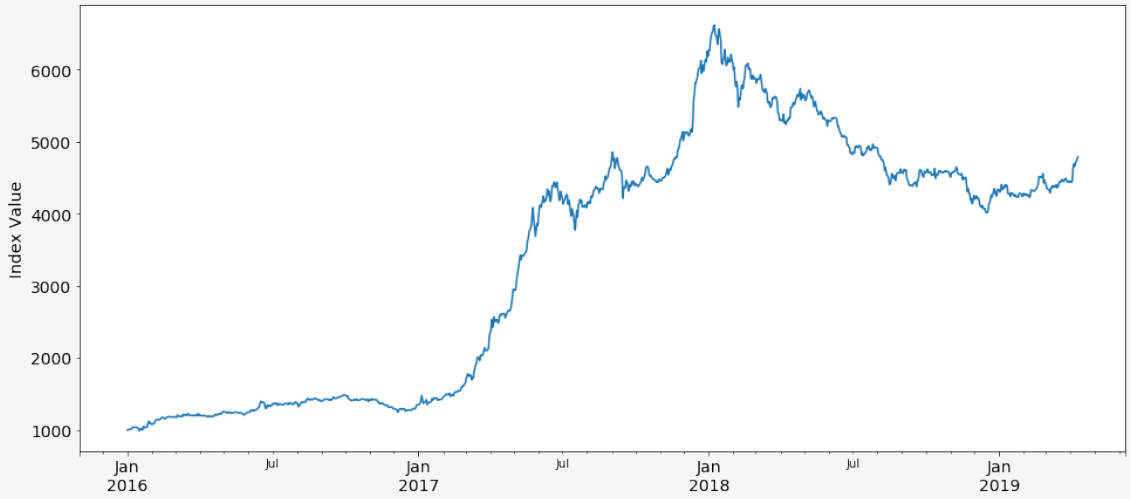

Figure 3.2: Index Value January 2016–April 2019

majority of nodes. However, where the fork is contentious enough that a non-negligible number of nodes continue to run the old version of the software, a chain split occurs.

The index features a Governing Committee which will evaluate all upcoming hard forks, especially in light of Rule 7 of Section 3.2.1.2. Treatment of hard forks are led by decisions of exchanges with respect to the ticker symbols used to represent the resulting cryptoassets and the markets that they maintain. Concretely, suppose some cryptoasset traded under ticker symbol T is expected to undergo (or undergoes) a hard fork resulting in an original chain C with cryptoasset C_a and a modified chain C' with cryptoasset C'_a.

There are a few scenarios to consider:

Scenario A C_a continues to trade under ticker symbol T while C'_a starts trading under a newly-created ticker symbol T'. The BTC–BCH fork is an example of this scenario. In this case, C_a continues as a constituent of the index. C'_a is not eligible to become a constituent of the index (lacking as it does the necessary pricing history), and does not contribute to the index value. C'_a may be sold by funds tracking the index as an excess return; the precise decision of when (or whether) to sell will be a matter of judgment for the tracking funds.

Scenario B C'_a now trades under ticker symbol T while C_a starts trading under a new ticker symbol T'. The ETH–ETC fork is an example of this scenario. In this case, C'_a replaces C_a as a constituent of the index. The pricing history for C'_a is taken as being that of C_a prior to the fork. C_a is no longer a constituent of the index, does not contribute to the index value, and may be sold by funds tracking the index as an excess return.

Scenario C C'_a now trades under ticker symbol T while trading in C_a is (largely) abandoned. Hard forks to upgrade the consensus mechanism of Monero usually follow this pattern. In this case, C'_a replaces C_a as a constituent of the index and the pricing history for C'_a is taken as being that of C_a prior to the fork.

Scenario D There is substantial disagreement amongst exchanges as to the ticker symbols that C'_a and C_a should trade under. Usually this scenario would arise as the result of a contentious hard fork. Since cryptoassets due to undergo contentious hard forks before the next selection date are not eligible for selection, it is expected that this situation would apply to index constituents only in very rare circumstances. In this case, an extraordinary meeting of the Governing Committee will be convened in order to decide on an appropriate course of action which may include replacing C_a by the next eligible cryptoasset, or rebalancing across the remaining constituent cryptoassets.

Airdrop Policy An 'Airdrop' occurs when a blockchain project distributes free cryptoassets to investors in the hopes of attracting more people to use their platform. Occasionally some projects offer more established cryptoassets to do an Airdrop but most of the time, the project Airdrops their own native token or cryptocurrency. Requirements to qualify for an Airdrop vary as well; in some cases the participant has to hold the cryptoasset in their wallet while other times they have to promote the project on an online forum.

Airdropped cryptoassets are not included in the index. Fund managers tracking the index may sell these at their earliest convenience, contributing to excess returns over the base index.

3.2.2 Performance Evaluation

3.2.2.1 Methodology and Data Source

In order to evaluate the effectiveness of a Weighted Risk Contribution (WRC) strategy in the cryptoasset and gold case, the performance of a respective risk distribution portfolio is measured and compared against various strategies including buy-and-hold bitcoin (BTC), buy-and-hold gold (GLD), market capitalisation weighted pure cryptoassets, Shannon's Demon using bitcoin and gold, and Equal Risk Contribution (ERC) cryptoassets. The dataset used for the implementation and backtesting of the described allocation method includes daily values of historical free float market capitalisation and USD prices for more than 3 000 cryptoassets, obtained from CoinGecko as well as daily adjusted USD prices of SPDR Gold Shares (GLD). The backtest that is performed covers the period between January 2016 and April 2019, a time span that reflects a wide variety of market conditions for the cryptoasset space. The datasets produce daily returns for both asset classes and assumes monthly rebalancing for all active strategies.

Table 3.1 shows the results of monthly selection of cryptoasset constituents that meet the eligibility criteria. Note that only dates where the constituents change are presented. BTC consistently appears as a leading constituent, underscoring its dominance and acceptance in the crypto market. The entry of ETH in March 2016 is significant, reflecting its rising popularity after its introduction. The subsequent consistent presence of BTC and ETH in the top spots indicates the market preference for established, well-known assets. Similarly, XRP and LTC maintain a frequent presence, suggesting their robust positions as well. We further notice some fluctuation in the fifth constituent, alternating among DASH, ETC, BCH and others. This variability highlights the competitive and volatile nature of the market.

Table 3.1: Top 5 Eligible Cryptoassets – Monthly Reselection

Date	Constituent 1	Constituent 2	Constituent 3	Constituent 4	Constituent 5
2016-01-01	Bitcoin (BTC)	Ripple (XRP)	Litecoine (LTC)	Dash (DASH)	Dogecoin (DOGE)
2016-03-01	BTC	XRP	LTC	Ethereum (ETH)	DASH
2017-02-01	BTC	ETH	XRP	LTC	Ethereum Classic (ETC)
2017-04-01	BTC	ETH	XRP	LTC	DASH
2017-07-01	BTC	ETH	XRP	LTC	ETC
2017-09-01	BTC	ETH	XRP	LTC	DASH
2018-03-01	BTC	ETH	XRP	Bitcoin Cash (BCH)	LTC
2018-11-01	BTC	ETH	XRP	Stellar (XLM)	LTC
2019-01-01	BTC	ETH	XRP	BCH	EOS (EOS)

The crypto-basket composition is defined according to an Equally Weighted scheme, whose historical returns and volatility are studied towards the dynamic allocation between the cryptoassets and gold. We opt for a WRC allocation scheme between the two classes. Given the historical level of correlation between gold and crypto assets, an equal risk distribution among the two asset classes would be expected to be heavily concentrated towards gold as the lower volatility asset. Nevertheless, the chosen WRC setting, with a risk ratio that results to 80% of the total risk emanating from the crypto-basket component ($\alpha = 4$), ensures a good level of diversification, balancing the two components in the denominator of Eq. 3.3, as seen in Figure 3.3.

The blue bars in Figure 3.3 represent the risk contribution-based allocation of the crypto-basket to the overall portfolio. Despite the inherent volatility of cryptoassets, the allocation remains substantial, due to the chosen WRC setting. This highlights the index's strategic emphasis on cryptoassets, aligning with the interests of investors seeking to gain exposure to the market. The orange bars denote the respective derived allocation in gold. While less volatile, gold's risk contribution is managed to complement that of the crypto-basket, ensuring that it does not dominate the risk profile of the portfolio despite its inherent stability.

Throughout the observed period there are some fluctuations in the risk contribution weights for both asset classes. This reflects the dynamic adjustments made in response to changes in market conditions and volatility across the two asset classes. Despite the fluctuations, the overall strategy

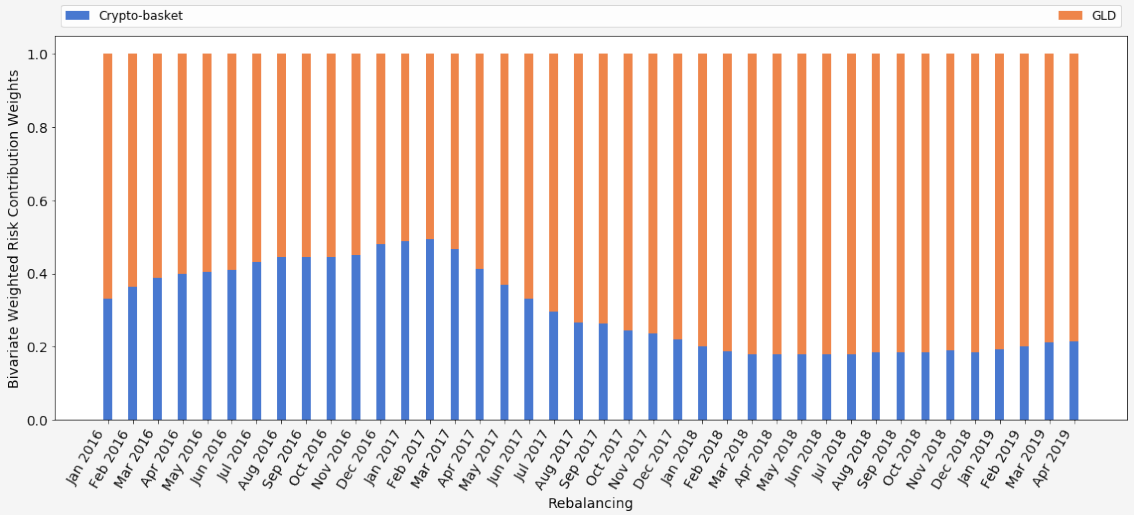

Figure 3.3: Weighted Risk Contribution Allocation – EW Crypto Basket Base – $\alpha = 4$

appears consistent with the objective of maintaining a crypto-basket risk contribution of approximately 80%. The strategy's responsiveness to market conditions suggests that it is designed to adapt to varying levels of volatility which is particularly important in the crypto market, known for its rapid changes. Overall, the historical allocations demonstrate the WRC scheme's ability to adapt and maintain the desired risk exposure over time.

3.2.2.2 Analysis and Results

The results obtained from the bivariate WRC allocation with an EW crypto-basket base (WRC-EW Base) are directly compared with the following:

1. Bivariate WRC allocation with a 6-month rolling mean Market Capitalisation weighted crypto-basket base (WRC-MC Base)
2. Equally-weighted cryptoassets (EW)
3. Market capitalisation weighted cryptoassets (MC)
4. Equal Risk Contribution weighted cryptoassets (ERC)
5. Bitcoin and GLD weighted in accordance with the Shannon's Demon (SD)
6. Bitcoin only (BTC)
7. Gold only (GLD)

As seen in Table 3.2 and Figure 3.4, the proposed allocation scheme outperforms the rest in terms of historical risk-adjusted returns, as measured by the Sharpe Ratio, indicating that the risk taken is well-compensated by the returns.

Moreover, a comparison with a typical index profile of the cryptoasset space, namely the MVIS Digital Assets 5 Index [105] (MVDA5) – a market capitalisation weighted index which tracks the performance of the five largest and most liquid cryptoassets – also reveals superiority in terms

of the risk–return profile. Annualised returns are higher than a buy-and-hold GLD-only investment while annualised volatility levels are much lower than the crypto-market's. The ERC and EW present similar behaviour due to the assets' correlation structure; similarly, passive bitcoin and Market-Cap driven strategies do not reveal major differences.

Table 3.2 also reports portfolio turnover, which reflects the total proportion of portfolio value traded (bought and sold) while rebalancing the portfolio, on an annualised basis as defined in [41]. The ERC and EW strategies exhibit the highest turnover, implying frequent rebalancing, which could result in higher transaction costs. This factor should be considered when interpreting their high returns.

The bivariate WRC allocation's performance is characterised by significantly lower volatility, and a more stable risk profile. While some strategies may offer high returns, they often come with increased volatility and turnover which can impact net performance. Overall, The WRC-EW Base scheme appears to offer a particularly effective balance of risk and reward.

Table 3.2: Annualised Performance of Allocation Schemes , Jan 2016–Apr 2019

Allocation Scheme	Annualised Returns	Annualised Volatility	Annualised Sharpe Ratio	Annualised Turnover
WRC-EW Base	0.4797	0.2411	1.9894	1.6906
WRC-MC Base	0.3199	0.2318	1.3800	1.1196
ERC	0.9878	0.8062	1.2253	2.8512
EW	1.0284	0.8292	1.2252	2.9556
MC	0.6734	0.7560	0.8908	1.2240
SD	0.4085	0.3889	1.0502	1.0800
BTC	0.7629	0.7680	0.9934	0.0000
GLD	0.0812	0.1452	0.5591	0.0000
MVDA5	1.1160	0.8757	1.2744	Not Computed

The stability of the strategy's performance is further reflected in Figure 3.5. In 2016, ERC and EW appear to have the highest volatility while GLD exhibits the lowest, which is consistent with gold's reputation as a stable asset. The volatility trends seem to continue in 2017, with ERC and EW showing high volatility. The volatility of BTC has noticeably increased, indicating a turbulent year for Bitcoin. Similarly in 2018, ERC and EW exhibit high volatility. Most allocation schemes show increased volatility compared to previous years, possibly suggesting a more volatile market environment overall.

In terms of annualised returns, the crypto-heavy EW allocation scheme stands out with the highest returns in 2016, followed by ERC. The WRC-EW Base and WRC-MC Base show modest returns, while GLD shows very low levels of returns. In 2017, returns for all allocation schemes continue to be positive, with EW and ERC leading. A drastic change is observed during 2018, where all schemes except GLD show negative returns, indicating a challenging year for all assets. GLD's return being close to zero, could be seen as a relative safe haven during this turbulent period.

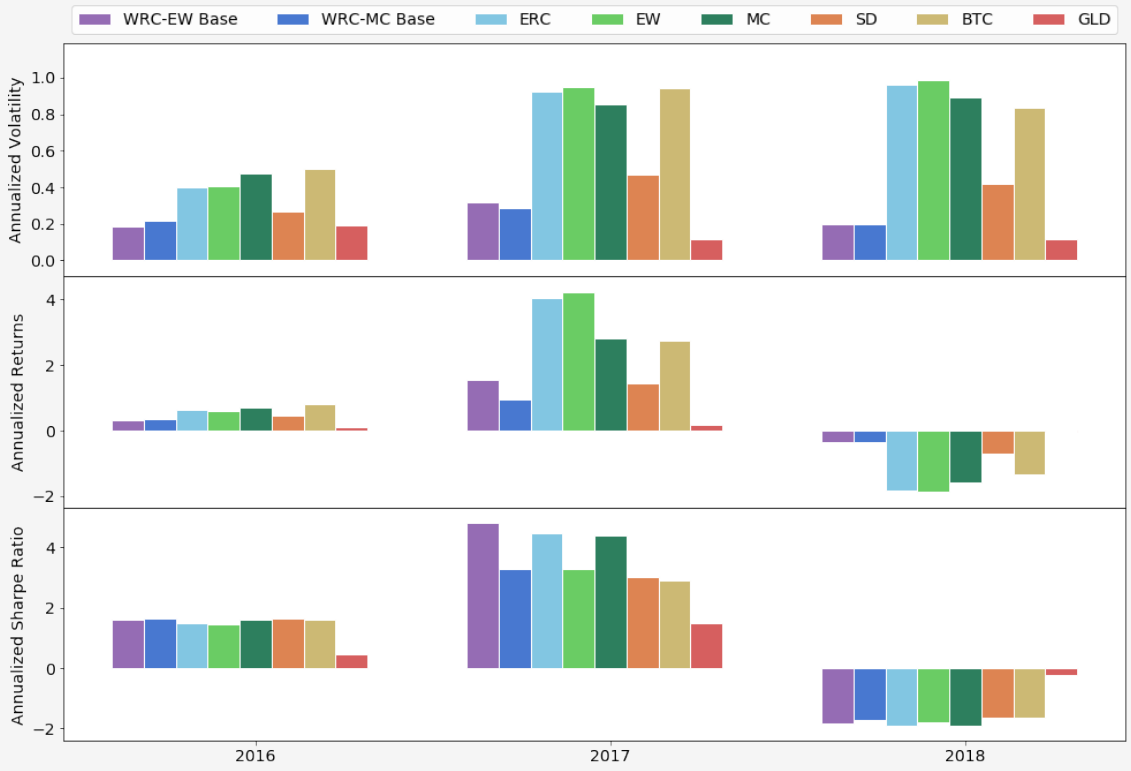

Figure 3.4: Annualised Returns, Volatility & Sharpe Ratio Jan 2016–Dec 2018

In terms of risk-adjusted performance, the WRC-MC Base exhibits the highest Sharpe ratio (albeit marginally), suggesting a superior performance. All schemes have positive Sharpe ratios, indicating favorable returns per unit of risk. A similar picture is observed for 2017. The Sharpe ratios higher lower across all allocation schemes, with WRC-EW Base leading, still by a small margin. The Sharpe ratios turn negative for all schemes in 2018, with GLD having the least negative ratio. This indicates that none of the strategies provided positive returns over the risk-free rate, reflecting a difficult market year.

While 2018 is an interesting period to evaluate, it is important to note that a negative Sharpe ratio is difficult to interpret because the metric is designed to measure excess returns per unit of risk taken above the risk-free rate. When the investment's returns are less than the risk-free rate, resulting in a negative Sharpe ratio, it suggests that the investment has underperformed on a risk-adjusted basis, but it does not provide a clear measure of the investment's risk relative to its negative return. Moreover, a negative Sharpe ratio does not indicate the magnitude of the underperformance or risk, making it challenging to use as a comparative tool for investment performance. In the next chapters we will introduce more robust methodologies to assess performance.

Figure 3.5 displays the performance of the aforementioned strategies over a span of more than three years, highlighting the trajectories of cumulative returns and the depth of drawdowns. In terms of returns, the ERC and EW portfolios dominate the chart, highlighting their performance

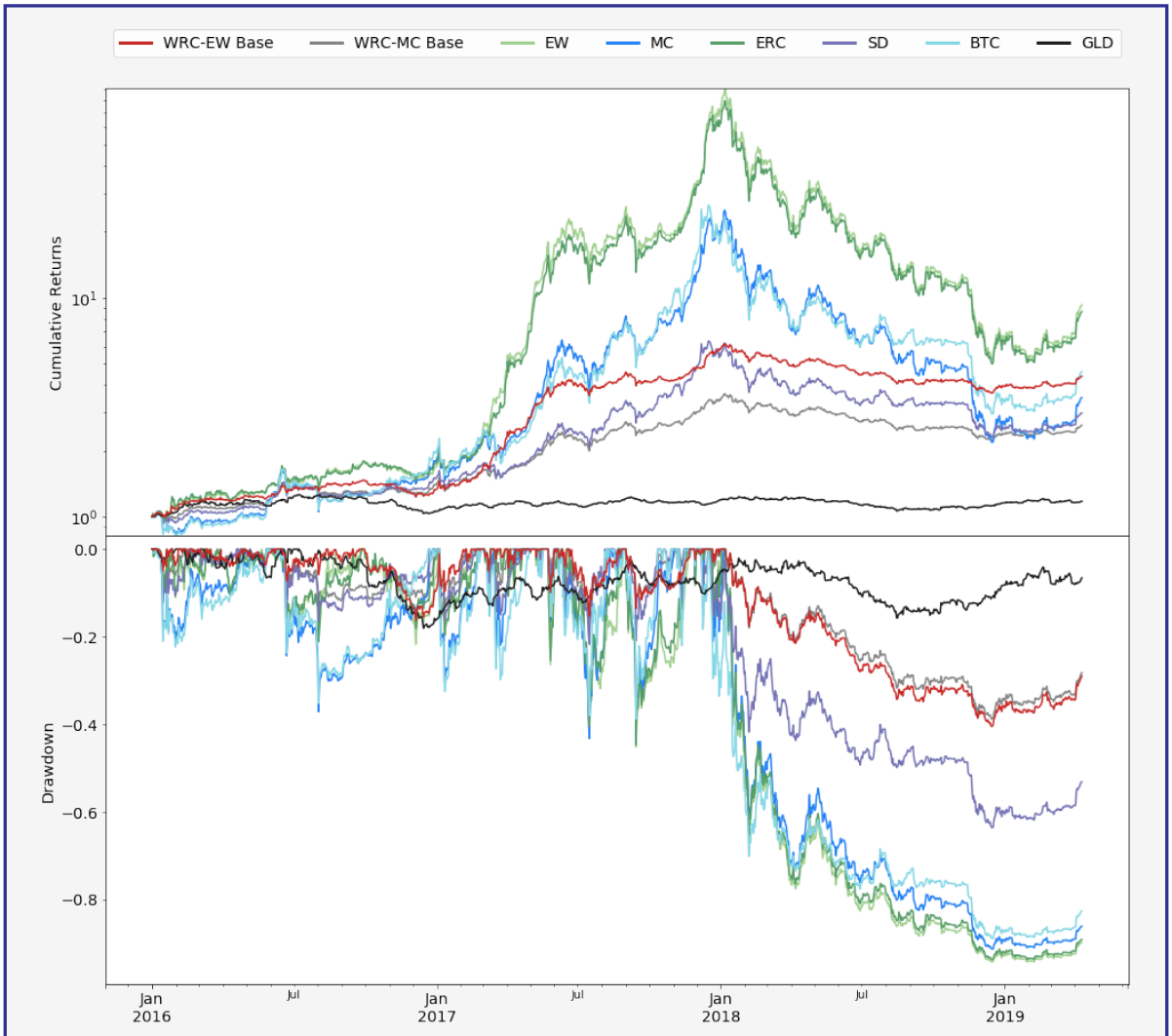

Figure 3.5: Cumulative Returns & Drawdown Jan 2016–Apr 2019

through most of the observed period. However, their success comes with the caveat of significant volatility, as seen in the drawdown portion of the graph, where these strategies also register the steepest declines from their peaks. On the other hand, gold stands out for its stability. Although it does not match the soaring highs of ERC or EW, it also does not succumb to the same lows, maintaining a relatively flat line throughout the period. This reflects gold's historical role as a safe haven asset. BTC, true to the crypto-market's reputation, oscillates dramatically, with sharp increases in cumulative returns that are susceptible to equally rapid declines.

The WRC-EW Base and WRC-MC Base settings demonstrate a more stable and consistent growth trajectory with moderate cumulative returns and relatively contained drawdowns. This is further confirmation that the WRC setting succeeds to smooth out the volatility associated with the cryptoasset market.

3.2.3 Summary

In this chapter we have proposed the construction of an index that offers investors exposure to alternative assets. By exploiting the characteristics of the two asset classes of cryptoassets and gold – namely the extremely high volatility of the former, the low volatility of the latter and the lack of correlation between the two – it is characterised by an attractive ability to reduce price instability while raising the average return per unit of volatility. By generalising the theory of equal risk contribution, one can obtain a sophisticated, albeit intuitive, way of tuning the exposure of an index to uncorrelated asset classes. Another important feature of the index lies in the associated moderate turnover, which translates into moderate operating costs. Finally, by taking into account a variety of events unique to the cryptoasset space such as hard forks and airdrops and by proposing corresponding policies, the end result is an investable product whose distinctive elements make it a unique form of investment.

Chapter 4

Stress Testing Cryptoasset Portfolios for Resilience

Stress testing involves the use of simulation to assess the resilience of investment portfolios to changes in market regimes and extreme events. The quality of stress testing is a function of the realism of the market models employed, as well as the strategy used to determine the set of simulated scenarios. In this chapter, we consider both of these parameters in the context of diversified portfolios, with a focus on the emerging class of cryptoasset-containing portfolios. Our analysis begins with univariate modelling of individual risk factors using ARMA and GJR–GARCH processes. Extreme Value Theory is applied to the tails of the standardised residuals distributions in order to account for extreme outcomes accurately. Next, we consider a family of copulas to represent the dependence structure of the individual risk factors. Finally, we combine the former approaches to generate a number of plausibility-constrained scenarios of interest, and simulate them to obtain a risk profile. We apply our methodology to the presented CoinShares Gold and Cryptoassets Index, a monthly-rebalanced index which comprises two baskets of risk-weighted assets: one containing gold and one containing cryptoassets. We demonstrate a superior risk-return profile as compared to investments in a traditional market-cap-weighted cryptoasset index.

This chapter was published at the 2nd International Conference on Mathematical Research for Blockchain Economy in 2020 [84].

4.1 Background and Methodology

4.1.1 Motivation

As mentioned in section 2.4, beyond its traditional use in banking, stress testing has become an essential tool for assessing investment portfolios. The process of stress testing involves developing methodologies grounded in realistic market scenarios to assess and mitigate potential risks. In the cryptocurrency sector, despite extensive research on price dynamics, there remains a notable void in risk management for cryptoasset investment products. This gap is increasingly recognized within the industry, with steps like the US Federal Reserve contemplating the inclusion of a bitcoin market crash scenario in their stress tests. On that note, the primary analysis target in this chapter is the CoinShares Gold and Cryptoassets Index (CGCI). In the case of the CGCI, the goal is to isolate its main design principles and propose a framework for scenario-based risk management that is able to unveil vulnerabilities in certain market conditions.

In the case of CGCI, we identify two main risk factors (the crypto-basket and gold component respectively) and we attempt to model their evolution using stochastic processes. The credibility of results when we apply risk measures to the portfolio distribution, is heavily dependent on the choice of model, and as highlighted by Nyström et al. [109], one should consider a series of stylised facts when simulating the evolution of risk factors. McNeil et al. [100] discuss those stylised facts that characterise the returns of financial time series which can also be observed in the CGCI components. The following sections discuss the design of a stress testing framework, directly applicable to cryptoasset portfolios.

4.1.2 Multivariate Stress Testing of Cryptoasset Portfolios

The concepts described in Section 2.3 are combined towards a scenario generation framework that combines sophisticated statistical methods with financial risk modeling techniques. Starting with the construction of a risk factor vector and proceeding to model fitting using asymmetric ARMA-GARCH models, the framework can capture both typical market conditions and the asymmetry often observed in financial time series data. By leveraging the flexibility of copulas to model dependency structures separately from the marginal distributions, the framework can more accurately reflect the complex interactions between different risk factors.

The scenario generation process is particularly notable for its robustness. It employs a Monte Carlo simulation approach to generate a wide range of potential future states, enabling a thorough exploration of the risks faced by a portfolio over different time horizons. This method also allows for the empirical estimation of the distribution of returns, taking into account the heavier tails often encountered in financial return distributions. Once the potential future states of risk factors are generated, they are translated into standardized innovations to drive the ARMA-GARCH

models, which then simulate paths for each risk factor. The final step of translating these into portfolio paths and P&L distributions provides a clear, actionable output for stress testing. Overall, the framework's integration of empirical distribution fitting with simulation techniques will offer a comprehensive tool for assessing and managing financial risk.

The overall framework can be summarised in the following steps:

Model Fitting

1. Define the d-dimensional risk factor vector $\boldsymbol{X}_t = (X_{t,1}, \ldots, X_{t,d})'$, observable at time t, and obtain the logarithmic returns time series $\boldsymbol{r}_t = (r_{t,1}, \ldots, r_{t,d})'$
2. Fit an appropriate asymmetric ARMA–GARCH model to $\boldsymbol{r}_t$, and obtain the standardised residuals $\hat{\boldsymbol{Z}}_t = (\hat{Z}_{t,1}, \ldots, \hat{Z}_{t,d})'$
3. Estimate the marginal distribution functions $F_1(Z_1), \ldots, F_d(Z_d)$ of the i.i.d. standardised residuals, empirically for the body and with a GPD for the tails
4. Transform $\hat{\boldsymbol{Z}}_t$ to uniform variates $\hat{\boldsymbol{U}}_t = (\hat{U}_{t,1}, \ldots, \hat{U}_{t,d})'$ by inversion
5. Estimate parameters $\boldsymbol{\theta}$ of an appropriate copula $C_{\boldsymbol{\theta}}$ with MLE, given the pseudo-observations $\hat{\boldsymbol{U}}_t$

Scenario Generation

1. For a given sample size m, horizon n and parameters $\boldsymbol{\theta}$, simulate $n \times m$ points of the random vector $\boldsymbol{U} = (U_{t,1}, \ldots, U_{t,d})'$, with distribution function $C_{\boldsymbol{\theta}}$
2. Given the margins $F_1, \ldots, F_d$ from step 3 of the fitting process, use quantile transformation to translate to $\boldsymbol{Z}_t = (F_1^{\leftarrow}(U_{t,1}), \ldots, F_d^{\leftarrow}(U_{t,d}))'$
3. Provide the $n \times m$ standardised innovations matrix pairs to the calibrated ARMA–GARCH models and simulate m paths for each risk factor, $\boldsymbol{X}_{t,\ldots,t+n}$
4. Given the risk factor mapping $V_t = f(t, \boldsymbol{X}_t)$ and the simulated returns, construct m portfolio paths and obtain the P&L distribution

In regards to step 2 of the model fitting process, we selected the GJR-GARCH model to capture volatility, as described in section 2.3. This approach was chosen due to its robust capability in capturing asymmetries and persistence in volatility, phenomena commonly known as volatility clustering.

When examining the credibility of stress test results, plausibility is an important quality criterion that has been studied extensively by existing literature [26, 104, 136]. The problem setting in the former studies consists of a set of elliptically distributed risk factors $\boldsymbol{X}_t$, a set of scenarios that represent factor movements, and a linear P&L function (dependent on a fixed weighting scheme and the aforementioned scenarios). The Mahalanobis distance is introduced as tool that can restrict scenarios, based on a desired level of plausibility, while respecting the elliptical symmetry.

Authors utilise this concept to define the most likely scenarios given a pre-defined quantile of loss and extend it to meta-elliptical distributions and non-linear P&Ls.

In this study, the ultimate goal is to observe variations in the P&L distribution on a longer horizon; we do not examine the intersection of iso-P&L lines with iso-plausibility ellipses. Nevertheless, we utilise the concept of excluding scenario outliers, as it can bolster the credibility of long-horizon simulations. To this end, preceding step 5 of the described scenario generation procedure, for each set $\boldsymbol{X}_{t,\ldots,t+n}$, we obtain P&L sets $\mathrm{PL}_1, \ldots, \mathrm{PL}_d$; we compute the robustly estimated Mahalanobis distance $\mathrm{MD}(\mathrm{PL}_i)$ and filter out all samples that exceed a pre-specified percentile of the underlying Chi-Squared distribution of MD.

A schematic diagram that summarises the scenario generation procedure in a 2-dimensional risk factor environment is presented in Fig. 4.1. This visual summary begins with a copula simulation, where the fitted two-dimensional copula generates simulated values of the two uniform variates $U_{t,1}$ and $U_{t,2}$. These are then transformed through their respective marginal cumulative distribution functions $F_{t,1}$ and $F_{t,2}$ to obtain the standardised residuals $Z_{t,1}$ and $Z_{t,2}$. Residuals are fed into the separately fitted ARMA–GARCH models to simulate the factor returns, presented in the left and right sides of the middle row of the diagram.

The central plot combines the two simulated factor returns and forms a baseline scenario. The baseline scenario plot is enhanced by an overlay of the Mahalanobis distance contours, which aim to filter out implausible extreme scenarios, ensuring that the simulated paths stay within a plausible range. Once a cut-off point has been chosen and extreme values have been separately eliminated, the process leads to the final cumulative distribution function of the P&L, which gives a visual representation of the likelihood of different levels of portfolio loss or gain.

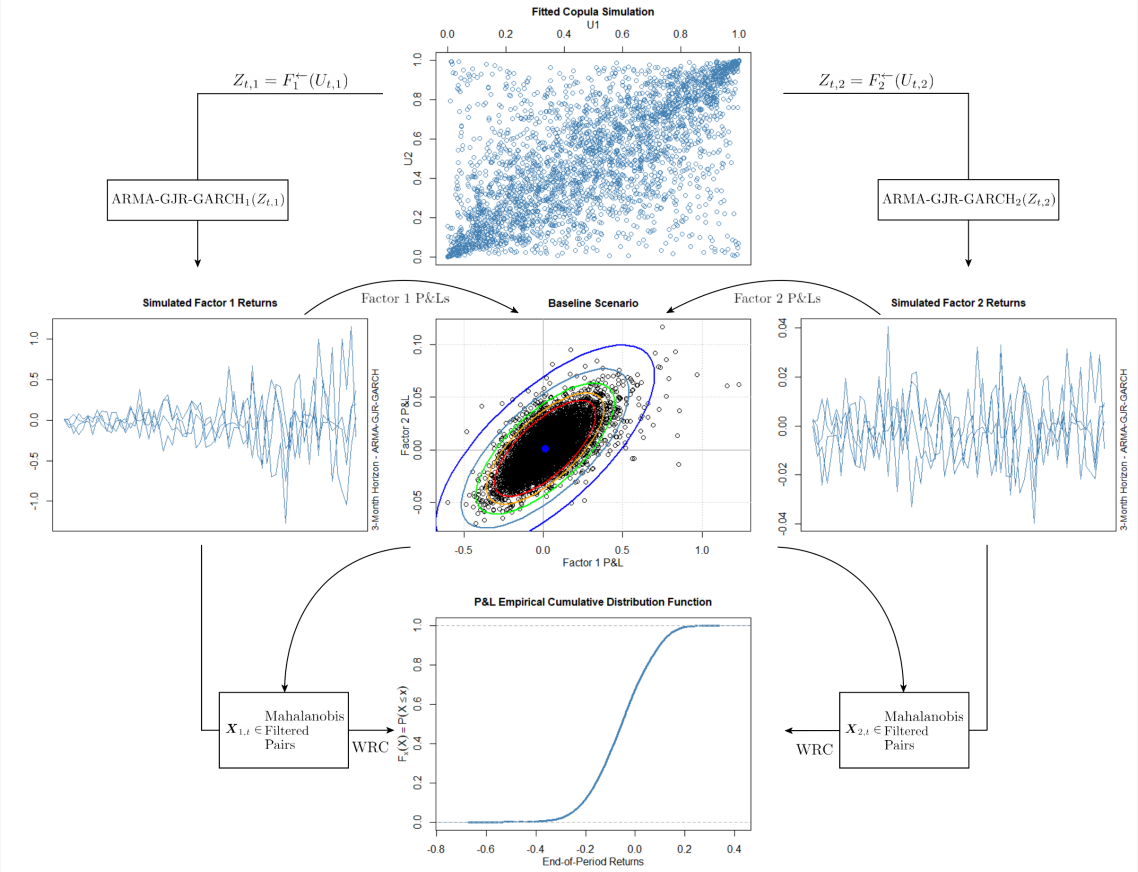

Figure 4.1: Scenario generation procedure for 2 risk factors

4.2 Applications

4.2.1 The Case of the CGCI

4.2.1.1 Index Replication and Risk Factor Mapping

In the case of CGCI, we isolate two risk factors, namely the crypto-basket and the gold component. The crypto-basket is formulated as an equally-weighted basket of 5 cryptoassets, each with a weight of 0.2. The crypto-basket price base level is set on 100 on July 1st, 2015 and on day t from July 2nd, 2015 onwards is calculated as:

$$\text{EW}_t = \left(1 + \sum_{i \in N_{c,t}} x_{i,R(t)} \times \left(\frac{P_{i,t}}{P_{i,R(t)}} - 1\right)\right) \times \text{EW}_{R(t)} \tag{4.1}$$

where

- $N_{c,t}$ is the set of the 5 cryptoassets constituents on day t
- $R(t)$ is the most recent CGCI rebalancing date preceding t
- $P_{i,t}$ is the closing price for cryptoasset i on day t, expressed in USD
- $P_{i,R(t)}$ is the closing price for cryptoasset i on the last rebalancing date preceding t, in USD
- $x_{i,R(t)}$ is the weight of cryptoasset i on the last rebalancing date preceding t, equal to 0.2
- $\text{EW}_{R(t)}$ is the crypto-basket price level on the last rebalancing date preceding t

The weighting between the crypto-basket and gold in the CGCI is computed through Eq. 3.3. It is reminded that the Index base level is set on 1 000 on January 1st, 2016 and on day t from January 2nd, 2016 onwards it is calculated as:

$$\text{Index}_t = \left(1 + \sum_{i \in N_t} x_{i,R(t)} \times \left(\frac{P_{i,t}}{P_{i,R(t)}} - 1\right)\right) \times \text{Index}_{R(t)} \tag{4.2}$$

where

- N_t is the set of the 2 CGCI components (crypto-basket and gold) on day t
- $R(t)$ is the most recent CGCI rebalancing date preceding t
- $P_{i,t}$ is the closing price for constituent i on day t, expressed in USD
- $P_{i,R(t)}$ is the closing price for constituent i on the last rebalancing date preceding t, in USD
- $x_{i,R(t)}$ is the weight of constituent i on the last rebalancing date preceding t, equal to the WRC allocation result
- $\text{Index}_{R(t)}$ is the CGCI price level on the last rebalancing date preceding t

We follow equation Eq. 4.1 and replicate the price time series for both and transform to logarithmic returns.

4.2.1.2 Baseline Scenario Generation

In this section we simulate a number of scenarios and evaluate the impact of stress in the main assumptions of the CGCI. We differentiate between three different types the baseline, historical and hypothetical scenario. The first simulation aims to describe as realistically as possible a recent index profit and loss profile, without the impact of any stress. This should serve as a benchmark to evaluate the severity of volatility or correlation shocks in the P&L distribution of the index. The calibration period for the baseline scenario is chosen to include all daily observations of 2019.

The validity of stylised facts (i)–(iii) presented in Section 2.3.3.1 is verified in Fig. 7.4–7.9 for both the crypto-basket and gold components of the CGCI; therefore asymmetric ARMA–GARCH processes are likely to explain the behaviour of the risk factors' daily returns $\boldsymbol{X}_{t,c}$ and $\boldsymbol{X}_{t,g}$. We assume a t-distribution for the underlying residuals for the ML process, iterate through pair-wise values of $p \in [1,4], q \in [0,4]$ and choose the combination that yields the minimum AIC. The results of the ARMA–GJR–GARCH fitting to the crypto-basket and gold returns time series is presented in Table 4.1.

Next, we estimate the semi-parametric distribution function of the ARMA–GJR–GARCH standardised residuals. As highlighted in Section 2.3.3.3, their i.i.d. behaviour allows the tails to be approximated by a GDP. The linearity of the mean excess function given by Eq. 2.35 can be used as a diagnostic to assist the selection of appropriate thresholds for the tails. Since the shape and scale parameters in Eq. 2.35 will be estimated after the threshold is defined, we use an empirical estimator for the mean excess function for positive-valued data $X_1, \ldots, X_n$, given by:

$$e^{\text{EMP}}(u) = \frac{\sum_{i=1}^{n}(X_i - u)I_{\{X_i > u\}}}{\sum_{i=1}^{n} I_{\{X_i > u\}}} \tag{4.3}$$

Based on Eq. 4.3, we inspect the plot $\big(Z_i, \quad e^{\text{EMP}}(Z_i)\big)$, first for the positive innovations (Upper tail, Figs. 7.10 and 7.12) and then for absolute values of the negative ones (Lower tail, Figs. 7.11 and 7.13). For each tail, we define the threshold $u := Z_i$ for such i, from which the sample becomes approximately linear for higher values. Given the thresholds, we obtain the parametric GPD tails through a negative log-likelihood function. The shape and scale parameters for the baseline scenario can be found in Table 4.1. Combined with a Gaussian kernel smoothed interior, we obtain the final semi-parametric distribution function for the baseline scenario's standardised residuals, displayed in Figs. 4.2 and 4.3.

In terms of the dependence structure, given the semi-parametric distribution functions F_c, F_g, we perform inverse transform sampling to the fitted ARMA–GJR–GARCH standardised residuals, and attempt to fit a copula to the pseudo-sample. The fitting results for considered copulas can be found in Table 4.1. We proceed with the t-copula for the remainder of this chapter, as it yields the maximum log-likelihood and provides the means for correlation stress testing through its parameters (ρ, ν).

Table 4.1: ARMA-GJR-GARCH, GPD and Copula Parameters and diagnostics

ARMA-GJR-GARCH Fitting						
	Crypto-basket Baseline	Crypto-basket Historical	Gold Baseline	Gold Historical	MDVA5 Baseline	MDVA5 Historical
Order (ARMA) (GJR-GARCH)	$(4,4)$ $(1,1)$	$(4,4)$ $(1,1)$	$(4,3)$ $(1,1)$	$(4,4)$ $(1,1)$	$(4,2)$ $(1,1)$	$(4,2)$ $(1,1)$
Parameters (Eq. 2.3)	ϕ_1: -0.95408 ϕ_2: -0.35581 ϕ_3: -1.07815 ϕ_4: -0.99300 θ_1: 1.03614 θ_2: 0.37295 θ_3: 1.11033 θ_4: 1.06890 ω: 0.000007 α_1: 0.02770 γ_1: -0.06146 β_1: 1.00000	ϕ_1: 0.05108 ϕ_2: 0.45840 ϕ_3: 0.06855 ϕ_4: -0.76304 θ_1: 0.08024 θ_2: -0.42010 θ_3: -0.02407 θ_4: 0.92655 ω: 0.00267 α_1: 0.22360 γ_1: 0.10915 β_1: 0.13794	ϕ_1: -0.90692 ϕ_2: -1.00161 ϕ_3: -0.72425 ϕ_4: 0.01181 θ_1: 0.79031 θ_2: 1.11737 θ_3: 0.74846 ω: 0.000001 α_1: 0.06469 γ_1: -0.13793 β_1: 0.98006	ϕ_1: 0.59656 ϕ_2: 1.08368 ϕ_3: -0.58776 ϕ_4: -0.39986 θ_1: -0.79959 θ_2: -1.00687 θ_3: 0.76978 θ_4: 0.26998 ω: 0.00000 α_1: 0.00000 γ_1: -0.00200 β_1: 1.00000	ϕ_1: -1.21805 ϕ_2: -1.19354 ϕ_3: -0.19727 ϕ_4: 0.02250 θ_1: 1.07132 θ_2: 1.03795 ω: 0.000002 α_1: 0.03245 γ_1: -0.06707 β_1: 1.00000	ϕ_1: -1.93720 ϕ_2: -1.12456 ϕ_3: -0.12869 ϕ_4: -0.02543 θ_1: 1.94084 θ_2: 1.03890 ω: 0.000003 α_1: 0.000001 γ_1: 0.08400 β_1: 0.94997
AIC	-3.6341	-2.7398	-7.2120	-7.4216	-4.0542	-3.2292
Residual Distribution Shape (KS Test p-value)	3.32702 (0.7003)	3.94689 (0.9604)	19.83051 (0.6673)	5.93231 (0.8674)	2.55280 (0.8684)	4.52857 (0.8335)
Generalised Pareto Distribution Fitting						
Threshold u (Upper) (Lower)	1.10114 -0.60602	0.54891 -0.75895	0.60316 -1.15400	0.75454 -0.61262	0.63667 -0.51043	0.64902 -1.25717
Parameters (Upper)	ξ: 0.27178 β: 0.39605	ξ: -0.03047 β: 0.62530	ξ: -0.49452 β: 1.10766	ξ: 0.15642 β: 0.53995	ξ: 0.09272 β: 0.59313	ξ: -0.14684 β: 0.66304
(Lower)	ξ: 0.01501 0.64541	ξ: 0.13459 β: 0.57712	ξ: -0.46581 β: 0.82030	ξ: -0.34770 β: 1.02221	ξ: 0.10358 β: 0.52568	ξ: 0.28828 β: 0.59477
LogLik (Upper) (Lower)	9.66944 30.58602	28.99699 28.07471	44.36422 8.06560	27.00540 40.44401	33.08554 203.4029	25.21121 27.66995

CGCI Copula Fitting				
	Gaussian Copula Loglik	t-Copula Loglik	t-Copula Parameters (ρ, ν)	Goodness-of-fit (p-value)
Baseline Scenario	0.41348	0.61102	$(0.05917, 23.62447)$	0.7737
Historical Scenario	0.24004	0.58172	$(-0.03363, 16.62352)$	0.3112

With the fitted ARMA–GJR–GARCH parameters, the cumulative distribution functions and fitted t-copula for the residuals, and a 3-month simulation horizon, we produce 10 000 paths for each risk factor, $\boldsymbol{X}_{t,c}, \boldsymbol{X}_{t,q}$. We filter out all path pairs that yield an MD value that exceeds the 99th percentile of the underlying MD Chi-Squared distribution, and use the remaining path pairs to produce $m' < m$ paths for the CGCI. Finally, we compute the P&L at the end of period for each path pair, and get the empirical P&L distribution function that should serve as risk profile benchmark. The generated

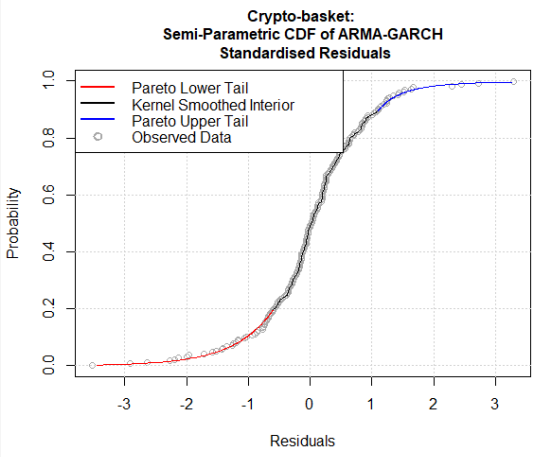

Figure 4.2: Semi-parametric CDF Crypto-basket residuals

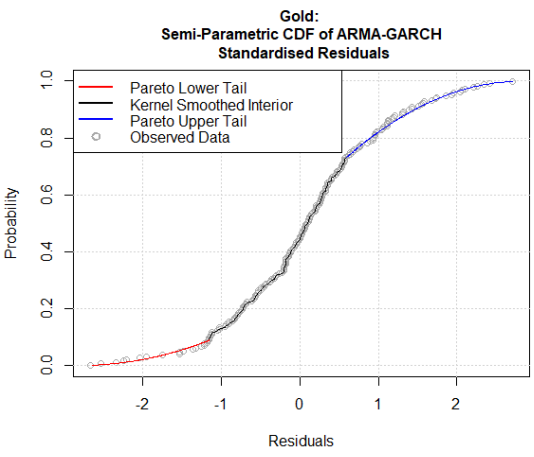

Figure 4.3: Semi-parametric CDF Gold residuals

scenarios with the Mahalanobis plausibility bound, and the final baseline P&L distribution can be found in Figs. 4.4 and 4.5.

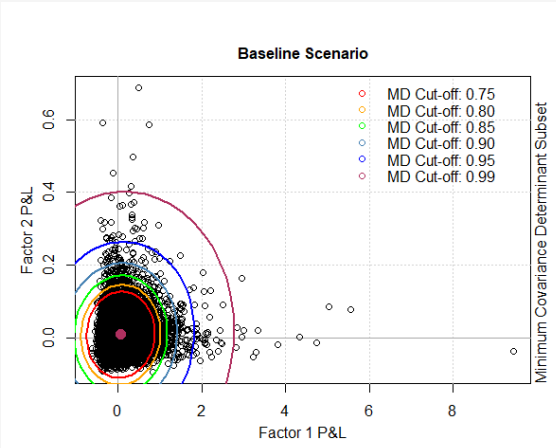

Figure 4.4: CGCI baseline scenarios: Mahalanobis plausibility ellipses

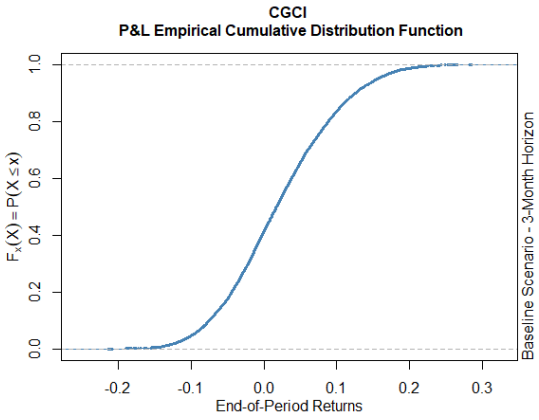

Figure 4.5: CGCI baseline scenarios: P&L distribution

We can also choose to generate a baseline scenario for single risk factor portfolios. In this case, the pseudo-random observations of the residuals can be derived directly from the cumulative distribution functions. We use this approach to generate 10 000 paths of returns for the MVIS Digital Assets 5 Index [105] (MVDA5) – a market capitalisation-weighted index which tracks the performance of the five largest and most liquid cryptoassets – and compare its P&L distribution with the one derived for the CGCI. The details of the fitting process for the MVDA5 baseline scenario and the plot of the semi-parametric residual distribution can be found in Table 4.1 and Fig. 7.14 respectively.

4.2.1.3 Historical and Hypothetical Scenarios

The process described in Section 4.1 can be further modified to support the generation of stress scenarios that can be compared against the baseline. First, we can change the calibration period to reflect stressful market conditions. Those historical scenarios are commonly used in practice because they are based on events that are observed, and therefore likely to reoccur. For the case of the CGCI, we generate the historical scenarios by calibrating the models in the period of 2018-01-01 to 2018-12-31, as it reflects very large downward price movements in the cryptoasset space.

To this end, we calculate the daily logarithmic returns over the aforementioned stressful period. We use this sample to fit the ARMA–GJR–GARCH model for both risk factors and obtain the i.i.d. standardised residuals. Following the same steps as in Section 4.2.1.2, we model the tails and produce the semi-parametric cumulative distribution functions. Both the new ARMA–GJR–GARCH and GPD parameters can be found in Table 4.1. We further transform the residuals to uniform variates and fit an appropriate t-copula (Table 4.1). With the new parameters we can proceed with the generation of 10 000 paths for each risk factor, filter out implausible pairs, compute the P&L at the end of the period and obtain the new P&L distribution that corresponds to the historical scenario. A single-factor approach is also used to produce the MVDA5 historical P&L distribution. While the historical scenarios can be used to assess the portfolio's performance under realised stressful market conditions, it is biased towards past experience and fails to examine plausible stress events that have not occurred yet.

In order to reveal additional vulnerabilities that historical scenarios fail to capture, we need to generate a number of hypothetical scenarios that assess the portfolio's sensitivity to shocks in various statistical patterns, such as increased volatility or correlation. In order to test the CGCI's resilience to a potential increase in correlation between the cryptoasset space and physical gold, we can choose to increase the correlation parameter ρ of the t-copula when generating pseudo-samples. We can further choose to decrease the degrees of freedom in order to increase the likelihood of joints extremes. Additionally, when providing the i.i.d. residuals to the fitted ARMA–GJR–GARCH model, we can shock the risk factors' volatilities by changing the constant, ω, in order to produce very volatile risk factor paths.

For this study, we modify those parameters such that $\rho = 0.9$, $\nu = 2$ and $\omega = 10\omega_b$, where ω_b denotes the volatility constant value of the baseline fitted ARMA–GJR–GARCH. The P&Ls that are derived through the modified copula reflects the new correlation structure, as seen in Fig. 7.15. The same volatility shock is introduced to the MVDA5 volatility constant to obtain its hypothetical scenario risk profile.

Fig. 4.6 and Fig. 4.7 present a comparison of the Baseline, Historical and Hypothetical Scenarios for the case of CGCI and MVDA5.

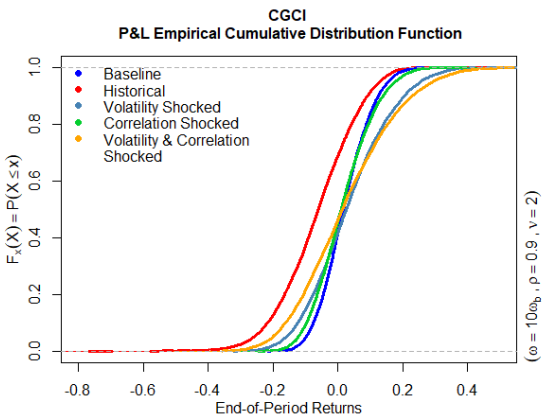

Figure 4.6: CGCI P&L Distributions

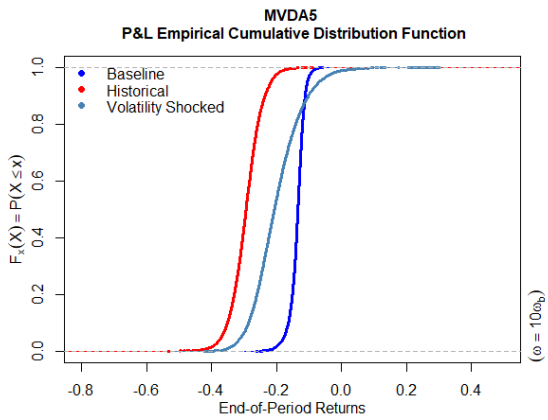

Figure 4.7: MVDA5 P&L Distributions

For CGCI, the P&L curves are closely bunched together, suggesting a strong resilience to market shocks. The "Volatility & Correlation Shocked" scenario which can be viewed as the most severe stress test, indicates only a modest deviation from the baseline scenario. This implies that the index's underlying components and weighting methodology are effective in mitigating the impact of increased volatility and correlation changes, which are common during market turbulence.

In contrast, the MVDA5 index, which is market cap weighted, shows a more pronounced separation between the baseline and shocked scenarios. The "Volatility Shocked" scenario reveals a substantial shift to the left, indicating a higher probability of negative end-of-period returns. This is attributed to the inherent concentration risk of market cap weighted strategies, where larger assets can disproportionately affect the index performance, especially in volatile market conditions.

Additionally, in the case of the CGCI, the slope of the P&L distribution for the historical scenario is visibly less steep compared to the baseline P&L. The heavier lower tail further confirms the increased risk in the historical scenario. The probability of a positive end-of-period return in the historical scenario lies around 31% compared to 58% for the CGCI baseline. When it comes to the volatility-shocked scenario, it does not differ significantly around the mid-section, with the probability of profit remaining around 58%, but the CDF is slightly heavier on the upper and lower tail. A single correlation shock impacts the risk profile even less, while a simultaneous shock in both volatility and correlation bring the probability of profit down to approximately 53%.

In the case of MVDA5, the baseline P&L distribution reveals significantly higher levels of risk, with no prospect of profit on the 3-month horizon. The historical scenario is more severe, displaying 85% probability of at least a 25% loss on the initial investment. The volatility-shocked MVDA5 on the other hand is heavier on the upper tail, but the probability of a positive end-of-period return barely exceeds 1%. Overall, CGCI's WRC allocation scheme is characterised by a much more stable risk profile in all the scenarios considered in this study.

4.2.2 Summary

In this chapter we have proposed a framework for scenario-based risk management and have described how it can be applied to assess the risk profile of diversified portfolios with cryptoasset components. Our approach ensures that the joint evolution of the identified risk factors are modelled in a realistic way and that the analysed scenarios are severe, yet plausible. By taking into account a variety of plausible future events related to volatility and correlation levels, we demonstrate the superiority of diversified strategies, such as the CGCI, as a means of mitigating risk. While this application focuses in generating basic stress scenarios specifically for the case CGCI, it can be further modified to include arbitrary combinations of risk factor shocks. Additionally, the presented procedure can potentially be used as a forward-looking portfolio optimisation approach.

Chapter 5

Cryptoasset Market Regimes

Regime-switching models are frequently used to explain the tendency of financial markets to change their behavior, often abruptly. Such changes usually translate to structural breaks in the average means and volatilities of financial indicators, and partition their time-series into distinct segments, each with unique statistical properties. In this chapter, we address the problem of identifying the presence of such regimes in the constituents of diversified, cryptoasset-containing portfolios, ultimately to define high-risk market conditions and assess portfolio resilience. For each portfolio component, we first consider a Gaussian Hidden Markov Model (HMM) in order to extract intermediate trend-related states, conditional on the weekly returns distributions. We further apply a Markov-switching GARCH model to the demeaned daily returns to describe changes in the conditional variance dynamics and isolate volatility-related states. We combine the former approaches to generate a number of price paths for each constituent, simulate the portfolio allocation strategy and obtain a risk profile for each combination of the trend and volatility regimes. We apply the proposed method to the CoinShares Gold and Cryptoassets Index, a diversified, monthly-rebalanced index which includes two main risk-weighted components; a cryptoassets basket and physical gold. Results demonstrate an overall stable risk-reward profile when compared against the individual components and suggest a superior performance in terms of Omega ratio for investors that target wealth preservation and moderate annual returns. We detect underperformance regions in bear-low volatility market regimes, where diversification is hindered.

This chapter was published at the Cryptoeconomic Systems Blockchain Journal in 2021 [86].

5.1 Background and Methodology

5.1.1 Motivation

The study of market regimes is important in many fields, including governmental policy, financial markets and regulation. Different market regimes exhibit different levels of volatility and understanding them can help investors and traders to better manage their portfolios, adjusting their positions and strategies overtime. Identifying them can also improve the portfolio construction process. This may involve diversifying across assets that behave differently in various market conditions or employing dynamic asset allocation strategies that adapt to regime changes. Additionally, regulators and financial institutions can monitor market regimes to identify potential imbalances, vulnerabilities or systemic risks that may arise from certain market conditions. Policymakers can also use this information to tailor their policy responses and better address challenges posed by prevailing regimes to work towards achieving macroeconomic stability.

Notwithstanding past studies on the crypto-market dynamics and the diversification properties of cryptoassets, it is not clear how traditional allocation strategies (a) behave in relation to different market conditions and (b) meet individual investor's expectations. The primary goal of this chapter is the application of regime-switching models to unveil high-risk market states for the diversification strategy employed by the CoinShares Gold and Cryptoassets Index (CGCI) and assess how appropriate it is for investors with different annual return targets. For this purpose, the index's two main market determinants are isolated, namely the crypto-basket and gold. Additionally, we study the dynamics of their price evolution both in terms of volatility and intermediate trend. In the proposed setting, there are four trend states and three volatility states for the crypto-basket and three trend states and three volatility states for gold. In terms of simulation, we produce 1 000 paths for each CGCI component and report the Omega ratio, both in isolation and combined, following the index rebalancing scheme. Finally, the proposed framework allows to detect regions where the weighting scheme does not improve risk-adjusted returns due to limited diversification opportunities.

5.1.2 Simulating Market Regimes

The proposed framework for simulating market regimes combines econometric modeling with a Monte Carlo approach. In the model fitting phase, the process begins with the normalization of daily logarithmic returns using an AR(1) filter to correct for autocorrelation, which is a common issue in time-series data that can lead to spurious inference if not addressed. The application of a regime-switching ARCH model further acknowledges the presence of different volatility regimes in financial markets, capturing the dynamics of changing market conditions over time. The transition matrix and ARCH parameters obtained for each state provide an understanding of (i) the possible states the market can transition into and (ii) the nature of volatility within each state. Moving to

weekly returns, the framework employs an HMM, which is useful for capturing latent states in the time series, reflecting the unobserved processes that influence market movements.

In the simulation process, the framework takes the parameters estimated from the regime-switching ARCH and HMM models to generate daily and weekly return paths. This allows for a granular day-to-day simulation that is adjusted for weekly trends, providing a more realistic trajectory of returns that accounts for both short-term fluctuations and longer-term patterns. By offsetting daily returns by the weekly returns raised to the power of 1/7, the framework bridges the gap between daily and weekly data, ensuring coherence in the simulation.

The translation of these returns into daily values, provides a simulated path of the index's value over the horizon of interest. This approach will offer a comprehensive view of the risk profile by incorporating the effects of autocorrelation, regime switches, and hidden states. We use an initial price level to anchor the simulation to a known starting point, allowing for the assessment of the CGCI's performance relative to its historical behaviour.

More specifically, we let V_t denote the daily value of a financial instrument at day t and we express its weekly log-return with $R_t = \ln(V_{t,n}/V_{t,1})$, where $V_{t,1}$ is the value on the first day and $V_{t,n}$ is the value on the last day of the week. The regime-switching models we discussed in Subsection 2.3.1 can be used to describe and simulate the evolution of V_t according to the regime switching behaviour of the market, both in terms of volatility and intermediate trend. In the case of regime-switching volatility, a Markov-switching ARCH(1) model is fitted on the daily logarithmic returns, while intermediate trend regime changes are observed in the weekly logarithmic returns.

Assuming the specifications of the previous sections and a discrete space of K_T distinct trend states $S_i,\ i \in \{1, \dots, K_T\}$ and K_V volatility states $s_i,\ i \in \{1, \dots, K_V\}$, the fitting and simulation process can be summarised in the following steps:

Model Fitting

1. Given V_t, observable on day t, obtain the daily logarithmic returns r_t and demean using an AR(1) filter to eliminate autocorrelation effects.
2. Fit the regime-switching ARCH(1) model to the demeaned r_t and obtain the $K_V \times K_V$ transition matrix $\boldsymbol{P_v}$ and the ARCH parameter vector $\boldsymbol{\theta_k} = [a_{0,k}, a_{1,k}]$ for each state s_k, $k \in \{1, \dots, K_V\}$
3. Translate V_t to weekly logarithmic returns R_t and demean using an AR(1) filter to eliminate autocorrelation effects.
4. Fit the Gaussian HMM to demeaned returns and obtain the $K_T \times K_T$ transition matrix $\boldsymbol{P_t}$ and the distribution parameter vector $\boldsymbol{\phi_k} = [\mu_k, \sigma_k]$ for each state $S_k, k \in \{1, \dots, K_T\}$

Simulating Process

1. Given a simulation horizon of T days and parameters $\boldsymbol{\theta_k}$, simulate process y_t for $t = 1, \ldots, T$, according to the fitted regime-switching ARCH(1) model, and translate to daily returns r_t according to the previously fitted AR(1)
2. Simulate process Y_t for $t = 1, \ldots, T$, according to the Gaussian HMM with distribution parameter vector $\boldsymbol{\phi_k} = [\mu_k, \sigma_k]$, and translate to weekly returns R_t through the previously fitted AR(1)
3. For day t, offset r_t by $(1 + R_t)^{1/7}$
4. Convert the simulated daily logarithmic returns r_t, where $t \in \{1, \ldots, T\}$, to daily values $V_t = V_0 e^{c_t}$, where $c_t = \sum_{i=1}^{t} r_i$ are the daily cumulative logarithmic returns and V_0 the initial price level on day $t = 0$

The produced time series evolve according to $K_V \times K_T$ combinations of the volatility states $s_i \; i \in \{1, \ldots, K_V\}$ and trend states $S_i \; i \in \{1, \ldots, K_T\}$, with the two Markov processes progressing independently (Fig. 5.1).

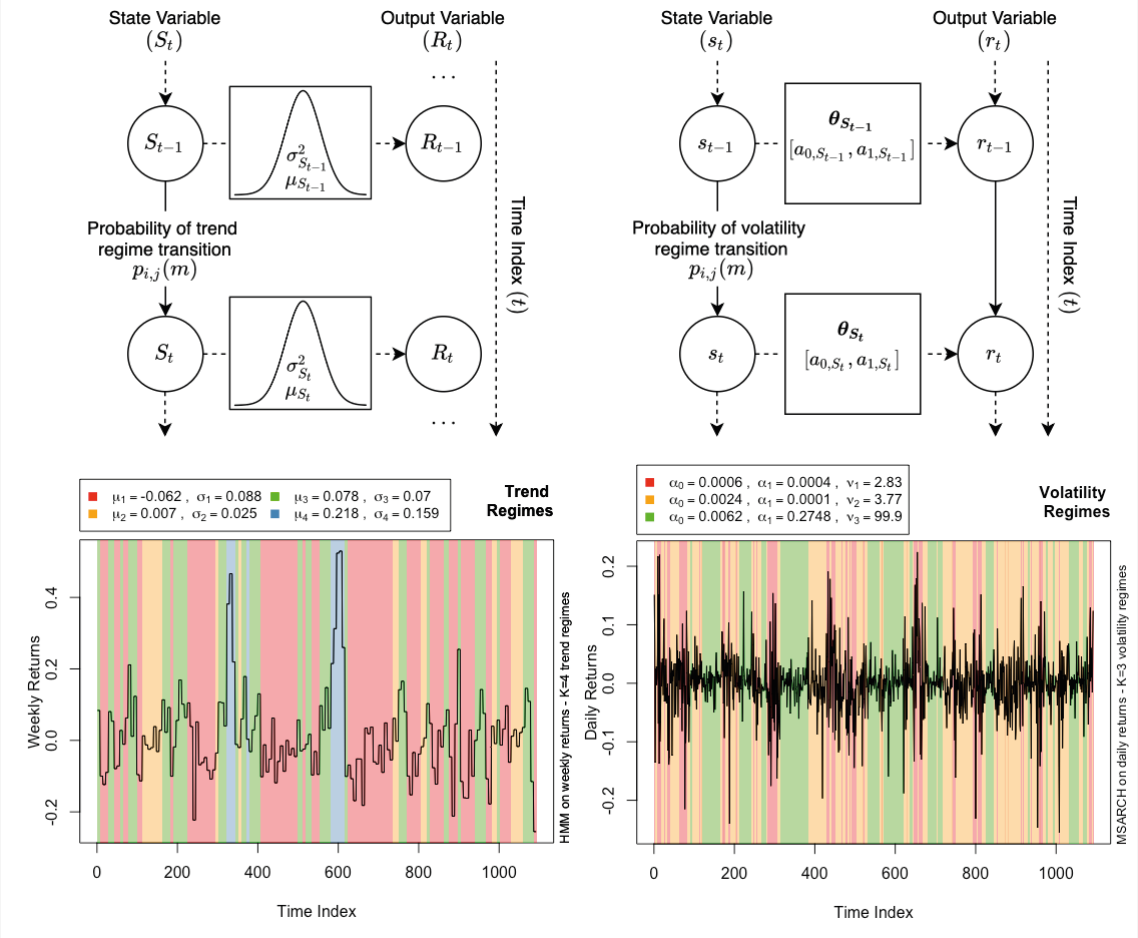

Figure 5.1: Market regime simulation procedure

5.2 Applications

5.2.1 CGCI Risk Factors: Characteristics and Regime Identification

The aim of this section is to test the resilience of the CoinShares Gold and Cryptoassets Index (CGCI) [87] during different market regimes. For this purpose, we examine the return profile in relation to the volatility and trend states of its main market determinants. The CGCI is a low-volatility index that aims to maintain a prudent risk profile through diversification and regular rebalancing. The two uncorrelated risk factors driving the value of CGCI are the crypto-basket and the gold component, with the crypto-basket being an equally-weighted basket of 5 cryptoassets. The weighting among the crypto-basket and gold in the CGCI is computed through Eq. 3.3.

The estimation of the regime-switching models is performed on a sample of 1231 price observations, ranging from July 1st 2015 to May 31st 2020. Both the crypto-basket and gold time series correspond to the prices used for the calculation of the CGCI, with the crypto-basket price being calculated using historical tick-by-tick trade data provided by Kaiko and the gold price corresponding to the LBMA Gold Price PM data provided by ICE Benchmark Administration (IBA). For a detailed view on the full pricing methodology of both the crypto-constituents and the CGCI, readers can consult the official methodology document.[1]

5.2.2 Trend Regime Estimation

We denote by $P_{c,t}$ the price of the crypto-basket component on day t and by $P_{g,t}$ the daily gold prices. Both time-series are expressed in USD. For the detection of the trend regimes we compute the weekly logarithmic returns, $R_{c,t}$ and $R_{g,t}$ respectively. As mentioned in previous sections, we aim to model the weekly return series as an HMM with Gaussian distributions for the observations, while the regimes change according to a discrete Markov Process. A Durbin–Watson test reveals the presence of serial autocorrelation in the weekly logarithmic returns of both the crypto-basket ($d = 1.338,\ p < 0.001$) and gold ($d = 1.574,\ p < 0.001$) time-series. Therefore, in order to respect the output independence assumption, $R_{c,t}$ and $R_{g,t}$ are demeaned prior to the HMM fitting, using an AR(1) filter. The same test on the demeaned time series rejects autocorrelation (Crypto-basket: $d = 2.078,\ p = 0.7347$, gold: $d = 1.971,\ p = 0.4080$).

In regards to the crypto-basket, taking into consideration that the sample dataset includes the historic 2017 price run, we assume the presence of $K_{c,T} = 4$ states, namely the bear, sideways, bull and outlier regimes. We expect the former states to reflect a downwards, stable, upwards and extreme intermediate trend respectively. The parameters of the four regimes and the diagnostics of the expected log-likelihood maximisation are displayed in Table 4.1. Kolmogorov-Smirnov tests across all regimes confirm that observations, conditional to the prevailing latent state, are normally

[1] Available online by the index owner, CoinShares (Holdings) Limited (www.coinshares.com), and the Benchmark Administrator and Calculation Agent, Compass Financial Technologies (www.compassft.com).

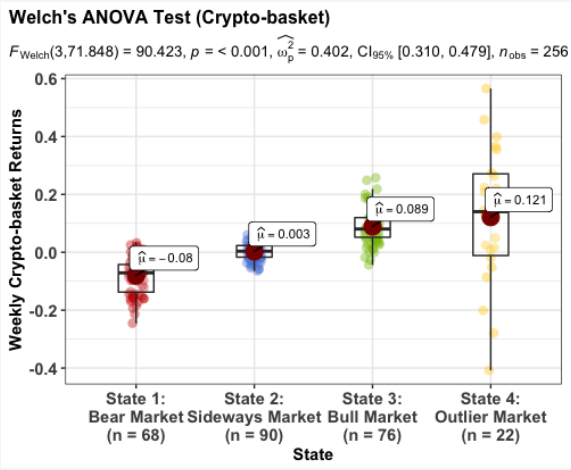

Figure 5.2: Welch's ANOVA – Crypto-basket Trend Regimes

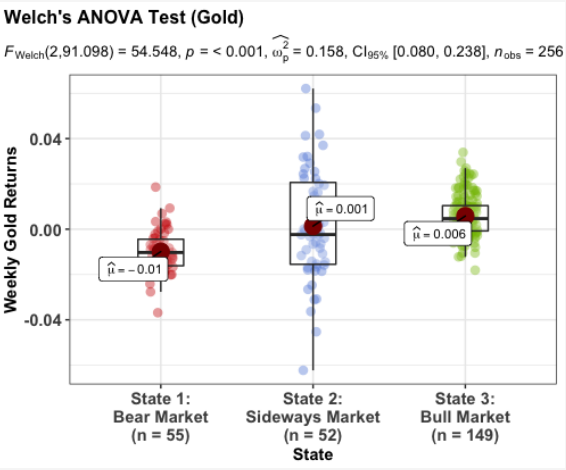

Figure 5.3: Welch's ANOVA – Gold Trend Regimes

distributed, as expected by the HMM specification (Bear: $D = 0.140, p = 0.1260$, sideways: $D = 0.067,\ p = 0.7901$, bull: $D = 0.105,\ p = 0.3385$, outlier: $D = 0.073,\ p = 0.9993$)

Latent states 1–3 correspond to the bear, sideways and bull market regimes and display a negative, zero and positive mean respectively. Levene's test reveals variance homogeneity across the bear and bull markets ($F = 0.973,\ p = 0.3256$), while the variance of the sideways market is slightly lower, something not atypical for neutral market periods. Welch's ANOVA test confirms that the sample's means differ significantly across regimes ($F = 90.423,\ p < 0.001$) (Fig. 5.2). Latent state 4 corresponds to the outlier regime, and describes the dynamics of the 2017 crypto-market price run, displaying extreme volatility and a mean similar to the one of the bull regime. Overall, the bear, sideways, bull and outlier states each constitute 26.46%, 35.02%, 29.96% and 8.56% of the 256 analysed weeks respectively.

For the evolution of gold's prices we follow the same approach and assume a simple HMM with $K_{g,T} = 3$ states that correspond to bear, sideways and bull market regimes (Fitting diagnostics in Table 5.1). Response normality across the three regimes is confirmed through Kolmogorov–Smirnov tests (Bear: $D = 0.071,\ p = 0.9176$, sideways: $D = 0.073, p = 0.4155$, bull: $D = 0.124,\ p = 0.3736$). Welch's ANOVA test further confirms that the sample means differ significantly across all regimes ($F = 54.548,\ p < 0.001$) (Fig. 5.3) and the bear, sideways and bull latent states each constitute 22.18%, 20.23% and 57.59% of the 256 analysed weeks respectively.

5.2.3 Volatility Regime Estimation

For the detection of the volatility states in the historical dataset, we transform the constituent prices $P_{c,t}$ and $P_{g,t}$ to daily logarithmic returns, $r_{c,t}$ and $r_{g,t}$. To account for different specifications in volatility dynamics of the daily returns, we express them in terms of a Markov-switching ARCH

model, as specified in Section 2.3.1.4. We assume that the ARCH residuals are Student-t distributed (as it is commonly used in practice and considered adequate for most financial applications [100]). Prior to the fitting process, we filter both time-series with an AR(1) filter. A Durbin–Watson test on the demeaned time series rejects autocorrelation (Crypto-basket: $d = 2.001,\ p = 0.5080$, gold: $d = 1.9708,\ p = 0.4076$).

We assume that the crypto-basket time-series contains $K_{c,V} = 3$ states, namely the low, moderate and high volatility states. The ARCH parameters of the three regimes and the diagnostics of the expected log-likelihood maximisation are displayed in Table 4.1. In this case our aim has been to specify a regime switching set of rules for the daily returns only based on volatility dynamics. Indeed, Levene's test rejects variance homogeneity across the low, moderate and high volatility regimes ($F = 209.52,\ p < 0.001$). Welch's ANOVA test further fails to reject mean equality across the specified regimes ($F = 1.199,\ p = 0.3037$). The identified low, moderate and high volatility latent states each constitute 21.88%, 64.59%, 13.53% of the 256 analysed weeks respectively.

Similarly for the gold prices, we assume a Markov-switching ARCH model with $K_{g,T} = 3$ volatility specifications and Student-t distributed innovations (Table 4.1). Variance homogeneity is rejected ($F = 95.228,\ p < 0.001$) and mean equality across regimes cannot be rejected ($F = 0.428,\ p = 0.653$). The low, moderate and high volatility latent states each constitute $59.45\%, 37.55\%, 3.00\%$ of the 256 analysed weeks.

Table 5.1: Regime Fitting Parameters and diagnostics

HMM & MSGARCH Fitting				
	Crypto-basket Trend Regimes	Crypto-basket Volatility Regimes	Gold Trend Regimes	Gold Volatility Regimes
Transition Parameters Trend States: 1:Bear, 2:Sideways, 3:Bull, 4:Outlier (Crypto-basket only) Volatility States: 1:Low, 2:Moderate, 3:High	$p_{1,1} = 0.3887,\ p_{1,2} = 0.2049,$ $p_{1,3} = 0.4064,\ p_{1,4} = 0.0000,$ $p_{2,1} = 0.0000,\ p_{2,2} = 0.8007,$ $p_{2,3} = 0,1993,\ p_{2,4} = 0.0000,$ $p_{3,1} = 0.4927,\ p_{3,2} = 0.0000,$ $p_{3,3} = 0.4523,\ p_{3,4} = 0.0551,$ $p_{4,1} = 0.0041,\ p_{4,2} = 0.0000,$ $p_{3,4} = 0.1468,\ p_{4,4} = 0.8491,$	$p_{1,1} = 0.9575,\ p_{1,2} = 0.0425,$ $p_{1,3} = 0.0000,\ p_{2,1} = 0.0202,$ $p_{2,2} = 0.9243,\ p_{2,3} = 0.0555,$ $p_{3,1} = 0.0000,\ p_{3,2} = 0.2268,$ $p_{3,3} = 0.7732$	$p_{1,1} = 0.0506,\ p_{1,2} = 0.1202,$ $p_{1,3} = 0.8294,\ p_{2,1} = 0.9994,$ $p_{2,2} = 0.0006,\ p_{2,3} = 0.0000,$ $p_{3,1} = 0.1253,\ p_{3,2} = 0.2586,$ $p_{3,3} = 0.6161$	$p_{1,1} = 0.9956,\ p_{1,2} = 0.0043,$ $p_{1,3} = 0.0001,\ p_{2,1} = 0.0000,$ $p_{2,2} = 0.9878,\ p_{2,3} = 0.0122,$ $p_{3,1} = 0.0265,\ p_{3,2} = 0.0431,$ $p_{3,3} = 0.9304$
Parameters Trend States: $N \sim (\mu_k, \sigma_k)$ Volatility States: ARCH: (a_0, a_1)	$(\mu_1 = -0.088, \sigma_1 = 0.060)$ $(\mu_2 = -0.003, \sigma_2 = 0.027)$ $(\mu_3 = 0.057, \sigma_3 = 0.069)$ $(\mu_4 = 0.045, \sigma_4 = 0.202)$	$(a_{0,1} = 0.0005, a_{1,1} = 0.0001)$ $(a_{0,2} = 0.0022, a_{1,2} = 0.0000)$ $(a_{0,3} = 0.0084, a_{1,3} = 0.0027)$	$(\mu_1 = -0.009, \sigma_1 = 0.008)$ $(\mu_2 = 0.001, \sigma_2 = 0.025)$ $(\mu_3 = 0.004, \sigma_3 = 0.011)$	$(a_{0,1} = 0.0000, a_{1,1} = 0.0001)$ $(a_{0,2} = 0.0001, a_{1,2} = 0.0001)$ $(a_{0,3} = 0.0003, a_{1,3} = 0.0001)$
Convergence AIC BIC Log-Likelihood	AIC : -471.5804 BIC : -390.0413 LL : 261.1289	AIC : -4232.4121 BIC : -4170.9959 LL : 2128.206	AIC : -1436.939 BIC : -1387.252 LL : 732.4695	AIC : -8436.9141 BIC : -8375.5076 LL : 4230.4571

5.2.4 Portfolio Performance Evaluation

Given the fitted model parameters and a 7-year simulation horizon, we produce $N = 1\,000$ price paths for the crypto-basket and gold components, with the initial prices set to the last recorded prices of the historical dataset on May 31st 2020. We use the weighted risk contribution allocation scheme (Eq. 3.3) and produce $N = 1\,000$ corresponding paths for the CGCI, each one containing

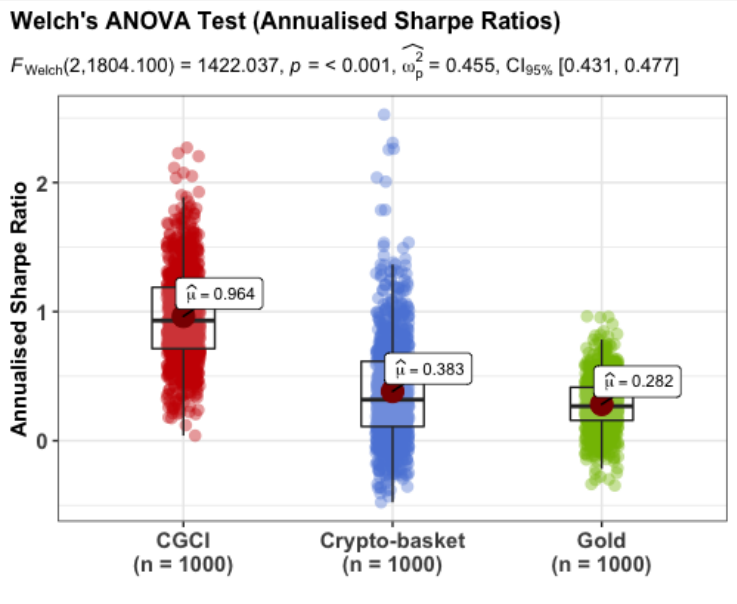

Figure 5.4: Welch's ANOVA – Annualised Sharpe Ratios

numerous of the $K_{c,T} \times K_{c,V} \times K_{g,T} \times K_{g,V} = 108$ possible combinations of its price determinants' states. We are ultimately interested in examining both the overall performance of the three time series as well as the index risk-adjusted return profile in relation to its constituents' ongoing trend and volatility regimes.

First, we assess the performance of the CGCI, crypto-basket and gold in terms of their annualised Sharpe ratio, taking into consideration the entire dataset, regardless of the prevailing trend and volatility regimes. Fig 5.4 displays a Welch's ANOVA test comparing the annualised Sharpe Ratios across the three different investment styles: the CGCI, the crypto-basket and gold in isolation. The test has yielded a highly significant p-value ($p < 0.001$), indicating strong evidence of a difference in the mean annualised Sharpe Ratios between at least two of the groups. From the boxplot, it is evident that the CGCI strategy has a much higher mean annualised Sharpe Ratio ($\hat{\mu} = 0.964$) compared to the crypto-basket ($\hat{\mu} = 0.383$) and gold ($\hat{\mu} = 0.282$).

The suitability of gold as a safe-haven asset is underscored, not by its higher mean ratio but by its tighter interquartile range, suggesting a more consistent risk-adjusted return compared to the other two. The spread of Sharpe Ratios for the gold is narrower (SD $= 0.1982$), indicating less variability in the performance. The crypto-basket has a wider dispersion of outcomes, which reflects higher risk and less consistency in returns. The lower mean Sharpe Ratio suggests that the risk-adjusted return of the crypto-basket in isolation is less favorable than CGCI.

The large F-statistic value from Welch's ANOVA ($F = 1422.037$) confirms the statistical significance of the differences in means, while the partial omega-squared ($\omega_p^2 = 0.455$) indicates a substantial effect size. The confidence interval for the partial omega-squared, ranging from 0.431

to 0.477, does not cross over any threshold of triviality, which further strengthens the argument that the differences observed are not only statistically significant but also meaningful in practice.

Overall, the diversified index strategy yields a superior risk profile, with an average annualised Sharpe ratio equal to 0.964 (SD $= 0.3540$) and a positive value for all simulation paths. The crypto-basket displays a less competitive performance and greater variability, yielding an average annualised Sharpe ratio of 0.383 (SD $= 0.4001$). Gold's risk profile is more stable, with M $= 0.282$ and SD $= 0.1982$. Welch's ANOVA test further confirms the highly significant difference in the Sharpe ratios ($F = 1422.037,\ p < 0.001$).

While the Sharpe ratio is a widely used risk–return assessment metric by investors, its main drawback is the fact that it takes into consideration only the first two moments of the returns distribution. One way to account for all return distribution moments is through the Omega ratio, as introduced by Keating and Shadwick [79]. The Omega ratio is defined as as the probability-weighted ratio of gains over losses given a specific level of threshold return (θ). We let X represent the observed returns of an asset and F its cumulative probability distribution function of returns. Given a selected target return threshold θ, the Omega ratio is given by:

$$\Omega(\theta) = \frac{\int_{\theta}^{\infty}[1 - F(r)]dr}{\int_{-\infty}^{\theta} F(r)dr} \tag{5.1}$$

When θ is set to be equal to zero, we get the gain–loss ratio of Bernardo and Ledoit [14]. The Omega ratio is used to rank investments similarly to the Sharpe ratio. The threshold is first chosen to a desired target level at will and investments can then be ranked accordingly, with higher values preferred to lower. The metric can further be extended to a portfolio optimisation strategy that aims to maximise quantity $\Omega(\theta)$ for a selected value of the returns threshold θ.

In this study we inspect the average annual return of each component. Given a simulated price path $P_i,\ i \in 1, \ldots, 1\,000$, the annualised return is obtained through:

$$R_i = \left(P_{i,1+l}/P_{i,1}\right)^{\frac{365}{l}} - 1, \tag{5.2}$$

where l denotes the length of the simulated prices expressed in number of days. This yields 1 000 values of annualised returns for the CGCI, crypto-basket and gold respectively.

Fig. 5.5 - 5.6 present the index cumulative distribution function and a graphical representation of the Omega ratio respectively. Given a benchmark threshold $\theta = 0.01$ (translating to a target return of 1% annually), the ratio is defined as the ratio of the blue over the red shaded area.

In Fig. 5.5 the slope of the crypto-basket CDF appears visibly less steep compared to the gold and the index, with significantly heavier tails. Its rightward spread indicates that it still offers the potential for significant gains, albeit with less consistency than CGCI. The CGCI's CDF is visibly steeper

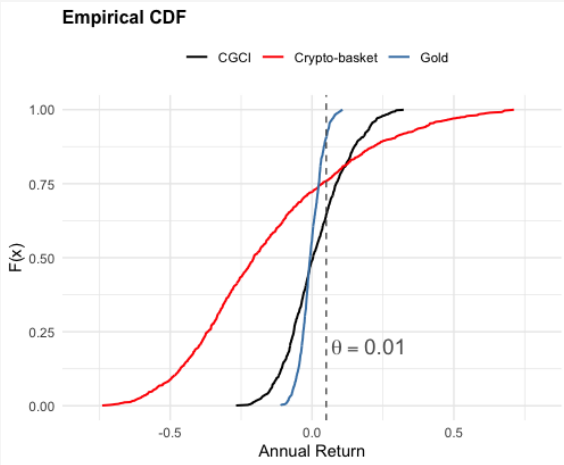

Figure 5.5: Empirical Cumulative Distribution Functions

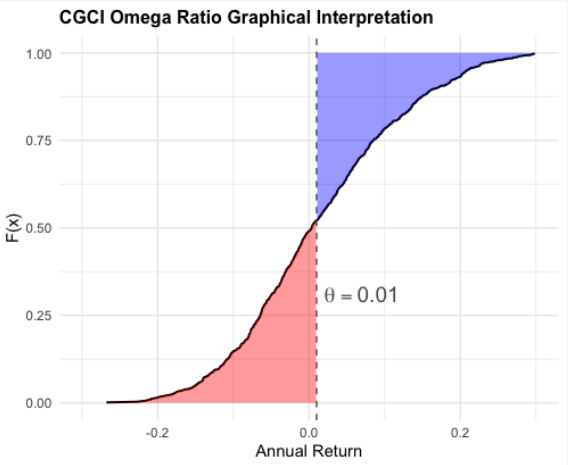

Figure 5.6: Omega Ratio Graphical Interpretation

and also shifts to the right, indicating a higher probability of achieving higher returns compared to the other strategies. It also crosses the threshold of $\theta = 0.01$ sooner, which suggests that CGCI reaches higher returns with less probability of loss, a sign of stronger performance in terms of both risk and return. Gold's CDF is the flattest, especially near the median, which denotes a higher likelihood of achieving modest returns with less extreme outcomes either in gains or losses. This is consistent with gold's reputation as a conservative investment, less likely to experience wide swings in returns.

We further investigate the ranking among the three components given different levels of expected profitability θ. For large negative values of θ, all three Omega ratios tends to infinity, while for large positive values of θ, they tend to zero. Fig. 5.7 presents on a log scale the Omega ratio of the CGCI, the crypto-basket and gold as a function of θ. The intersection point of the CGCI and gold Omega lines reveals that the index strategy is more appropriate for investors aiming for moderate positive returns up to 10.6% annually. The area for $\theta < 0$ reveals that gold provides protection against negative market developments more effectively than the other two components. When it comes to the crypto-basket, it overperforms the index when the target is set higher than a 10.6% annual return, making it a more appropriate for investors with high risk tolerance. Examining the three components wealth preserving capabilities, a threshold of value $\theta = 0$ yields an Omega ratio of $\Omega(0)_{\text{CGCI}} = 1.4018$ for the index, and $\Omega(0)_{\text{CB}} = 0.3056$, $\Omega(0)_{\text{Gold}} = 0.7747$ for the two components respectively.

5.2.5 Regime-Conditional Performance

Each of the simulated paths is then factorised according to the constituents' prevailing states and eventually split into 144 subsets of the original time-series. For each subset we compute the average monthly return for both the CGCI and its two constituents, across all $1\,000$ paths. Given

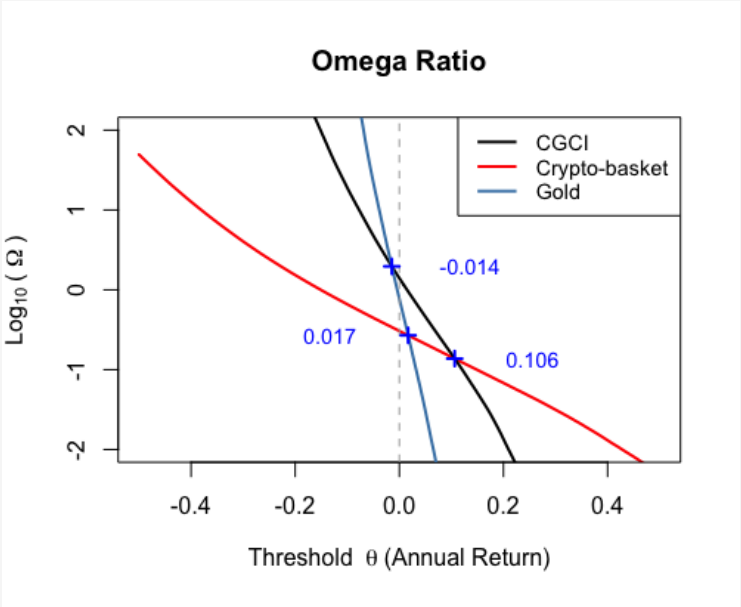

Figure 5.7: Omega Ratios - Log Scale

the high number of possible regime combinations, especially in the case of CGCI, we expect their duration to correspond to a few days. The average regime duration for the index is indeed approximately 3.44 days, with a total of $K_{c,T} \times K_{c,V} \times K_{g,T} \times K_{g,V} = 108$ possible regime combinations. Accordingly, in the case of the crypto-basket, with $K_{c,T} = 4$ trend states and $K_{c,V} = 3$ volatility states, we have $K_{c,T} \times K_{c,V} = 12$ regime combinations with an average duration of 4.27 days. Finally for gold, we observe $K_{g,T} \times K_{g,V} = 9$ different regime combinations with an average duration of 9.15 days.

Given the short duration of regimes, we express the return profile of each regime in terms of monthly return instead of annual. If we denote with $\boldsymbol{r}_j^i$ the vector of returns that correspond to regime j and simulation path i, we divide $\boldsymbol{r}_j^i$ in N partitions, each with a duration of 21 days, and obtain the average monthly return of regime j through:

$$\bar{R}_j^i = \sum_{j=1}^{N} \left(\prod_{t=1}^{21} (1 + r_{j,t}) - 1 \right) / N, \quad i \in 1, \ldots, 1\,000 \tag{5.3}$$

We consider the risk-adjusted return profile of each component per regime combination. As mentioned before, a main drawback of the Sharpe ratio when assessing the performance, is the fact that it fails to consider the entire distribution of returns. An additional disadvantage of the Sharpe ratio is evident in this case because we need to consider the presence of negative returns during bear market periods. A negative Sharpe ratio is generally problematic to interpret when persistent (during market downturns) because a large amount of volatility, given negative excess returns, wrongfully insinuates that the examined performance is not as poor as expected. To this end, when

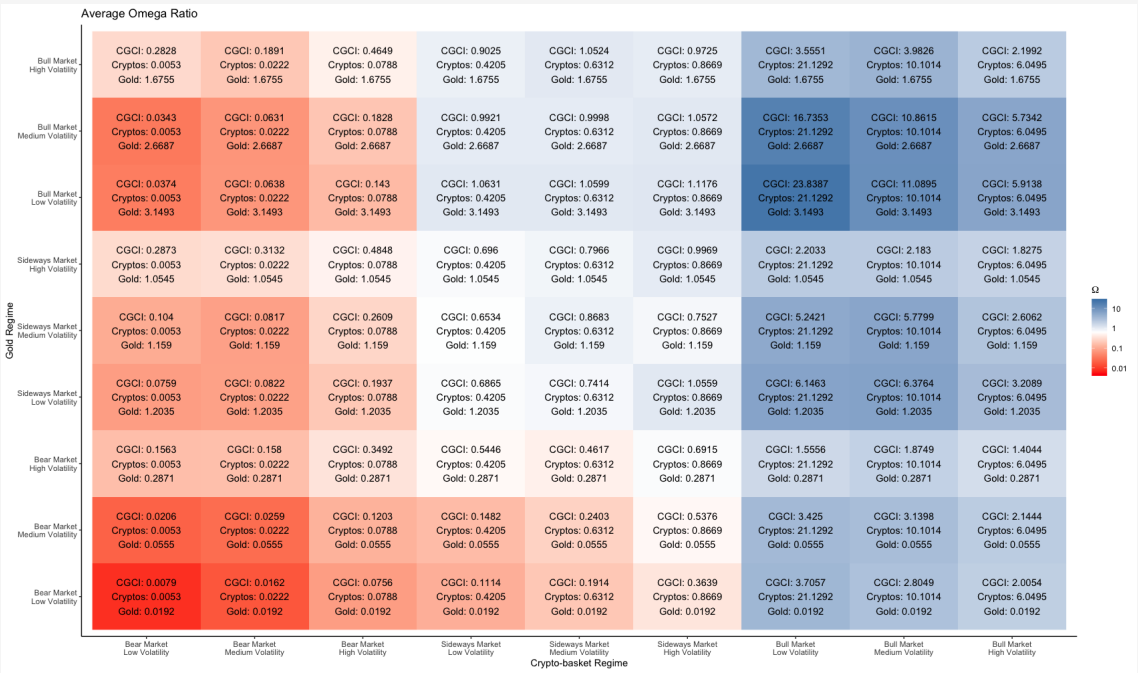

Figure 5.8: Average Simulated Omega Ratios (Monthly returns, $\theta = 0.0008$)

evaluating the regime-conditional risk-adjusted returns, we use the Omega ratio as well.

For each regime combination, we calculate the Omega ratio through 1 000 values of $\bar{R}$, corresponding to the 1 000 simulated time-series. We use a benchmark value of $\theta = 0.0008$ for the monthly returns, which roughly translates to a 1% annual return. The produced heatmap in Fig. 5.8 reveals high-risk regime combinations for the index diversification and rebalancing strategy. Moreover, it allows for a comparative analysis between the CGCI, the cryptoasset market and gold. For ease of exposition, and since we are interested in the three main trend regimes of bear, sideways and bull market periods, the outlier trend regime is omitted from the heatmap. Overall, the color gradient reveals that the main driver of the CGCI price is the crypto-basket component.

The heatmaps in Fig. 5.9 display the variability of the CGCI Omega ratio across different regimes, in comparison with its two components. All Omega ratios are estimated using the same target return benchmark value, $\theta = 0.0008$. In bull market conditions, all three components perform better in low volatility regimes. The highest value for the CGCI Omega ratio, $\Omega_{\text{CGCI}} = 23.8387$, is observed when both components experience low volatility and have an upward intermediate trend. In this case, the Omega ratios for the two index components are $\Omega_{\text{CB}} = 21.1292$ and $\Omega_{\text{Gold}} = 3.1493$ respectively. In regions that correspond to bear conditions for both the cryptoasset and gold markets, the CGCI performs best when both components are in a high-volatility state, with $\Omega_{\text{CGCI}} = 0.3492$, $\Omega_{\text{CB}} = 0.0788$ and $\Omega_{\text{Gold}} = 0.2871$. This is in line with the primary goal of the index to protect against unfavorable market conditions and to control and benefit from risk through diversification and frequent rebalancing.

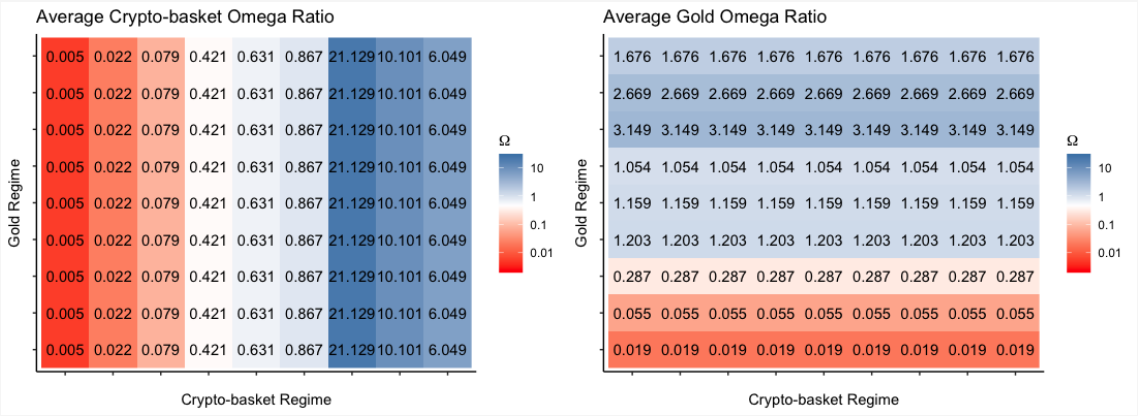

Figure 5.9: Regime-Conditional Average Omega Ratios, Crypto-basket & Gold (Monthly returns, $\theta = 0.008$)

Likewise, the regions that negatively affect the index performance the most lie around the bottom-left corner of the heatmap. Those regions correspond to periods when the two components simultaneously experience bear markets with low volatilities, therefore, providing limited opportunities for successful diversification. In this case, the Omega ratios of the CGCI and the crypto-basket lie closer to zero, $\Omega_{\text{CGCI}} = 0.0079$, $\Omega_{\text{CB}} = 0.0053$. Gold seems to offer better protection in times of market decline, with $\Omega_{\text{Gold}} = 0.0192$.

5.2.6 Summary

In this chapter we have proposed a way to describe the dynamic behavior of the two market determinants of the CGCI. The proposed framework includes a Gaussian Hidden Markov Model to extract the intermediate trend regimes, given through the weekly logarithmic returns, and a Markov-switching ARCH approach to describe the variability of the conditional variances, through the demeaned daily logarithmic returns. Their combination attempts to produce a realistic set of simulated price paths for the index and its two risk factors, each one containing numerous combinations of the identified regimes.

Taking into consideration the evolution of the index and its two risk factors, their overall performance is reported in terms of Sharpe and Omega ratio and assess their suitability for investors, according to their individual return targets and willingness to take on certain levels of risk. The Sharpe ratios across the entire datasets demonstrate the overall superiority of the diversified approach when seeking exposure in the cryptoasset market. Computations of the Omega ratio for different values of the target return threshold reveal that the index is more suitable for wealth-preserving investors and investors who target moderate returns, up to 10.6% on an annual basis. For investors with higher risk tolerance, portfolios with cryptoasset components only are more appropriate, whereas gold is the best choice when seeking protection against periods of persistently declining markets.

Chapter 6

Diversification Benefits of Cryptoassets for Traditional Asset Classes

The aim for balance between risk and reward in investment portfolios often requires studying the diversification contribution of its constituents. This objective requires to specify whether investors can extend their exposure in certain asset classes and benefit their portfolios in a statistically significant way. In this chapter, we address this issue of diversification in the context of cryptoasset portfolios and examine whether their risk-adjusted performance can be enhanced through seeking exposure into the commodities class. For an equally-weighted portfolio of five cryptoassets, we first consider the addition of physical gold, as conceptualised by the CoinShares Gold and Cryptoassets Index, a diversified, monthly-rebalanced index that seeks exposure to both asset classes. We further consider modifying the index composition by replacing physical gold with a basket of five commodities. Mean-variance spanning tests reveal that the addition of physical gold in the original cryptoasset portfolio translates to a significant shift in the efficient frontier, both in terms of the global minimum variance and the tangency portfolios. Additionally, expanding the exposure in the commodity side confirms a statistically significant improvement, with the diversification benefit arising from a shift in the tangency portfolio. We further generate a number of price paths for the original index, the modified index and their components, according to a Dynamic Conditional Correlation GARCH specification, to assess the efficiency of the index weighted risk contribution scheme. Results demonstrate a superior performance of the two indices when compared against their constituents in terms of Omega ratio. The modified index appears more appropriate for investors that seek higher annual returns, while the original composition would be more appropriate for individuals with moderate annual return goals.

This chapter was published at the IEEE International Conference on Blockchain and Cryptocurrency (ICBC) in 2021 [85].

6.1 Applications

6.1.1 Background

The inclusion of risky assets, such as cryptoassets, in investment portfolios requires careful consideration of the impact on the risk-adjusted performance. A key aspect of this understanding involves analyzing the portfolio's efficient frontier, which represents a collection of optimal portfolios offering the maximum possible returns for a given level of risk. Graphically, the efficient frontier is formed by plotting the portfolio's expected return against its standard deviation and is curved because each unit of risk added to a portfolio gains a diminishing amount of return. Huberman and Kandel [68] propose a multivariate test setting that examines the hypothesis that the efficient frontier of a benchmark set of K assets is the same as the efficient frontier of an augmented set of $K + N$ assets. Failure to reject the proposed hypothesis would suggest that the initial portfolio setting cannot be benefited by investing in the additional N assets under consideration. Kan and Zhou [77] conduct a comprehensive study of tests for mean-variance spanning based on the regression framework of Huberman and Kandel [68] and present in detail the Likelihood Ratio, Wald, Lagrange multiplier and step-down F tests.

Building on the aforementioned studies, a significant area yet to be fully explored is how the integration of cryptoassets with traditional asset classes affects portfolio dynamics. This chapter aims to fill this gap by investigating the diversification benefits that commodities might offer within the cryptoasset space. Specifically, it seeks to understand how the inclusion of such assets in cryptoasset portfolios impacts the mean-variance frontier.

We first consider the case of the CoinShares Gold and Cryptoassets Index and assess the diversification benefit of physical gold for a portfolio of five equally-weighted crypto-constituents. We further consider a case of diversified commodity exposure by replacing physical gold with a basket of five commodities and assess whether there exist opportunities to improve the index risk-adjusted performance. We also isolate the main market determinants of the formed portfolios, namely the crypto-basket, gold and the commodity basket, and study the dynamics of their conditional correlation. We produce 1 000 paths for each component and report the Omega ratio following the index rebalancing scheme. Our aim is to investigate how various strategy configurations align with diverse investor goals.

6.1.2 Datasets

In this chapter, we initially examine the CoinShares Gold and Cryptoassets Index to assess the diversification benefits of physical gold within a portfolio composed of five equally-weighted cryptoassets. We then explore a scenario of diversified commodity exposure, where physical gold is replaced with a basket of five commodities, to evaluate potential improvements in the index's

risk-adjusted performance. Utilizing the concept of mean-variance spanning, as presented in Section 2.3.2.3, we aim to determine the validity of the mean-variance spanning null hypothesis and investigate whether gold (and the commodity basket) influences both the global minimum variance and tangency portfolios. Additionally, employing DCC-GARCH models, detailed in Section 2.3.1.3, we will isolate and analyze the primary market determinants of the constructed portfolios—namely, the crypto-basket, gold, and the commodity basket—and examine the dynamics of their conditional correlation

Both the estimation of the DCC-GARCH parameters and the mean-variance tests are performed on a historical dataset of 1 308 price observations ranging from July 2nd, 2015 to November 2nd, 2020. The dataset contains the price time-series of the crypto-basket component of the CGCI rather than the individual prices of its crypto-constituents because (i) this study is not examining any alterations in the crypto-basket composition and (ii) the CGCI selection rules around the crypto-basket composition would make the simulation process unnecessarily complex. The crypto-basket historical prices are calculated using tick-by-tick trade data provided by Kaiko. The dataset also contains the time-series of five commodities. Gold prices, under the original CGCI calculations, correspond to the LBMA Gold Price PM data provided by ICE Benchmark Administration (IBA). The rest correspond to the respective price observations of iShares Silver Trust (SLV), Aberdeen Standard Physical Platinum Shares ETF (PPLT), Aberdeen Standard Physical Palladium Shares ETF (PALL) and West Texas Intermediate Crude Oil (WTI).

6.1.3 Regression-based Spanning Hypothesis Testing

The CGCI is designed based on the premise that the addition of physical gold in a cryptoasset portfolio improves the risk-return profile of the initial crypto-investment. We will seek to confirm this diversification benefit as statistically significant through the spanning tests of Section 2.3.2.3. Since spanning tests are not explicitly concerned with a specific allocation style, but rather examine the shift of the frontier hyperbola as a whole, we define the benchmark investment universe as the collection of any cryptoasset c that has historically been a constituent of the CGCI. We denote their daily logarithmic returns, R_c, R_{GLD}, R_{SLV}, R_{PPLT}, R_{PALL} and R_{WTI}. The regression setting for the tests is given by:

$$\boldsymbol{R}_i = \boldsymbol{\alpha} + \sum_{j=1}^{K} \beta_j \boldsymbol{R}_j + \boldsymbol{\epsilon}, \tag{6.1}$$

where $\boldsymbol{R}_j$ is the set of constituents comprising the cryptoasset-only benchmark portfolio and $\boldsymbol{R}_i$ denotes the test asset under consideration for addition. In this first case, the test asset $\boldsymbol{R}_i$ corresponds to physical gold. All three tests of spanning reject the null hypothesis, with LR $= 3160$, $p < 0.001$, W $= 27723$, $p < 0.001$ and LM $= 891$, $p < 0.001$, W $\geq$ LR $\geq$ LM. We conclude that the benchmark portfolio does not span the augmented portfolio and the diversification benefit is statistically significant.

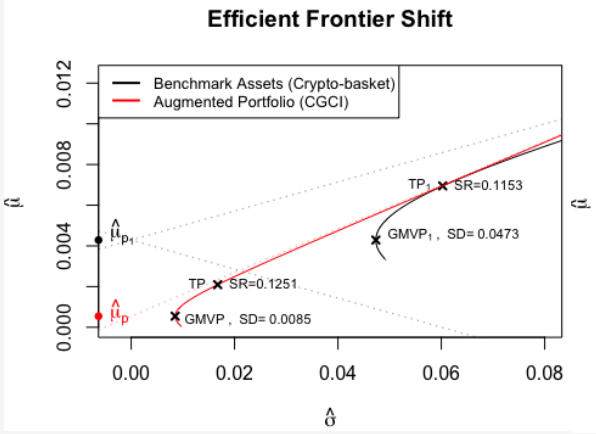

Figure 6.1: Spanning Test 1: Efficient Frontiers

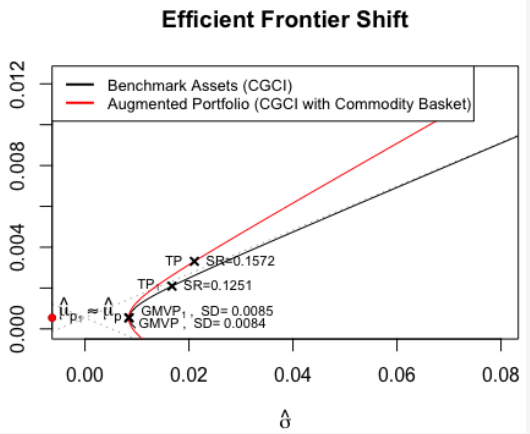

Figure 6.2: Spanning Test 2: Efficient Frontiers

The constants that describe the efficient frontier hyperbola on the $(\hat{\sigma}, \hat{\mu})$ space of the benchmark portfolio of K assets are $\hat{\alpha_1} = \hat{\mu_1}'\hat{V}_{11}^{-1}\hat{\mu_1}$, $\hat{b_1} = \hat{\mu_1}'\hat{V}_{11}^{-1}1_K$, $\hat{c_1} = 1_K'\hat{V}_{11}^{-1}1_K$ and $\hat{d_1} = \hat{\alpha}\hat{c} - \hat{b}^2$. Accordingly, the constants that define the location of the efficient frontier of the augmented portfolio of $N+K$ assets are, $\hat{\alpha} = \hat{\mu}'\hat{V}^{-1}\hat{\mu}$, $\hat{b} = \hat{\mu}'\hat{V}^{-1}1_{N+K}$, $\hat{c} = 1_{N+K}'\hat{V}^{-1}1_{N+K}$ and $\hat{d} = \hat{\alpha}\hat{c} - \hat{b}^2$, where $\hat{\mu} = \frac{1}{T}\sum_{t=1}^{T} R_t$ and $\hat{V} = \frac{1}{T}\sum_{t=1}^{T}(R_t - \hat{\mu})(R_t - \hat{\mu})'$. Here $\hat{\mu}$ and $\hat{V}$ represent the maximum likelihood estimates of the expected return and covariance matrix of the augmented portfolio and $\hat{\mu_1}$ and $\hat{V}_{11}$ represent the maximum likelihood estimates of the expected return and covariance matrix of the benchmark assets. We denote the global minimum variance and tangency benchmark portfolios by GMVP_1 and TP_1 and the global minimum variance and tangency augmented portfolios by GMVP and TP. The slopes of the asymptotes to the efficient hyperbolae of the benchmark and augmented portfolios are given by $\sqrt{\hat{d}_1/\hat{c}_1}$ and $\sqrt{\hat{d}/\hat{c}}$ respectively. Figure 6.1 displays the two frontier hyperbolae for the first round of spanning tests, where the benchmark portfolio only contains cryptoassets, while the augmented portfolio corresponds to the CGCI. The diversification benefit of gold is mainly attributed to a significant reduction of risk. The augmented global minimum variance portfolio corresponds to a risk level of $0.85 * \sqrt{252} = 13.5\%$ annualised volatility, compared against $4.73 * \sqrt{252} = 75.1\%$ for the cryptoasset-only benchmark. In terms of Sharpe ratio, the benchmark tangency portfolio is characterised by an annualised Sharpe value of 1.83, while the diversified portfolio presents an average simulated annualised value of 2.0. The efficient hyperbolae are characterised by asymptotes with slopes $\sqrt{\hat{d}_1/\hat{c}_1} = 0.0051$ and $\sqrt{\hat{d}/\hat{c}} = 0.0115$.

Following the rejection of the joint spanning hypothesis and the geometrical interpretation of the two portfolios, we follow the step-down procedure described in Section 2.3.2.3 and derive the F_1, F_2 statistics and their p-values. The separation of the two tests therefore allows us to isolate the reasons for rejection if the original null hypothesis is rejected. If the rejection derives from F_1, we can conclude that there is a statistically significant difference between the two tangency portfolios,

while a rejection of F_2 will indicate that a significant difference is observed between the two global minimum variance portfolios. Another benefit of the step-down procedure is that it allows us to adjust the significance levels of the two tests, according to the perceived economical significance of each. Given that investors are typically interested in risk-adjusted returns rather than solely volatility, and since a statistically significant shift in the tangency portfolio is much more difficult to detect [77], it is generally advisable to set the significance level of F_1 higher and that of F_2 lower. Nevertheless, the interpretation of the p-values in the separated tests is not a trivial task. For the purposes of this study, where the tangency portfolio shift is of great economical significance, we will accept the F_1 test for p-values that exceed a value of 0.15 and reject the F_2 null for p-values falling below 0.0005. This difficulty in interpreting the F_1 test results becomes specifically relevant in this case where, despite the improvement of the annualised Sharpe ratio from 1.83 to 2, we would fail to reject the null given a 5% significance level. For this case, we derive $F_1 = 2.12,\ p = 0.146$ and $F_2 = 27432,\ p < 0.0001$ and recognise a significant statistical shift both in the tangency and global minimum variance portfolio.

An additional interest of this study is to examine whether further diversification on the commodity side can benefit the CGCI. Here we denote by $\boldsymbol{R}_j$ the set of all the CGCI constituents (both cryptoassets and physical gold), while $\boldsymbol{R}_i$ denotes the four additional commodities, SLV, PPLT, PALL and WTI. All three tests of spanning reject the null hypothesis again at a significance level of 0.05, with LR $= 27.3,\ p = 0.0006$, W $= 27.5,\ p = 0.0006$ and LM $= 27,\ p = 0.0006$, W $\geq$ LR $\geq$ LM. We conclude that the benchmark portfolio does not span the augmented portfolio and is significantly benefited by the four additional commodities. Figure 6.2 displays the two frontier hyperbolae, where the benchmark portfolio corresponds to the CGCI setting, while the augmented portfolio corresponds to a CGCI portfolio that uses a commodity-basket rather than physical gold only. In this case, the diversification benefit of the commodity basket is attributable to an increase in expected returns. The augmented global minimum variance portfolio corresponds to a risk level of 13.3% volatility and does not drift away from the benchmark, which lies around the same level. In terms of the Sharpe ratio, the augmented tangency portfolio has managed to drive the risk-adjusted performance up to 2.5, compared to the previous value of 2. The slope of the hyperbola of the augmented portfolio increases to $\sqrt{\hat{d}/\hat{c}} = 0.0207$ compared to its previous benchmark of $\sqrt{\hat{d}_1/\hat{c}_1} = 0.0115$.

We follow up the joint hypothesis testing with the step-down approach. For this case, $F_1 = 2.03,\ p = 0.0889$ and $F_2 = 4.78,\ p = 0.0008$ and recognise a significant statistical shift only in the tangency portfolio. The p-value of the F_2 test in this case similarly highlights the importance of adjusting the significance levels of the step-down approach. A significance level of 0.05 would in this case indicate a significant shift in the global minimum variance portfolio, even though the test assets merely reduce its annualised standard deviation from 13.5% to 13.3%.

6.1.4 DCC-GARCH Estimations

The spanning test results from the previous section confirm that the addition of commodities in cryptoasset portfolios significantly shifts the efficient frontier. In this section, we examine how this diversification benefit is reflected in the WRC weighting scheme. We compare the risk-performance profiles of a cryptoasset-only portfolio, a portfolio that adds gold, following the CGCI weighting scheme, and a portfolio that replaces gold with five commodities, also following the CGCI weighting scheme. We denote the daily value of a given financial instrument i at time t by $V_{i,t}$ and its daily logarithmic returns by $r_{i,t}$. We first form a monthly-rebalanced commodity-basket, similarly to the crypto-basket component of the CGCI. The commodity-basket base level is set on 100 on July 1st, 2015 while the price level on day t from July 2nd, 2015 onwards is calculated as:

$$\text{CoB}_t = \left(1 + \sum_{i \in N_{c,t}} x_{i,R(t)} \times \left(\frac{V_{i,t}}{V_{i,r(t)}} - 1\right)\right) \times \text{CoB}_{R(t)}, \tag{6.2}$$

In Eq. 6.2, $N_{c,t}$ is the set of 5 commodities constituents on day t, $R(t)$ is the most recent rebalancing date preceding t, and similarly $V_{i,R(t)}$ is the value of commodity i, $x_{i,R(t)}$ is the weight of commodity i, equal to 0.2, and CoB_t is the commodity-basket price level on the last rebalancing date preceding t. The crypto-basket daily price observations are formed using the same formula and are denoted with CrB. All prices are expressed in USD. The DCC-GARCH is estimated on the three main components of interest, CrB, CoB and Gold. Table 6.1 contains the fitted model parameters.

6.1.5 Omega Ratio Comparison

Given the fitted model and a 5-year simulation horizon, we produce $N = 1\,000$ price paths for the CrB, CoB and gold, with the initial prices set to the last recorded prices of the historical dataset on November 2nd, 2020. We use the WRC allocation scheme (cf. Eq. 3.3) and produce $N = 1\,000$ paths for the CGCI, and $N = 1\,000$ paths for the modified CGCI, where the CoB replaces physical gold. We are ultimately interested in examining the individual baskets' risk-adjusted return profiles compared against the two diversified strategies.

Following the examination of the tangency portfolio shift, we also examine the risk-adjusted performance of the different portfolio specifications. We let X represent the returns of an asset and F its cumulative probability distribution function of returns. It is reminded that, given a selected target return threshold θ, the Omega ratio is given by:

$$\Omega(\theta) = \frac{\int_{\theta}^{\infty}[1 - F(r)]dr}{\int_{-\infty}^{\theta} F(r)dr} \tag{6.3}$$

In this study we inspect the average annual return of each component. Given a simulated price path

Table 6.1: DCC-GARCH Parameters and diagnostics

DCC-GARCH Fitting			
	Crypto-basket	**Commodity basket**	**Gold**
ARMA-GJR-GARCH Parameters (Eq. 2.3)	ϕ_1: 0.9669 θ_1: -0.9521 ω: 0.00003 α_1: 0.1168 γ_1: -0.06346 β_1: 0.9140	ϕ_1: 0.5044 θ_1: -0.4797 ω: 0.00002 α_1: 0.1925 γ_1: -0.0397 β_1: 0.7345	ϕ_1: -0.7792 θ_1: 0.7960 ω: 0.000001 α_1: 0.0669 γ_1: -0.0259 β_1: 0.9323
Residual Distribution Shape (Kolmogorov-Smirnov Test p-value)	3.3128 (1.0000)	4.5797 (0.8000)	5.3186 (0.7170)
Information Criteria Akaike Bayes	-14.784 -14.670		

Spanning Tests Results					
	LR	**W**	**LM**	F_1	F_2
CGCI Scenario Benchmark Assets (K): Crypto-basket Test Assets (N): Physical Gold	3160 (≤ 0.001)	27723 (≤ 0.001)	891 (≤ 0.001)	2.12 (0.1461)	27432 (≤ 0.0005)
Modified CGCI Scenario Benchmark Assets (K): Crypto-basket Test Assets (N): Commodity-basket	27.3 (0.0006)	27.5 (0.0006)	27 (0.0006)	2.03 (0.0889)	4.78 (0.0008)

P_i, where $i \in 1, \ldots, 1\,000$, the annualised return is obtained through $R_i = (P_{i,1+l}/P_{i,1})^{\frac{365}{l}} - 1$ where l denotes the length of the simulated prices expressed in number of days. This yields 1 000 values of annualised returns for the CGCI, crypto-basket and gold respectively.

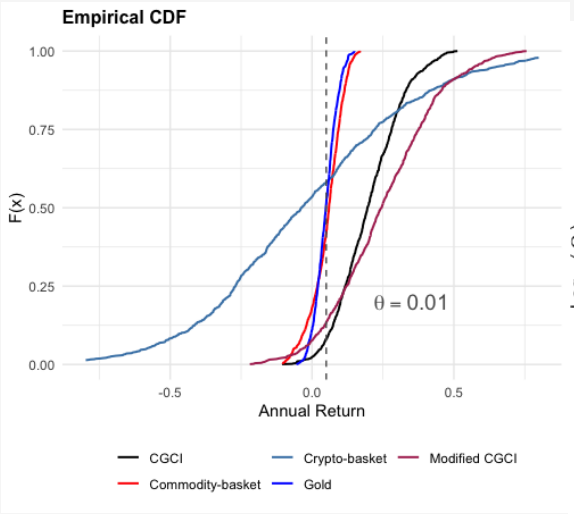

Figure 6.3: Empirical Cumulative Distribution Functions

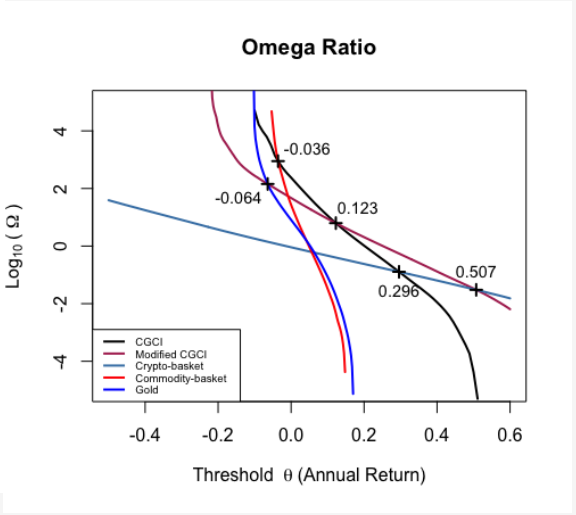

Figure 6.4: Omega Ratios - Log Scale

Fig. 6.3 presents a comparison of annual return distributions for the four different investment styles. The slope of the crypto-basket cumulative distribution function appears visibly less steep compared to the rest of the components, with significantly heavier tails. Both physical gold and the formed commodity basket display a reduced profit and loss range, with the commodity basket presenting signs of slightly heavier tails.

The two mixed portfolios that follow the CGCI weighting schemes appear to be relatively robust against the crypto-market's potential severe losses, while at the same time they display much higher chances of profit when compared against the commodity market. The CDF for the original CGCI is notably steep and progresses rapidly towards 1, crossing the $\theta = 0.01$ threshold quickly. The modified CGCI shows a CDF very close to the original, suggesting that the modifications do not significantly alter the return distribution. There is a slight shift to the left, indicating a marginal increase in the likelihood of lower returns compared to the original CGCI.

We also plot the Omega ratio as a function of the expected profitability parameter θ, to investigate the ranking among the five portfolios given different levels of target returns. For large negative values of θ, all three Omega ratios tend to infinity, while for large positive values of θ, they tend to zero. Fig. 6.4 presents on a log scale the Omega ratio of the CGCI, the modified CGCI, the crypto-basket, the commodity-basket and gold as a function of θ and allows us to rank the portfolios according to the intersection points of the five curves.

In the graph, the threshold θ is set at 0.1, consistent with the previous CDFs, serves as a benchmark to evaluate how much reward an investor gets for each unit of risk taken beyond the 10% annualised return threshold. The higher the Omega Ratio, the more favorable the trade-off between gains and risks. From the graph, the CGCI strategy exhibits a higher Omega Ratio at the $\theta = 0.1$ point, indicating a better return per unit of risk compared to the other strategies. The Modified CGCI, while

close to the original, shows a slightly lower Omega Ratio, therefore suggesting that the modifications have led to a minor reduction in the risk-reward measure. Both versions of CGCI outperform the other strategies at this particular point.

The intersection point of the CGCI and gold Omega lines reveals that the original index strategy is more appropriate for investors aiming for moderate positive returns up to 29.6% annually. Accordingly, gold is more effective in providing protection against negative market developments. The intersection point of the crypto-basket and original CGCI curves confirms that complete exposure to the crypto-space is appropriate for risk-tolerant investors who target annual returns that exceed 29.6%. When it comes to the modified CGCI setting, it manages to extend the range of overperformance. Specifically, the modified CGCI appears more appropriate for investors aiming up to 50.7% annual returns. When it comes to selecting between the two index methodologies, the original setting is more appropriate for investors who are interested in wealth preservation and moderate annual returns up to 12.3%, while the modified methodology is better suited for less risk-averse individuals that set a target annual return at up to 50.7%. Both physical gold and the commodity-basket are wealth-preservation tools, with the commodity basket displaying a more volatile profile.

6.1.6 Summary

In this chapter we have examined the diversification properties of the commodity class from the perspective of a cryptoasset investor. We utilise the concept of mean-variance spanning tests and examine how the addition of commodities in cryptoasset portfolios shifts the efficient frontier in a statistically significant way. A step-down approach using two separate F tests further allows us to examine changes in the global minimum variance and tangency portfolios. We first take into consideration the setting of the CoinShares Gold and Cryptoassets Index and confirm that the addition of physical gold to a basket of five equally-weighted cryptoassets translates to a significant shift in the mean-variance frontier, in both of the efficient portfolios. We also consider a second setting where gold is replaced by a basket of five commodities. The spanning tests reject the null hypothesis and the rejection is found to be due to a significant shift in the tangency portfolio.

We have additionally taken into consideration the two portfolio compositions and compared the two approaches in terms of their suitability for investors. The evolution of the portfolio risk factors have been described using a dynamic conditional correlation model, which is used to generate 1 000 different price paths. Computations of the Omega ratio for different values of the target return threshold reveal that the original index composition is more suitable for wealth-preserving investors and investors who target moderate returns. For investors with higher return expectations, up to 50.7%, the modified index approach is more appropriate.

Chapter 7

Conclusions

This thesis has presented a comprehensive approach to creating novel, investable indices for the cryptoasset space, in a way that offers exposure to alternative assets while balancing risk and return. To compliment the index design arguments, we have provided a scenario-based risk management framework which highlights the superiority of diversified strategies in mitigating risk. We have further examined the diversification properties of commodities from a cryptoasset investor's perspective, confirming that their addition to a basket of cryptoassets significantly shifts the mean-variance frontier.

This chapter summarises the findings of Chapter 3, Chapter 4, Chapter 5 and Chapter 6 and discusses some topics that can be considered for future work.

7.1 Conclusions

7.1.1 Summary of Contributions

In this thesis, we have developed and analysed an innovative investment approach that combines alternative assets, specifically cryptoassets and commodities, to offer investors exposure to a diversified and risk-adjusted product. We have extended the the equal risk contribution theory towards a weighted risk contribution scheme and have taken into account unique events in the cryptoasset space. The resulting product showcases a balance between price instability reduction and average return per unit of volatility, with moderate operating costs.

To further validate this approach, a framework for scenario-based risk management was developed, demonstrating the effectiveness of diversified indices - such as the CoinShares Gold and Cryptoassets Index (CGCI) - in mitigating risk. The framework can be adapted to accommodate various risk factor shocks, both in terms of volatility and correlation.

In order to describe the dynamic behavior of the CGCI and its market determinants, a combination of Gaussian Hidden Markov Model and Markov-switching ARCH approach was utilized. This enabled the production of realistic simulated price paths for the index and its risk factors, ultimately revealing the superiority of diversified strategies in terms of Sharpe and Omega ratios. It was determined that the CGCI is more suitable for wealth-preserving investors and those targeting moderate returns, while portfolios with only cryptoasset components or gold are preferable for those with higher risk tolerance or seeking protection against declining markets, respectively.

Finally, the diversification properties of commodities from a cryptoasset investor's perspective were investigated, highlighting the statistically significant shift in the efficient frontier when commodities are added to a cryptoasset portfolio. The original index composition was deemed more suitable for wealth-preserving investors and those with moderate return targets, while the modified index approach was more appropriate for investors with higher return expectations.

The research presented in this thesis ultimately led to the release of a family of novel indices for the cryptoasset space:

1. **CoinShares Gold & Cryptoassets Index** (CGCI, Fig. 7.1), the first EU Benchmark Regulations (EU BMR) compliant index for the digital asset industry that combines cryptoassets and gold and a risk and return profile that is superior to holding gold or cryptoassets alone.
2. **CoinShares Equally Weighted Crypto Index** (CECI, Fig. 7.2), designed to provide a diversified exposure to the five most liquid cryptoassets.
3. **CoinShares Gold and Bitcoin Index** (CGBI, Fig. 7.3), which employs the same asset allocation mechanism as the CGCI and the crypto-basket is composed of Bitcoin only rather than a basket of the top five cryptoassets.

The full index methodology documents have been made available online by the index owner, CoinShares Limited, at www.coinshares.com/index-strategies/ and the calculation agent, Compass Financial Technologies, at www.compassft.com/indices/.

Figure 7.1: CoinShares Gold & Cryptoassets Index (CGCI)

Figure 7.2: CoinShares Equally Weighted Crypto Index (CECI)

Figure 7.3: CoinShares Gold and Bitcoin Index (CGBI)

7.1.2 Future Work

Possible extensions of the topics covered in this thesis include:

Exploring Alternative Assets Classes One possible extension of the presented work is to expand the proposed methodologies to additional asset classes. This could include an array of traditional asset classes such as equities, fixed income, commodities, and real estate, along with emerging asset types like green bonds, and technology-based securities. The aim would be to explore the interdependencies between those diverse assets and focus on how cryptoassets interact within the broader financial ecosystem. It also includes studying the influence of broader factors such as global economic policies, significant technological advancements and important geopolitical events.

Dynamic Constituent Allocation The proposed framework provides an application example of the weighted risk contribution scheme, with a fixed risk contribution ratio parameter (α). An exciting avenue for further work would be to investigate the use of a dynamic portfolio weighting approach, where such parameters are time-varying. This would lead to an innovative family of adaptive risk parity schemes that optimize the allocation of assets in response to changing market conditions and investor risk preferences. Furthermore, this family of adaptive models can be tuned to take into consideration more complex correlation structures. In the setting presented in this thesis, the correlation between cryptoassets and commodities is assumed to be equal to zero, an assumption that can break down when extending to other asset classes or when market conditions change, such as during periods of economic recession, market turmoil, or regulatory changes.

Investment Universe Expansion Another possible extension is to examine the possibility of creating a family of sub-indices that include a wider variety of cryptoassets, such as tokens from emerging blockchain projects or DeFi platforms and evaluate the potential improvements in risk-adjusted returns and the overall stability of the portfolio.

Environmental, Social & Governance (ESG) Considerations Finally, an additional area for further research would be to assess the potential integration of ESG factors into the index construction process to promote responsible investing and evaluate the impact on portfolio performance and risk characteristics.

References

[1] Abbate, J. *Inventing the Internet*. MIT Press, 1999.

[2] Antipova, V. "Building and Testing Global Investment Portfolios Using Alternative Asset Classes". MA thesis. Lithuania: Vytautas Magnus University, 2019.

[3] Antonopoulos, A. M. *Mastering Bitcoin: Unlocking Digital Cryptocurrencies*. O'Reilly Media, Inc., 2014.

[4] Ardia, D., Bluteau, K., Boudt, K., et al. "Forecasting risk with Markov-switching GARCH models: A large-scale performance study". In: *International Journal of Forecasting* 34.4 (2018), pp. 733–747.

[5] Ardia, D., Bluteau, K., and Rüede, M. "Regime changes in Bitcoin GARCH volatility dynamics". In: *Finance Research Letters* 29 (2019), pp. 266–271.

[6] *Bakkt Digital Asset Futures*. 2019. URL: https://www.bakkt.com/markets/bitcoin-futures.

[7] Basel Committee on Bank Supervision (BCBS). *Basel I: the Basel Capital Accord*. July 1988.

[8] Basel Committee on Bank Supervision (BCBS). *Basel II: International Convergence of Capital Measurement and Capital Standards: a Revised Framework*. June 2004.

[9] Baum, L. E., Petrie, T., Soules, G., et al. "A Maximization Technique Occurring in the Statistical Analysis of Probabilistic Functions of Markov Chains". In: *The Annals of Mathematical Statistics* 41.1 (1970), pp. 164–171.

[10] Baur, D. G., Dimpfl, T., and Kuck, K. "Bitcoin, gold and the US dollar – A replication and extension". In: *Finance Research Letters* 25 (2018), pp. 103–110. ISSN: 1544-6123.

[11] Bauwens, L., Preminger, A., and Rombouts, J. "Theory and Inference for a Markov Switching GARCH Model". In: *Econometrics Journal* 13.2 (2010), pp. 218–244.

[12] Bedi, P. and Nashier, T. "On the Investment Credentials of Bitcoin: A Cross-Currency Perspective". In: *Research in International Business and Finance* 51 (Aug. 2019).

[13] Benartzi, S. and Thaler, R. H. "Naive Diversification Strategies in Defined Contribution Saving Plans". In: *The American Economic Review* 91.1 (2001), pp. 79–98.

[14] Bernardo, A. E. and Ledoit, O. "Gain, Loss, and Asset Pricing". In: *Journal of Political Economy* 108 (2000), pp. 144–172.

[15] Berndt, E. R. and Savin, N. E. "Conflict among Criteria for Testing Hypotheses in the Multivariate Linear Regression Model". In: *Econometrica* 45.5 (1977), pp. 1263–1277.

[16] BlackRock. *Index Investing Supports Vibrant Capital Markets*. 2017.

[17] Bloomberg. *Index Methodology: Bloomberg Galaxy Crypto Index*. Index Methodology. Apr. 2019.

[18] Board of Governors of the Federal Reserve System. "Amendments to Policy Statement on the Scenario Design Framework for Stress Testing". In: *Federal Register* 84 (Feb. 2019), pp. 6651–6664.

[19] Bodie, Z., Kane, A., and Marcus, A. J. *Investments*. New York, NY: McGraw-Hill Education, 2014.

[20] Bollerslev, T. "Generalized Autoregressive Conditional Heteroskedasticity". In: *Journal of Econometrics* 31.3 (1986), pp. 307–327.

[21] Booth, D. and Fama, E. "Diversification Returns and Asset Contributions". In: *Financial Analysts Journal* 48.3 (1992), pp. 26–32.

[22] Bouchey, P., Nemtchinov, V., Paulsen, A., et al. "Volatility Harvesting: Why Does Diversifying and Rebalancing Create Portfolio Growth?" In: *The Journal of Wealth Management* 15.2 (2012), pp. 26–35. ISSN: 1534-7524.
[23] Brauneis, A. and Mestel, R. "Cryptocurrency-Portfolios in a Mean-Variance Framework". In: *Finance Research Letters* 28 (June 2018).
[24] Brauneis, A. and Mestel, R. "Cryptocurrency-portfolios in a mean-variance framework". In: *Finance Research Letters* 28 (2019), pp. 259–264.
[25] Bredin, D., Conlon, T., and Poti, V. "Does gold glitter in the long-run? Gold as a hedge and safe haven across time and investment horizon". In: *International Review of Financial Analysis* 41 (2015), pp. 320–328. ISSN: 1057-5219.
[26] Breuer, T., Jandacka, M., Rheinberger, K., et al. "How to Find Plausible, Severe, and Useful Stress Scenarios". In: *International Journal of Central Banking* 5 (Mar. 2009).
[27] Breusch, T. S. "Conflict Among Criteria for Testing Hypotheses: Extensions and Comments". In: *Econometrica* 47.1 (1979), pp. 203–207.
[28] Brière, M., Oosterlinck, K., and Szafarz, A. "Virtual Currency, Tangible Return: Portfolio Diversification with Bitcoin". In: *Journal of Asset Management* 16.6 (2015), pp. 365–373.
[29] Burniske, C. and Tatar, J. *Cryptoassets: The Innovative Investor's Guide to Bitcoin and Beyond*. 1st ed. New York: McGraw-Hill Education, 2017. ISBN: 1260026671.
[30] Buterin, V. *Ethereum: A Next-Generation Cryptocurrency and Decentralized Application Platform*. 2015. URL: https://bitcoinmagazine.com/technology/ethereum-next-generation-cryptocurrency-decentralized-application-platform-1390528211/.
[31] Casey, M. J. and Vigna, P. *The Truth Machine: The Blockchain and the Future of Everything*. St. Martin's Press, 2018.
[32] Castro, J. G., Tito, E. A. H., Brandão, L. E., et al. "Crypto-assets Portfolio Optimization Under the Omega Measure". In: *The Engineering Economist* 65 (2020), pp. 114–134.
[33] Chaum, D. "Blind signatures for untraceable payments". In: *Advances in Cryptology Proceedings of Crypto*. Vol. 82. 3. 1983, pp. 199–203.
[34] Cherubini, U., Luciano, E., and Vecchiato, W. *Copula Methods in Finance*. John Wiley & Sons, Jan. 2004. Chap. 5, pp. 178–180.
[35] Chu, J., Chan, S., Nadarajah, S., et al. "GARCH Modelling of Cryptocurrencies". In: *Journal of Risk and Financial Management* 10 (Oct. 2017), p. 17.
[36] CoinMarketCap. *Historical Snapshot - December 31, 2017*. 2018. URL: https://coinmarketcap.com/historical/20171231/.
[37] CoinMarketCap. *Bitcoin Historical Data*. 2021. URL: https://coinmarketcap.com/currencies/bitcoin/historical-data/.
[38] Cont, R. "Empirical Properties of Asset Returns: Stylized Facts and Statistical Issues". In: *Quantitative Finance* 1 (Mar. 2002), pp. 223–236.
[39] Costa, G. and Kwon, R. "Risk parity portfolio optimization under a Markov regime-switching framework". In: *Quantitative Finance* 19.3 (2018), pp. 453–471.
[40] CRYPTO20. *CRYPTO20: The First Tokenized Cryptocurrency Index Fund*. White Paper. Oct. 2017.
[41] Demiguel, V., Garlappi, L., and Uppal, R. "Optimal Versus Naive Diversification: How Inefficient is the 1/N Portfolio Strategy?" In: *Review of Financial Studies* 22 (May 2009).
[42] DeRoon, F. A. and Nijman, T. E. "Testing for Mean-Variance Spanning: a Survey". In: *Journal of Empirical Finance* 8.2 (2001), pp. 111–155.
[43] Dubikovsky, V. and Susinno, G. *Demystifying Rebalancing Premium and Extending Portfolio Theory in the Process*. May 2015. DOI: 10.2139/ssrn.2927791.

[44] Duprey, T. and Klaus, B. *How to Predict Financial Stress? An Assessment of Markov Switching Models*. Working Paper Series 2057. European Central Bank, 2017.
[45] Dyhrberg, A. "Hedging capabilities of bitcoin. Is it the virtual gold?" In: *Finance Research Letters* 16 (2016), pp. 139–144.
[46] Elendner, H. et al. "The Cross-Section of Crypto-Currencies as Financial Assets: Investing in Crypto-Currencies Beyond Bitcoin". In: *Handbook of Blockchain, Digital Finance, and Inclusion*. Elsevier, 2018, pp. 145–173.
[47] Elton, E. J., Gruber, M. J., Brown, S. J., et al. *Modern Portfolio Theory and Investment Analysis*. Hoboken, NJ: John Wiley & Sons, 2014.
[48] Engle, R. "Autoregressive Conditional Heteroscedasticity with Estimates of the Variance of United Kingdom Inflation". In: *Econometrica* 50.4 (1982), pp. 987–1007.
[49] Engle, R. and Kroner, K. "Multivariate Simultaneous Generalized ARCH". In: *Econometric Theory* 11 (2000), pp. 122–150.
[50] Engle, R. and Sheppard, K. "Theoretical and Empirical Properties of Dynamic Conditional Correlation Multivariate GARCH". In: *Department of Economics, UC San Diego, University of California at San Diego, Economics Working Paper Series* (Oct. 2001).
[51] Fang, F., Ventre, C., Basios, M., et al. *Cryptocurrency Trading: A Comprehensive Survey*. 2020.
[52] *Fidelity Digital Assets*. 2018. URL: https://www.fidelitydigitalassets.com/.
[53] Genest, C. and Remillard, B. "Validity of the parametric bootstrap for goodness-of-fit testing in semiparametric models". In: *Annales De L'Institut Henri Poincare – Probabilites et Statistiques* (Dec. 2008).
[54] Ghahramani, Z. "An Introduction to Hidden Markov Models and Bayesian Networks". In: *Hidden Markov Models: Applications in Computer Vision*. World Scientific Publishing Co., Inc., 2001, pp. 9–42.
[55] Glosten, L. R., Jagannathan, R., and Runkle, D. E. "On the Relation between the Expected Value and the Volatility of the Nominal Excess Return on Stocks". In: *Journal of Finance* 48.5 (1993), pp. 1779–1801.
[56] Graves, S. and Stevens, R. *What Is 'The Merge'? Ethereum's Move to Proof of Stake*. 2022. URL: https://decrypt.co/resources/what-merge-ethereum-move-proof-stake.
[57] Grayscale. *Grayscale Investments*. 2020. URL: https://grayscale.co/.
[58] Group, C. *CME Bitcoin Futures*. 2017. URL: https://www.cmegroup.com/trading/equity-index/us-index/bitcoin.html.
[59] Haas, M. "A New Approach to Markov-Switching GARCH Models". In: *Journal of Financial Econometrics* 2.4 (2004), pp. 493–530.
[60] Hamilton, J. "A New Approach to the Economic Analysis of Nonstationary Time Series and the Business Cycle". In: *Econometrica* 57.2 (1989), pp. 357–84.
[61] Hamilton, J. and Susmel, R. "Autoregressive Conditional Heteroskedasticity and Changes in Regime". In: *Journal of Econometrics* 64.1-2 (1994), pp. 307–333.
[62] Hassan, M. and Nath, B. "Stock Market Forecasting Using Hidden Markov Model: A New Approach". In: *Proceedings of the 5th International Conference on Intelligent Systems Design and Applications*. 2005, pp. 192–196.
[63] Henriques, I. and Sadorsky, P. "Can Bitcoin Replace Gold in an Investment Portfolio?" In: *Journal of Risk and Financial Management* 11.3 (2018), p. 48.
[64] HM Treasury, Financial Conduct Authority, and Bank of England. *Cryptoassets Task Force: final report*. Oct. 2018.
[65] Hood, M. and Malik, F. "Is gold the best hedge and a safe haven under changing stock market volatility?" In: *Review of Financial Economics* 22.2 (2013), pp. 47–52.

[66] Hosking, P. and Webster, P. "Chancellor on brink of second bailout for banks". In: *The Times* 69079 (Jan. 2009), p. 1.
[67] Howcroft, E. *Explainer: NFTs are hot. So what are they?* 2021. URL: https://www.reuters.com/article/us-crypto-currency-nft-explainer-idUSKBN2B92MA.
[68] Huberman, G. and Kandel, S. "Mean-Variance Spanning". In: *Journal of Finance* 42.4 (1987), pp. 873–88.
[69] Indices, S. D. J. *S&P Digital Market Indices Methodology*. Tech. rep. 2023.
[70] International Settlements, B. for. *Central bank digital currencies: foundational principles and core features*. 2021. URL: https://www.bis.org/publ/othp33.pdf.
[71] Investopedia. *Exchange-Traded Fund (ETF) Definition*. 2021. URL: https://www.investopedia.com/terms/e/etf.asp.
[72] Investopedia. *Index Definition*. 2021. URL: https://www.investopedia.com/terms/i/indexfund.asp.
[73] Investopedia. *Index Futures Definition*. 2021. URL: https://www.investopedia.com/terms/i/indexfutures.asp.
[74] Investopedia. *Index Option Definition*. 2021. URL: https://www.investopedia.com/terms/i/indexoption.asp.
[75] Investopedia. *Inflation-Linked Bond Definition*. 2021. URL: https://www.investopedia.com/terms/i/indexlinkedbond.asp.
[76] Jorion, P. "Bayes-Stein Estimation for Portfolio Analysis". In: *The Journal of Financial and Quantitative Analysis* 21.3 (1986), pp. 279–292.
[77] Kan, R. and Zhou, G. "Tests of Mean-Variance Spanning". In: *Annals of Economics and Finance* 13 (Mar. 2008), pp. 145–193.
[78] Katsiampa, P. "An Empirical Investigation of Volatility Dynamics in the Cryptocurrency Market". In: *Research in International Business and Finance* 50.C (2019), pp. 322–335.
[79] Keating, C. and Shadwick, W. "A Universal Performance Measure". In: *Journal of Performance Measurement* 6 (2002).
[80] Kiayias, A., Russell, A., David, B., et al. "Ouroboros: A Provably Secure Proof-of-Stake Blockchain Protocol". In: *Annual International Cryptology Conference* (2017), pp. 357–388.
[81] Kim, J.-M., Kim, S.-T., and Kim, S. "On the Relationship of Cryptocurrency Price with US Stock and Gold Price Using Copula Models". In: *Mathematics* 8 (Oct. 2020).
[82] Kjærland, F., Khazal, A., Krogstad, E., et al. "An Analysis of Bitcoin's Price Dynamics". In: *Journal of Risk and Financial Management* 11 (Oct. 2018), p. 63.
[83] Koki, C., Leonardos, S., and Piliouras, G. "Do Cryptocurrency Prices Camouflage Latent Economic Effects? A Bayesian Hidden Markov Approach". In: *Future Internet* 12 (2020), p. 59.
[84] Koutsouri, A., Petch, M., and Knottenbelt, W. J. "Stress Testing Diversified Portfolios: The Case of the CoinShares Gold and Cryptoassets Index". In: *Proc. 2nd International Conference on Mathematical Research for the Blockchain Economy (MARBLE 2020)*. May 2020.
[85] Koutsouri, A., Petch, M., and Knottenbelt, W. J. "Diversification Benefits of Commodities for Cryptoasset Portfolios". In: *2021 IEEE International Conference on Blockchain and Cryptocurrency (ICBC)*. 2021, pp. 1–9. DOI: 10.1109/ICBC51069.2021.9461107.
[86] Koutsouri, A., Petch, M., and Knottenbelt, W. J. "Performance of the CoinShares Gold and Cryptoassets Index Under Different Market Regimes". In: *Cryptoeconomic Systems* 1.2 (Oct. 2021). https://cryptoeconomicsystems.pubpub.org/pub/koutsouri-cgci-performance.
[87] Koutsouri, A., Poli, F., Alfieri, E., et al. "Balancing Cryptoassets and Gold: A Weighted-Risk-Contribution Index for the Alternative Asset Space". In: *Proc. 1st International Conference on Mathematical Research for the Blockchain Economy (MARBLE 2019)*. Santorini, Greece, May 2019.

[88] Kovach, S. *Tesla buys $1.5 billion in bitcoin, plans to accept it as payment*. 2021. URL: https://www.cnbc.com/2021/02/08/tesla-buys-1point5-billion-in-bitcoin.html.
[89] Lee, C. *Announcing Litecoin*. 2011. URL: https://web.archive.org/web/20171008042924/http://litecoin.org/.
[90] Li, L. "An Economic Measure of Diversification Benefits". In: *Yale School of Management, Yale School of Management Working Papers* (Jan. 2003).
[91] Li, W. and Mak, T. "On the Squared Residual Autocorrelations in Non-linear Time Series with Conditional Heteroscedasticity". In: *Journal of Time Series Analysis* (June 2008), pp. 627–636.
[92] Li, X. and Wang, C. A. "The technology and economic determinants of cryptocurrency exchange rates: The case of Bitcoin". In: *Decision Support Systems* 95 (2017), pp. 49–60. ISSN: 0167-9236. DOI: https://doi.org/10.1016/j.dss.2016.12.001.
[93] Lindberg, C. "Portfolio optimization when expected stock returns are determined by exposure to risk". In: *arXiv.org, Quantitative Finance Papers* 15 (May 2009). DOI: 10.3150/08-BEJ163.
[94] Liu, W. "Portfolio diversification across cryptocurrencies". In: *Finance Research Letters* 29 (2019), pp. 200–205.
[95] Lopez, J. "Stress tests: useful complements to financial risk models". In: *FRBSF Economic Letter* (Feb. 2005).
[96] Maillard, S., Roncalli, T., and Teiletche, J. *On the Properties of Equally-weighted Risk Contributions Portfolios*. Sept. 2008. DOI: 10.2139/ssrn.1271972.
[97] Mancini, G. "Stablecoins: The New Banknotes for a Crypto World?" In: *Journal of Alternative Investments* 21.2 (2018), pp. 15–20.
[98] *Manhattan U.S. Attorney Announces Seizure of Additional $28 Million Worth of Bitcoins Belonging to Ross William Ulbricht, Alleged Owner and Operator of "Silk Road" Website, Federal Bureau of Investigation*. 2013.
[99] Markowitz, H. "Portfolio Selection". In: *The Journal of Finance* 7.1 (1952), pp. 77–91.
[100] McNeil, A., Frey, R., and Embrechts, P. *Quantitative Risk Management: Concepts, Techniques, and Tools*. Vol. 101. Princeton University Press, Oct. 2005.
[101] Merkle, R. C. "Ethereum: A Next-Generation Smart Contract and Decentralized Application Platform". In: *Ledger* 1 (2016), pp. 99–101.
[102] Michaud, R. O. "The Markowitz Optimization Enigma: Is 'Optimized' Optimal?" In: *Financial Analysts Journal* 45.1 (1989), pp. 31–42.
[103] Mougayar, W. *The Business Blockchain: Promise, Practice, and Application of the Next Internet Technology*. Wiley, 2016.
[104] Mouy, P., Archer, Q., and Selmi, M. "Extremely (un)likely: a plausibility approach to stress testing". In: *Risk Magazine* (2017), pp. 72–77.
[105] MV Index Solutions. *MVIS CryptoCompare Digital Assets 5 Index*. Index Factsheet. Mar. 2019.
[106] Nakamoto, S. *Bitcoin: A Peer-to-Peer Electronic Cash System*. 2008. URL: https://bitcoin.org/bitcoin.pdf.
[107] Narayanan, A., Bonneau, J., Felten, E., et al. *Bitcoin and Cryptocurrency Technologies: A Comprehensive Introduction*. Princeton University Press, 2016.
[108] Nguyen, N. and Nguyen, D. "Hidden Markov Model for Stock Selection". In: *Risks* 3.4 (2015), pp. 455–473.
[109] Nyström, K. and Skoglundy, J. *A Framework for Scenario-based Risk Management*. Apr. 2002.

[110] Popper, N. *Digital Gold: Bitcoin and the Inside Story of the Misfits and Millionaires Trying to Reinvent Money*. Harper, 2015.
[111] Poundstone, W. *Fortune's Formula*. Hill and Wang, 2005.
[112] Raskin, M. and Yermack, D. *Digital Currencies, Decentralized Ledgers, and the Future of Central Banking*. Working Paper 22238. National Bureau of Economic Research, 2016.
[113] Remillard, B., Genest, C., and Beaudoin, D. "Goodness-of-fit tests for copulas: A review and a power study". In: *Insurance: Mathematics and Economics* (Apr. 2009), pp. 199–213.
[114] Reuters. *Factbox: Crypto's string of bankruptcies*. 2023. URL: https://www.reuters.com/business/finance/cryptos-string-bankruptcies-2023-01-20/.
[115] Rickards, J. *The New Case for Gold*. Portfolio/Penguin Random House UK, 2016.
[116] Salhi, K., Deaconu, M., Lejay, A., et al. "Regime Switching Model for Financial Data: Empirical Risk Analysis". In: *Physica A: Statistical Mechanics and its Applications* 461 (2015), pp. 148–157.
[117] Sandor, K. and Genç, E. *The Fall of Terra: A Timeline of the Meteoric Rise and Crash of UST and LUNA*. 2022. URL: https://www.coindesk.com/learn/the-fall-of-terra-a-timeline-of-the-meteoric-rise-and-crash-of-ust-and-luna/.
[118] Scherer, B. "Can robust portfolio optimisation help to build better portfolios?" In: *Journal of Asset Management* 7.6 (Mar. 2007), pp. 374–387. DOI: 10.1057/palgrave.jam.2250.
[119] Securities, U. and Commission, E. *SEC's 2021 Examination Priorities*. 2021. URL: https://www.sec.gov/files/2021-exam-priorities.pdf.
[120] Securities, U. and Commission, E. *SEC Charges Samuel Bankman-Fried with Defrauding Investors in Crypto Asset Trading Platform FTX*. 2022. URL: https://www.sec.gov/news/press-release/2022-219.
[121] Security and Exchange Commission. *Virtual Currencies: The Oversight Role of the U.S. Securities and Exchange Commission and the U.S. Commodity Futures Trading Commission*. Report. Feb. 2018.
[122] Sharpe, W. F. "Mutual Fund Performance". In: *The Journal of Business* 39.1 (1966), pp. 119–138.
[123] Shu, J.-J. and Wang, Q.-W. "Beyond Parrondo's Paradox". In: *Scientific reports* 4 (Feb. 2014), p. 4244.
[124] Son, H. *Goldman Is Setting Up a Cryptocurrency Trading Desk*. 2017. URL: https://www.bloomberg.com/news/articles/2017-12-21/goldman-is-said-to-be-building-a-cryptocurrency-trading-desk.
[125] Son, H. *JP Morgan is rolling out the first US bank-backed cryptocurrency to transform payments business*. 2019. URL: https://finance.yahoo.com/news/jp-morgan-rolling-first-us-105916377.html.
[126] SourceForge. *Bitcoin*. 2009.
[127] Statman, M. "The Diversification Puzzle". In: *Financial Analysts Journal* 60.4 (2004), pp. 44–53.
[128] Stein, D., Nemtchinov, V., and Pittman, S. "Diversifying and Rebalancing Emerging Market Countries". In: *The Journal of Wealth Management* 11.4 (2009), pp. 79–88. ISSN: 1534-7524.
[129] Studer, G. "Market risk computation for nonlinear portfolios". In: *The Journal of Risk* 1.4 (1999), pp. 33–53.
[130] Swan, M. *Blockchain: Blueprint for a New Economy*. O'Reilly Media, 2015.
[131] Szabo, N. *Secure property titles with owner authority*. 1998.
[132] Szabo, N. *Bit gold*. Unenumerated Blog. 2005.
[133] Tapscott, D. and Tapscott, A. *Blockchain Revolution: How the Technology Behind Bitcoin Is Changing Money, Business, and the World*. Penguin Publishing Group, 2016.

[134] The Law Library of Congress. *Regulation of Cryptocurrency in Selected Jurisdictions*. Report. June 2018.
[135] Thies, S. and Molnár, P. "Bayesian change point analysis of Bitcoin returns". In: *Finance Research Letters* 27 (2018), pp. 223–227.
[136] Traccucci, P., Dumontier, L., Garchery, G., et al. *A Triptych Approach for Reverse Stress Testing of Complex Portfolios*. 2019.
[137] Treasury, U. D. of the. *President's Working Group on Financial Markets Releases Report and Recommendations on Stablecoins*. 2021. URL: https://home.treasury.gov/news/press-releases/jy0454.
[138] Trimborn, S. and Härdle, W. K. "CRIX an Index for Cryptocurrencies". In: *Journal of Empirical Finance* 49 (Dec. 2018), pp. 107–122. ISSN: 0927-5398.
[139] Tsay, R. S. *Analysis of Financial Time Series*. John Wiley & Sons, 2010. Chap. 3, pp. 109–173.
[140] Tütüncü, R. and Koenig, M. "Robust Asset Allocation". In: *Annals of Operations Research* 132.1 (2004), pp. 157–187.
[141] Union, E. *The Fifth Anti-Money Laundering Directive (AMLD5)*. 2021. URL: https://eur-lex.europa.eu/legal-content/EN/TXT/?uri=CELEX%5C%3A32018L0843.
[142] Wood, G. "Ethereum: A Secure Decentralized Generalized Transaction Ledger". In: *Ethereum Yellow Paper* (2014).
[143] Wu, C. and Pandey, V. "The Value of Bitcoin in Enhancing the Efficiency of an Investor's Portfolio". In: *Journal of Financial Planning* 27 (Sept. 2014), pp. 44–52.
[144] Yermack, D. "Is Bitcoin a Real Currency? An Economic Appraisal". In: *Handbook of Digital Currency*. Elsevier, 2015. DOI: 10.1016/b978-0-12-802117-0.00002-3.
[145] Zhu, X. and Zhu, J. "Predicting stock returns: A regime-switching combination approach and economic links". In: *Journal of Banking & Finance* 37.11 (2013), pp. 4120–4133.
[146] Zohar, A. "Bitcoin: Under the Hood". In: *Communications of the ACM* 58.9 (2015), pp. 104–113.
[147] Zohar, A. *The Age of Cryptocurrency: How Bitcoin and the Blockchain Are Challenging the Global Economic Order*. St. Martin's Press, 2015.
[148] Zuckerman, G. *The Man Who Solved the Market: How Jim Simons Launched the Quant Revolution*. Penguin Press, 2019.

Appendices

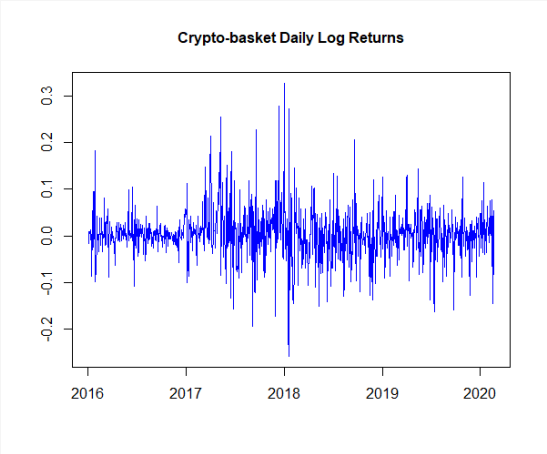

Figure 7.4: Crypto-basket log-returns

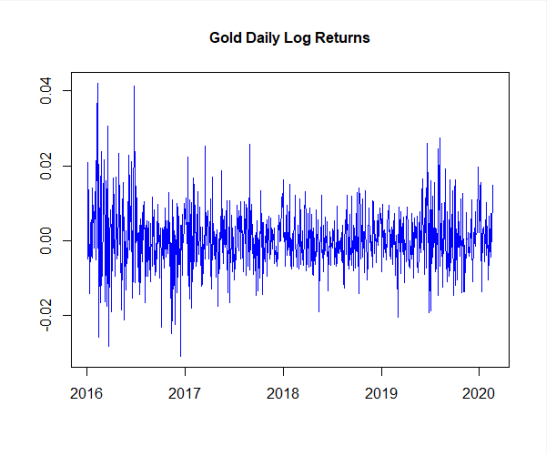

Figure 7.5: Gold log-returns

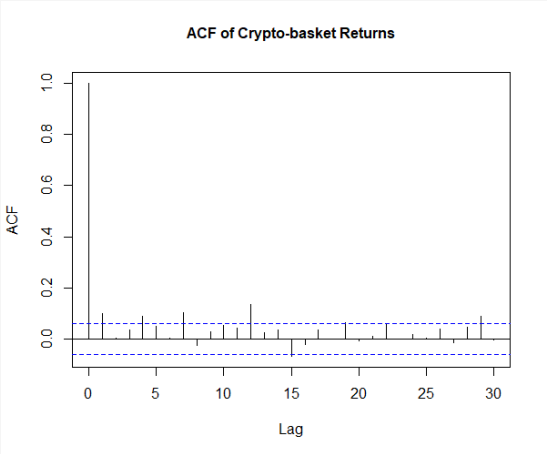

Figure 7.6: ACF of Crypto-basket returns

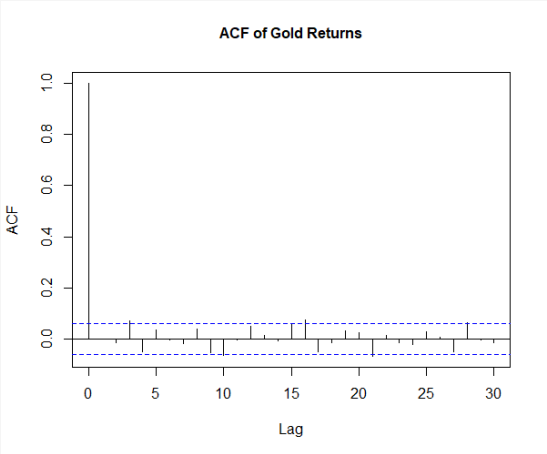

Figure 7.7: ACF of Gold returns

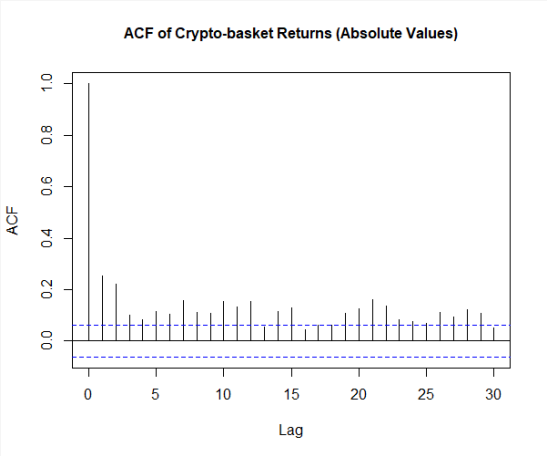

Figure 7.8: ACF of Crypto-basket returns (absolute values)

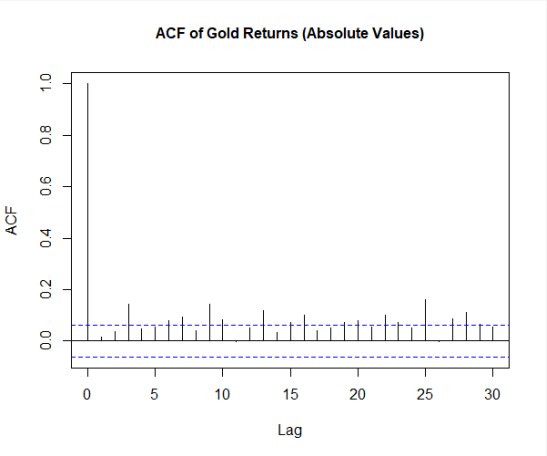

Figure 7.9: ACF of Gold returns (absolute values)

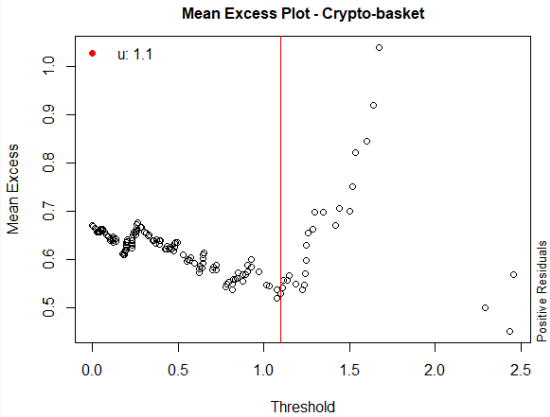

Figure 7.10: Crypto-basket mean excess plot Positive residuals

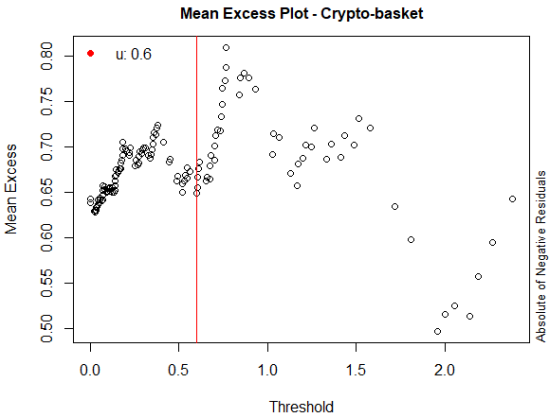

Figure 7.11: Crypto-basket mean excess plot Absolute of negative residuals

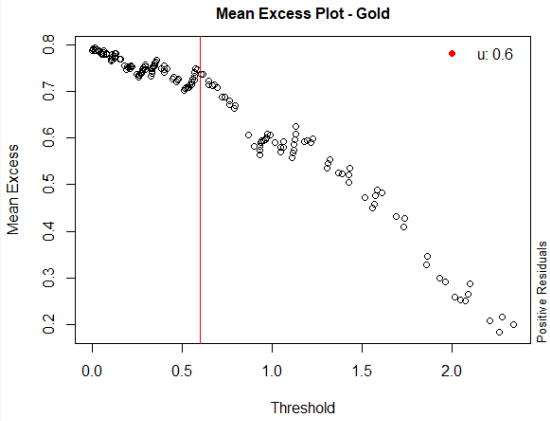

Figure 7.12: Gold mean excess plot Positive residuals

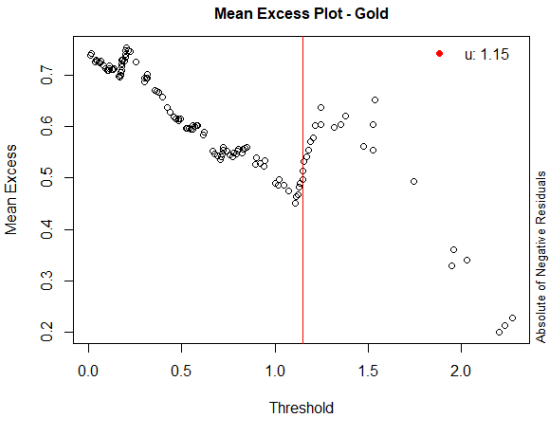

Figure 7.13: Gold mean excess plot Absolute of negative residuals

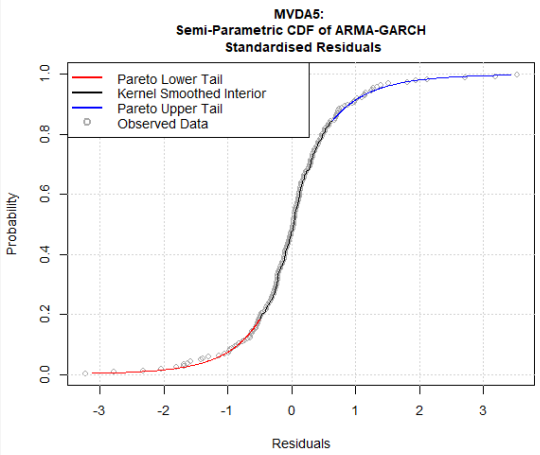

Figure 7.14: MVDA5 residuals baseline CDF

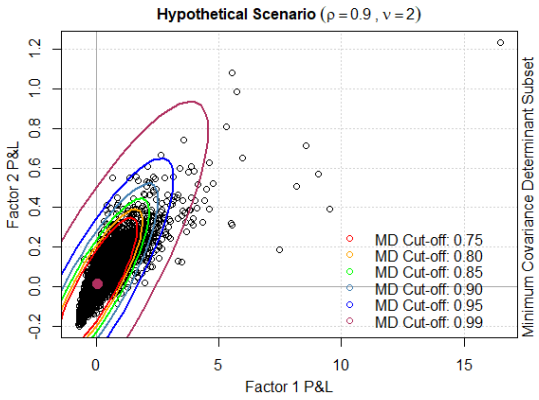

Figure 7.15: CGCI hypothetical scenarios